THE UNIVERSITY OF CALGARY

Vascular Adaptations after Surgical Incision of the Normal Rabbit Patellar Tendon

by

Michael Roman Doschak

A THESIS

SUBMITTED TO THE FACULTY OF GRADUATE STUDIES

IN PARTIAL FULFILMENT OF THE REQUIREMENTS FOR THE

DEGREE OF MASTER OF SCIENCE

DEPARTMENT OF MEDICAL SCIENCE

CALGARY, ALBERTA

APRIL, 1998

© Michael Roman Doschak 1998

National Library of Canada

Acquisitions and Bibliographic Services

395 Wellington Street
Ottawa ON K1A 0N4
Canada

Bibliothèque nationale du Canada

Acquisitions et services bibliographiques

395, rue Wellington
Ottawa ON K1A 0N4
Canada

Your file Votre référence

Our file Notre référence

The author has granted a non-exclusive licence allowing the National Library of Canada to reproduce, loan, distribute or sell copies of this thesis in microform, paper or electronic formats.

The author retains ownership of the copyright in this thesis. Neither the thesis nor substantial extracts from it may be printed or otherwise reproduced without the author's permission.

L'auteur a accordé une licence non exclusive permettant à la Bibliothèque nationale du Canada de reproduire, prêter, distribuer ou vendre des copies de cette thèse sous la forme de microfiche/film, de reproduction sur papier ou sur format électronique.

L'auteur conserve la propriété du droit d'auteur qui protège cette thèse. Ni la thèse ni des extraits substantiels de celle-ci ne doivent être imprimés ou autrement reproduits sans son autorisation.

0-612-31344-1

Canada

ABSTRACT

The clinical management of chronic, painful patellar tendinitis often involves open surgical debridement, which is thought to promote healing, possibly by means of an acute vascular response to the surgical injury. The objective of this study was to investigate and quantify vascular adaptations (both anatomical and physiological) to open surgical incision of the patellar tendon (PT), and the resultant effects on tendon microstructural organization.

Results indicated that longitudinal incision rapidly increases PT blood flow and vascular volume, whilst resulting in substantial changes to matrix organization that persisted for a long period after surgery. These findings suggest that longitudinal incision of the PT increases the vascular supply to deep tendon, but associated post-surgical remodelling activity causes collagenous disorganization possibly resulting in altered material composition.

The inability to discern new blood vessels over pre-existing ones led to studies evaluating developmental chondroepiphyseal neovascularization in long bones, as a suitable model for studying angiogenesis in connective tissues, and is presented in Appendix B.

ACKNOWLEDGEMENTS

I wish to express my gratitude to the many individuals, in the laboratory, and at the University of Calgary, who helped me to complete this work. I thank Drs Robert Bray, John Matyas, and David Hart for their helpful guidance, and many hallway discussions during the course of my studies. I also wish to thank Dr Anthony Russell for his constructive critique of this work.

I would like to sincerely thank the two individuals who have inspired, encouraged, and mentored my career in science, namely, Phillip Jacobsen and Robert Bray. You have helped me to go further and beyond, and I thank you for this.

In conclusion, I wish to sincerely thank my family for their encouragement and support, and for the hardships they have endured on my behalf. To my wife Lydia, her parents Lydia and Myron, my son Luke, and my parents Michael and Zirka - thanks!

DEDICATION

In memory of Anton Oleh Doschak, with love.

October 8, 1997

TABLE OF CONTENTS

Approval Page ii

Abstract iii

Acknowledgements iv

Dedication v

Table of Contents vi

List of Figures viii

CHAPTER 1: INTRODUCTION 1

CHAPTER 2: BACKGROUND AND RELATED RESEARCH 5
- 2.1 Joint Connective Tissues: General Overview 5
- 2.2 The Origins of Joint Blood Supply 6
- 2.3 The Vascular Organization of Tendon and Patellar Tendon 7
- 2.4 Vascular Volume and Responses to Injury 11
- 2.5 Tendon Blood Flow and Responses to Injury 14
- 2.6 Elevated Blood Flow and Fluid Compartment Changes 18
- 2.7 The Pathophysiology of Patellar Tendinitis 19
- 2.8 Study Rationale and Significance 20

CHAPTER 3: MATERIALS AND METHODS 23
- 3.1 Animal Handling and Experimental Design 23
- 3.2 Patellar Tendon (PT) Incision Surgery 24
- 3.3 Vascular Ink-injection with Tissue Clearing 27
- 3.4 Vascular Ink-injection, Histology, and Immunohistochemistry..... 27
- 3.5 Evaluation of Matrix Organization and PT Remodelling 29
- 3.6 Microsphere Techniques 30
- 3.7 Coloured Microsphere Processing and Water Content Analyses.. 33
- 3.8 Vascular Volume Determination..... 36
- 3.9 Statistical Analyses 38

CHAPTER 4: RESULTS.....40
- 4.1 Morphological Evaluations 40
- 4.2 Quantitative Evaluations 49
  - 4.2.1 Blood Flow 49
  - 4.2.2 Water Content Analyses 52
  - 4.2.3 Vascular Volume Analyses (Vascular Index) 52

4.2.4 Cross-sectional Area Measurements 55

CHAPTER 5: DISCUSSION 57
Future Directions 64

CHAPTER 6: REFERENCES 65

APPENDICES 72
APPENDIX A 72
Manuscript entitled: "Surgical Incision of the Normal Rabbit Patellar Tendon Causes Significant Vascular adaptations 72

APPENDIX B 91
Manuscript entitled: "Angiogenesis in the Distal femoral Chondroepiphysis of the rabbit during Development" 91

APPENDIX C 113
C.1 Digitized slides of cartilage canals traversing a serially sectioned distal femoral epiphysis from a 29 day kit 113
C.2 Digitized slides of serially sectioned distal femoral epiphyseal transplant in the chick chorio-allantoic membrane 131

LIST OF FIGURES

Figure 2.1: Anterior view of the right rabbit knee in full extension, demonstrating the patellar tendon and surrounding retinacular tissues. 9

Figure 3.1: Schematic representation of the rabbit knee joint, demonstrating the three longitudinal incisions in the patellar tendon midsubstance. Incisions are demarcated at the time of surgery with marker sutures. 25

Figure 3.2a: The experimental design of this investigation. Figure 3.2b: Materials and methods used to evaluate both morphological and quantitative aspects of vascular adaptations in the patellar tendon at each interval assessed. 26

Figure 3.3: The ink-perfusion setup. Both femoral arteries are cannulated and gelatin-ink is infused at a constant rate by means of a syringe pump. 28

Figure 3.4: Histological photomicrograph of rabbit patellar tendon demonstrating the collagen "crimp" waves. Marker sutures, cut in cross-section, are evident (black arrow)., as are the blood vessels which have been injected with gelatin-ink. Section Thickness = 20 μm. Bar Marker = 50 μm. 31

Figure 3.5: A specimen of rabbit patellar tendon clamped vertically in vice grips, awaiting cross-sectional area determination in the midsubstance. The black horizontal marker lines are used to monitor subsequent disruption of the patellar tendon. 32

Figure 3.6a: Physiological data acquisition of Electrocardiograph (EKG) and arterial blood pressure in the anaesthetized rabbit, in preparation for microsphere infusion. Figure 3.6b: Chart recording demonstrating the change in blood pressure waveform (blak arrow) as the infusion cannula enters the heart. 34

Figure 3.7: Schematic illustrating the protocol for coloured microsphere blood flow evaluation: (1) Brachial artery cannulation for withdrawal of the blood "reference" sample. (2) Transducer monitoring arterial pressure. (3) Transducer confirming placement of the infusion cannula in the left ventricle of the heart. (4) Electrocardiograph (EKG) reading. 35

Figure 3.8a: Anterior view of the rabbit patellar tendon following Gelatin-Carmine Red infusion used to quantify vascular volume. Figure 3.8b: View of the reflected patellar tendon demonstrating the posterior surface of the patella. 37

Figure 3.9a: Schematic illustrating the removal of a central square of patellar tendon midsubstance, as demarcated by the marker sutures placed at the time of surgery. Figure 3.9b: Both inner and outer pieces of tissue were subsequently processed to quantify vascular volume by measuring the Carmine Red dye content. 39

Figure 4.1: Macroscopic photographs of gelatin-ink injected blood vessels in control (A), & longitudinally incised patellar tendon at the indicated intervals (B - D). Rule graduations are in centimetres. 41

Figure 4.2: Photomicrographs of gelatin-ink injected blood vessels in control (A), and healing patellar tendon 3 days (B), 10 days (C), and 42 days (6 weeks) (D) following longitudinal incision.
Section Thickness = 20μm. Bar markers = 50 μm. 42

Figure 4.3: Cryomicrotome prepared sections of patellar tendon 3 days following surgical incision. The sections have been stained using Haematoxylin and Eosin, demonstrating cords of migrating endothelial cells (black arrows).
Section Thickness = 20 μm. Bar Marker = 50 μm. 43

Figure 4.4: Histological photomicrographs of migrating endothelial buds in patellar tendon 3 days following surgical incision. The sections have been stained using the Alcian blue-safranin method to highlight mast cells (black arrows), which promote angiogenesis through the action of heparin and other secreted factors (Whalen & Zetter, 1992).
Section Thickness = 20 μm. Bar Marker = 50 μm. 44

Figure 4.5a: Histological photomicrograph of gelatin-ink injected blood vessels in normal rabbit patellar tendon. Figure 4.5b: The same section co-localized with anti-thrombomodulin immunohistochemistry, demonstrating blood vessels not detected through gelatin-ink injection. Bar Marker = 50 μm. 45

Figure 4.6a: Histological photomicrograph of gelatin-ink injected blood vessels in normal rabbit patellar tendon. Figure 4.6b: The same section co-localized with anti-thrombomodulin immunohistochemistry, demonstrating blood vessels not detected through gelatin-ink injection. Bar Marker = 50 μm. 46

Figure 4.7a: Histological photomicrograph of gelatin-ink injected blood vessels in normal rabbit patellar tendon. Figure 4.7b: The same section co-localized with anti-thrombomodulin immunohistochemistry, demonstrating blood vessels not detected through gelatin-ink injection. Bar Marker = 50 μm. 47

Figure 4.8a: Histological photomicrograph of gelatin-ink injected blood vessels in normal rabbit patellar tendon. Figure 4.8b: The same section stained with anti-thrombomodulin immunohistochemistry, demonstrating blood vessels (black arrows) not detected through gelatin-ink injection. Bar Marker = 50 μm. 48

Figure 4.9: Haematoxylin and Eosin stained section of patellar tendon 42 days following surgical incision. The inclusion of a fatty defect (black arrow) at the location of an incised slit is evident. 50

Figure 4.10: Standardized blood flow in control and incised experimental patellar tendon. Values represent the Mean $\pm$ Std Error Mean. The significances noted are between Time Zero Controls and Incised Experimentals across groups. 51

Figure 4.11: Wet mass in control and incised experimental patellar tendon. Values represent the Mean $\pm$ Standard Error of Mean. 53

Figure 4.12: Dry mass in control and incised experimental patellar tendon. Values represent the Mean $\pm$ Standard Error of Mean. 54

Figure 4.13: The vascular volume for the entire PT (solid line) sampled at time-zero, 3 d, 10 d, and 42 d. The individual components of this vascular volume which supply the outer portions and inner square of PT substance are represented in the central dotted lines. Values represent the Mean $\pm$ Std Error Mean. 56

Figure B.1: Time-course of cartilage canal development in the distal femoral epiphysis of the fetal New Zealand White rabbit. 96

Figure B.2: A view of the freshly transplanted chondroepiphysis on the chorio-allantoic membrane. Magnification x10. 101

Figure B.3: Time-course of fetal New Zealand White rabbit growth, from 18 to 41 days post-conception (Log-Log plot). 102

Figure B.4: A metaphyseal vascular erosion of the 21 day chondroepiphysis stained with anti-thrombomodulin and viewed under epi-fluorescent illumination. Bar Marker = 50 μm. 103

Figure B.5: Angiogenesis from the chorio-allantoic membrane directed towards a 48 hour implant of 20 day chondroepiphysis. Magnifications x6.5 and x20 respectively. 106

Figure B.6: Angiogenesis from the chorio-allantoic membrane directed towards a 72 hour implant of 20 d chondroepiphysis. Mag x6.5 and x20 respectively. 108

CHAPTER 1

INTRODUCTION

Historically the blood supply to joint tissues has attracted only limited scientific enquiry, despite the well documented involvement of vasculature in the inflammatory and healing responses following injury (Whalen & Zetter, 1992). The fibrous connective tissues of joints were generally believed to be sparsely vascularized, if at all, with joint nourishment attributed to passive, diffusion-based mechanisms. However, as detailed anatomical and physiological studies evolve, our understanding of the diverse nature of joint tissue blood supply has also grown (Davies & Edwards, 1948; Scapinelli, 1968; Arnoczky, 1985; Alm & Stromberg, 1974; Bray et al. 1990). As awareness (and possibly incidence) of injury to joint tissues increases, the notably high level of morbidity and poor prognostic outcome has stimulated more intense interest in joint blood supply (Arnoczky et al, 1979; Banes et al, 1981; Gelberman et al, 1991; Torstensen et al, 1994).

Joint health is heavily dependent on homeostatic and precise mechanical function of the soft tissues binding and enclosing these load-bearing, freely-mobile structures. Injury signals a shift in joint homeostasis, and invariably, in joint function. If the healing response is inadequate in regaining structural and functional homeostasis, insidious deterioration of joint structure and function may result and surgical intervention may be the last viable therapeutic alternative.

Injured joint tissues, on the whole, do not heal well (Arnoczky et al, 1979; Fackelman, 1973). In many situations normal tissue structure, and material properties, are not restored and often predispose the joint to further deterioration. Surgical intervention addresses anatomic and structural faults in joint tissue architecture, often with attainment of near-perfect anatomic restoration. But what of the physiological processes and tissue remodelling responses in the healing state? Many joint tissues are not well vascularized, and as such, do not mount appreciable vascular, repair, and inflammatory responses to injurious stimuli. Ironically, those that do may create an altered environment which irritates and degrades adjacent uninjured tissues, resulting in "chronic joint damage", such as that seen in the reactive synovium of rheumatoid arthritis (Peacock et al, 1995).

One clinical example of surgical intervention designed to promote healing in a joint connective tissue involves the patellar tendon (PT) in cases of tendon overuse syndrome, or tendinitis. Surgical debridement of the PT is performed to treat refractory cases of tendinitis (Blazina et al, 1973; Henninger et al, 1992; Parker & Calabrese, 1994; Schepsis & Leach, 1987; Torstensen et al, 1994). In this procedure, a number of longitudinal incisions are introduced randomly in the tendon midsubstance in an effort to stimulate healing. The healing of tendon injuries has been well described, and occurs through fibrin clot organization, cellular recruitment and scar formation (Amadio, 1992; Ross, 1968). However, the vascular events have not been as clearly delineated. It has been suggested that longitudinal incision of normal tendons increases tendon vascularity (Stromberg et

al, 1974), but few studies have quantified vascular responses during tendon healing.

The present study is based on the rationale that longitudinal incision of tendons stimulates acute vascular responses to injury, and this response promotes healing. Vascular responses include changes in vessel numbers (through recruitment and angiogenesis), and changes in blood supply (vasoactive changes in vessel diameter and rate of blood flow). Previous investigators have shown that following tendon injury, blood vessels divide and vascularize the repair site (Gelbermann et al, 1991; Henninger et al, 1992; Stromberg et al, 1974). This constitutes a direct alteration of the tendon material composition, and ultimately may alter normal tendon physiology (Shrive et al, 1995). Furthermore, vasoactive changes in blood supply during the acute phase following injury is inherent for defining the classical inflammatory responses of redness, swelling, and heat. Often the immediate outcome of acute inflammation is "loss of function", and in the healing tendon, this process may possibly be mediated by the degree to which vascular adaptation alters normal tendon physiology and function.

The objectives of this study were to: a) determine the response and time course of vascular adaptations in the incised, healing PT; b) quantify the changes in PT blood flow and vascular volume; and c) assess the effects that longitudinal (non-transecting) incision has on PT geometric properties and matrix remodelling.

The hypothesis tested was that: "Longitudinal incision of the patellar tendon evokes vascular adaptations and stimulates tendon remodelling over time".

This investigation details a surgical model for studying changes in PT vascular supply, and will provide experimental evidence that PT incision stimulates vascular adaptation.

On a separate note, the vexing problem of distinguishing pre-existing vasculature from newly formed blood vessels in connective tissues was difficult in these studies of vascular adaptation. As a first step in understanding the process of neovascularization and vascular agenesis, neovascularization of the distal femoral chondroepiphysis in the fetal rabbit was investigated. This study staged the time-course for blood vessel invasion of the initially avascular femoral chondroepiphysis during the development of the secondary centre of ossification. In this system there is the potential for studying angiogenic markers in the total absence of pre-existing vasculature. The results of this study are included as Appendix B.

CHAPTER 2

BACKGROUND AND RELATED RESEARCH

2.1 Joint connective tissues: General overview

The load-bearing connective tissues of joints differ markedly from each other with respect to composition, morphology and function. They encompass such diverse structures as the tendons, ligaments, cartilage, menisci, bone, capsule and synovium. Most are, however, a composite of collagen fibrils embedded in a hydrophilic matrix of proteoglycans, populated sparsely by resident fibrocytic cells. These cells are predominantly fibrocytes, and are often named after their host tissue, such as tenocytes in tendon, or synoviocytes in synovium. Some definitive morphological and functional differences have been noted between resident fibrocytic cells in varying joint tissues, in particular with the chondrocytes of cartilage and the osteocytes of bone (Leeson & Leeson, 1970). It is reasonable to assume that these cells are at varying states of differentiation and have specialized functions suited to their resident tissues. Teleologically speaking, these cells have formed the structure and composition of their respective tissues that they maintain in adulthood.

The major structural component of connective tissues is collagen. The collagens are a family of 20 or more proteins with diverse organization and function, but which are ultimately defined by a common primary structure - namely the collagen chain. The collagen chain consists primarily of three repeating amino

acids - glycine, proline and hydroxyproline (Butler et al, 1978). Each collagen chain is arranged in a left-handed configuration, and three collagen chains are organized into a single collagen molecule. The three chains are woven into a right-handed triple-helix, which is held together by hydrogen and covalent bonds. In this manner, five collagen molecules combine to form ordered, parallel bundles of microfibrils that are oriented in a distinct longitudinal pattern. At this level, collagen is associated with water, proteoglycans and glycoproteins which form an extracellular matrix binding the fibrils together to form fascicles.

2.2 The origins of joint blood supply

The fascicular level of collagen organization heralds an important breakthrough-point for the blood supply. In the tendon, for example, fascicles are held together by loose connective tissue which facilitates the entry of blood vessels, lymphatics and nerves. The origins of arterial tributaries to joints are manifold. A number of arteries act as the principal sources of blood supply (Scapinelli, 1968). In general, veins follow the arteries, and usually one vein follows one artery. Exceptions occur, such as in the anastomosing superficial plexi of the synovium where two veins commonly follow one artery, and anastomose frequently across it (Davies & Edwards, 1948). Valves occur frequently in all the veins.

Blood vessels divide and anastomose freely, forming a complex network around the joint, and within the boundary circumscribed by the joint capsule and synovium-bone entheses. This network was described, in the knee, by Hunter in

1743 and was termed the "circulus articuli vasculosus" (Hunter, 1743). It is from this network that branches arise to supply virtually all of the surrounding structures. The vasculature of these structures have been elucidated in a progressive manner using anatomical observation with red ochre (Hunter, 1743), india ink injection (Davies & Edwards, 1948), barium sulphate radiography (Scapinelli, 1968), corrosion cast electron microscopy (Arsenault, 1987), and recently immunohistochemical markers (Bray et al, 1997; Kai et al, 1992; Schmidt et al, 1995).

2.3 The vascular organization of tendon and patellar tendon

From the circulus articuli vasculosus, vessels branch to supply the connective tissue structures of the joint, such as the tendons. Tendons receive their blood supply from vessels in the perimysium, the periosteal insertions and from surrounding vessels in the paratenon (or mesotenon), and epitendon. Tendons surrounded by paratenon are referred to as vascular tendons, while those surrounded by a tendon sheath are referred to as avascular tendons (Woo et al, 1994). In tendons surrounded by a paratenon, blood vessels enter from many points along the periphery and form a longitudinal system of vesels deep within the tendon substance. Frequent anastomoses are seen, with smaller vessels running transversely around the connective tissue bundles in a ladderlike fashion. In tendons surrounded by sheaths, the mesotenons are reduced to vinculae (or straps) through which blood vessels supply the tendon. The vincular vessels often

divide into branches once they enter the tendon substance, and become arranged as vertical vascular loops, leaving the remainder of the sheathed tendon avascular. These avascular regions have led many investigators to propose a dual pathway for sheathed tendon nutrition, namely direct vascular and a syovial (diffusion) pathway for the avascular regions (Neuberger et al, 1951; Woo et al, 1994).

The patellar tendon is an unusual tendon, as it consists of an insertion from "bone" to "bone-and-muscle", namely the tibia to the patella and quadraceps muscle (Figure 2.1). This has led many anatomists to classify the structure as the Patellar ligament, due to the bone to bone component. The structural composition of the PT, however, closely approximates other tendons found throughout the body, with the surrounding peritendinous and retinacular tissues being richly vascularized. Vascular ink-injection studies have demonstrated that the patellar tendon derives its blood supply from the underlying infrapatellar fat pad and from the surrounding retinacular tissues (Arnoczky, 1985). In the developing tendon, the blood supply is generous due to the large proportion of actively synthesizing fibroblasts. As the amount of intercellular substance increases, the circulation decreases until, in the mature tendon, it is sparse. Those vessels that do supply the tendon usually penetrate the paratenon or enter from the epitendinous junction (Liew & Carson-Dick, 1981). The endotenon carries blood vessels as well as lymphatics and nerves to the primary bundles. Few, if any, vessels traverse the osteotendinous junction, probably as a result of the fibrocartilage that is usually present. Similarly,

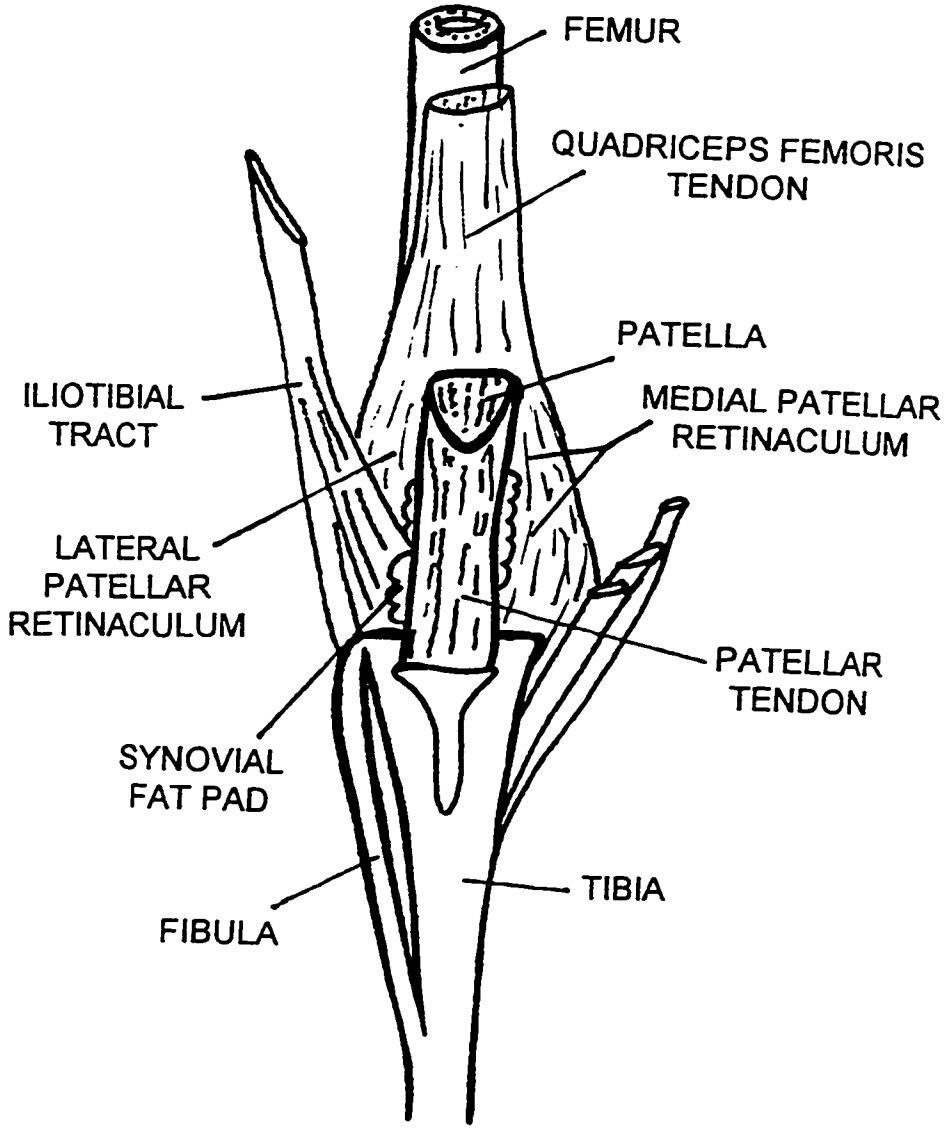

Figure 2.1: Anterior view of the right rabbit knee in full extension, demonstrating the patellar tendon and surrounding retinacular tissues.

the adjacent osseous surface is usually devoid of foramina with vessels (Leeson & Leeson, 1970; Scapinelli, 1968).

2.4 Tendon vascular volume and responses to injury

In contrast to the mere presence of vessels, of importance in determining blood supply to a structure is the total vascular volume, as well as the vasoregulatory state of the microcirculation. In this situation one considers the total area of vasculature available. This measure may be a reasonable index of volume when determining the vascular response mounted to injury.

Embryologically, blood vessels are derived from mesenchymal cells and first appear as a collection of endothelial cells, known as blood islands (Rifkin & Klagsbrun, 1987). These endothelial cells multiply to form independent vessels which at a later stage unite to form the circulatory system in a process termed vasculogenesis. Vessels initially appear as capillaries, which progressively increase in size and develop smooth mucle and connective tissue components by adjacent differentiating mesenchymal cells. Once the blood circulation has been established, new vessel formation occurs by outgrowths or buds of endothelial cells from the existing structure (Sandison, 1928). This process is termed angiogenesis (Angeion [Gr.] "vessel"; Genesis [Gr.] "production") or neovascularization (Neo [Gr.] "new"), and occurs relative, and in degree, to some form of stimulus.

The inner lining cell of the blood vessel is the endothelial cell. These cells form a single layer which lines the luminal surface of all vessels (Leeson & Leeson,

1970). In capillaries, they constitute the full thickness of the wall. While providing a barrier between the vessel lumen and underlying tissues, they remain well suited to allow the exchange of products and cells across their boundaries. Endothelial cells are curved, elongated, and flat, with a bulging ovoid nucleus which protrudes its mass into the lumen of the vessel. Endothelial cells are highly active metabolically, and are involved in the active transport of fluid across the capillary wall, as well as a multitude of chemically mediated events (Gross, 1983). Through the action of specific molecules, they provide a non-thrombogenic surface to the reactive components of the blood supply (cellular and plasma-borne), while retaining the ability to express receptors and synthesize vasoactive substances which effect interactions with these same blood components.

The theory of neovascularization (or angiogenesis) have mostly been derived from observations on experimental models, such as the rabbit ear chamber (Sandison, 1928), the hamster corneal pocket (Langham, 1953), and the chick chorioallantoic membrane assay (Auerbach et al, 1974). These studies demonstrated a rapid vascular response to an angiogenic stimulus. Not only is the response rapid in its formation, but it is equally as rapid in remodelling and resorptive events which regulate the degree of vascularization to a given tissue.

Measures of vascular volume followed anatomical visualization techniques for the vasculature. Vascular volumes were ascertained by the qualitative observation of dye-perfused vasculature, both macroscopically (after being rendered translucent with clearing agents) and microscopically. The inclusion of

gelatin in the perfused dye ensures the localization of the perfusate within the vasculature once the gelatin has set. Quantitative histomorphometric techniques have followed the morphological evaluations; however, the time-consuming nature of microscopic quantitation has limited the number of studies to date on the vascular volumes to various joint tissues. A recent technique for quantifying vascular volume in entire tissue samples has significantly simplified these measures (Colville-Nash et al, 1995). The vasculature is perfused using classical dye-injection techniques with gelatin and a dye (carmine red) whose concentration can be ascertained spectrophotometrically. Namely, the concentration of dye is directly, and linearly, proportional to the absorbance measured at the correct wavelength. Thus, once standardized to the mass of the tissue sample, a quantitative measure of vascular volume in the specimen can be obtained by eluting the trapped dye and measuring it spectrophotometrically.

For patellar tendon, no quantitative information is available to compare and contrast vascular volume or angiogenesis. Some literature exists for the sheathed flexor tendons in the forepaws of the dog, horse and rabbit, and for the knee ligaments (Arnoczky et al, 1979; Bray, Rangayyan, et al., 1996; Gelberman et al, 1991). These results will be considered as indicators of the vascular adaptations (in response to injury) seen in related joint connective tissues.

Arnoczky and colleagues demonstrated a pronounced vascular response in dog knee ligaments in response to injury using microangiography (Arnoczky et al, 1979). A marked proliferation of vessels was noted after two and a half weeks of

healing, and the new vessels extended up to the area of the lesion as well as to the ligament itself. Intraligamentous vessels were seen to be increased in number and larger in diameter.

Bray et al quantified the vascular volume of medial collateral ligament, and its responses to acute injury, namely complete disruption (Bray, Rangayyan, et al., 1996). When measured 3 wks following injury, a large and rapid angiogenic response of ligament tissue to injury was noted. Furthermore, this response is seen to be maximal around 6 weeks, giving an increase of 56% in vascular tissue to the injured ligament. Up to 17 weeks following the injury, the degree of vascularity remains elevated. These observations suggest the necessity of an increased blood supply, and/or a redistribution of the microvasculature is required during the healing and remodelling responses of ligaments. However, by 40 weeks, ligament vascular volume has been dramatically reduced to a level two-thirds below the peak of the injury, and marginally below that of even normally undisturbed ligament. Thus, with further progress of the healing response, the initially large amount of vessels serving the structure is apparently resorbed to a level more indicative of demand. This degree of vascularity may also be influenced in some fashion by the presence of scar tissue, and the effects of scar contraction following the healing process, as evidenced by the changing angular distribution of the blood vessels (Bray, Rangayyan et al., 1996).

Recent studies, using vascular injections of ink, have described the revascularization of acutely ruptured tendon in the forepaw of the dog (Gelberman

et al, 1991). It was noted that vessels in the surrounding epitenon progressively extended through normal avascular regions to reach the site of repair by 17 days post-injury. It was further noted that normally avascular volar segments of the tendon were also revascularized as a consequence of the adjacent injury. Thus, an extrinsic vascular response to tendon injury, in the case of sheathed tendons, may promote more rapid healing.

2.5 Tendon blood flow and responses to injury

The presence of blood vessels, their quantity and distribution suggest the magnitude of respective vascular requirements to a structure, be it in response to injury or simply in the course of normal function. Although vascular volume is an indicator of the degree of blood supplying a structure, it by no means constitutes a physiologically active measure.

The determination of blood flow, on the other hand, gives a quantitative measure at a point-in-time, at which the blood supply to a given structure was evaluated. A structure receiving a greater flow of blood (and therefore an increased blood supply) would receive greater amounts of nutrients, and this would suggest a heightened level of tissue metabolic activity, perhaps necessary to mount an appreciable healing response. But underlying the nutritional requirements of the structure are the parallel effects of increased blood flow, namely greater delivery and removal of active regulatory substances, elevated hydrostatic pressure dynamics, greater convective removal of heat, and recent studies in load-bearing

structures suggesting the loss of low-load viscoelastic properties (Doschak et al, 1994; Bray et al, 1997). Thus, it is plausible that changes in blood supply may alter the functional behaviour of joint connective tissues, and this premise will be reviewed shortly.

It is possible to measure blood flow by a number of accepted techniques, including radioisotope clearance (Whiteside & Sweeney, 1980), chromium-tagged red blood cell washout (Shim & Leung, 1986), hydrogen washout (Brookes & Harrison, 1967), microspheres (Riggi et al, 1990), and more recently by laser doppler flowmetry/imaging (Schlehr et al, 1987). Of these techniques, microsphere evaluation of blood flow is attractive as it provides a measure of total tissue perfusion, rather than individual major vessel blood flow. Furthermore, it constitutes an absolute measure, and not a relative one as seen with laser doppler flowmetry/imaging.

Blood flow to connective tissues of the joint varies considerably from tissue to tissue; however, in general, flow values are relatively low when compared to richly perfused organs such as lung, kidney and heart. In such a comparison, differences are in orders of magnitude when tissues are compared after standardization with respect to mass. Bone tissue is measured to have the greatest blood perfusion, with canine bone flow values ranging from 18.2 ml/min/100g (millilitres/minute/100 grams of tissue) for the tibial plateau and 13.0 ml/min/100g for the femoral condyle (Simkin et al, 1990) to 2.3 ml/min/100g for femoral endosteal cortex (Li et al, 1989).

Blood flow to synovial tissue is consistently among the highest observed in articular soft tissues. Baseline values for knee synovium ranging from 10.5 to 2.6 ml/min/100g have been shown in the horse and dog repectively (Hardy et al, 1993; Simkin et al, 1990). This range at first seems immense, however it is more likely a reflection of the heterogeneous nature of synovial tissue, with its superficial layers of lining cells and underlying areolar tissue, and the degree of "demand" offered by this metabolically active tissue at the point in time samples are obtained. Variation in tissue sampling results in variable ratios of tissue components, and also may account for the broad range of flow values reported.

Tendon blood flow assessments using microspheres have quantitatively proven the "low-flow" nature of tendinous tissue. McFarland et al demonstrated blood flow to canine patellar tendon was in the order of 2.5 - 3.0 ml/min/100g of tissue (McFarland et al, 1986). Similarly, a study in blood flow to canine flexor tendons resulted in flow rates of 2.0 to 7.0 ml/min/100g (Weidman, 1984). When compared to highly vascularized tissues (eg. muscle, skin), these flow rates for tendon indicate a lower, but very functional, blood supply (Hooper et al, 1984). However little information exists for healing tendon blood flow in response to injury.

Tendon and ligament blood flow have proved to be similar in nature. Hooper and colleagues demonstrated blood flow in canine deep flexor, calcaneal, superficial flexor and extensor tendon, and determined the range of flow values to be between 0.18 to 1.08 ml/min/100g (Hooper et al, 1984). Similarly, articular ligament blood flow has been evaluated between 0.74 to 2.36 ml/min/100g for MCL

and PCL respectively (Bray, Butterwick et al, 1996). Of importance to note is the range in values obtained from anatomically similar tissue types. It is evident from the reported values that flow, and therefore blood supply, differs between individual ligaments and tendons. This variation could well be attributed to many individual differences, such as content, location, function, the mechanical stimuli, and degree of vascularization to name a few.

As seen with vascular volume, the blood flow to an articular tissue increases rapidly after acute injury. Trifitt et al demonstrated that following osteotomy of the rabbit tibial diaphysis, cortical flow increased 2 to 3-fold, but marrow flow did not change (Trifitt et al, 1992). This implied that the increases in cortical flow were mediated by an arterial supply paralleling that of the marrow. An increase in blood flow in response to injury has also been shown with healing ligament. Following complete rupture of the rabbit MCL, blood flow in the healing MCL is seen to rise up to 30-fold that of resting values by three weeks of healing (Bray, Butterwick et al, 1996). This elevated flow is still evident at a six week interval; however, it has returned near to control normal values by seventeen weeks of healing. This temporal increase and decrease parallels that of the increasing vascular volume resultant from angiogenetic processes, followed by the decrease due to remodelling and resorptive events.

The cause of the initial increase in blood flow to the injured tissues is believed to be due to an increase in the vascular volume supplying the tissue. A known mechanism involves the increased activity of local vasoregulatory

substances which can alter vascular tone through vasodilatory events, and thus regulate flow to tissues (Khoshbaten & Ferrell, 1993). The presence of a vascular response to injury is of great importance to a healing tissue, but on the other hand, a persistence of this elevated response might be detrimental to the homeostatic functioning of some of the tissues involved (Doschak et al, 1994; Gross et al, 1995; Bray et al, 1997).

2.6 Elevated blood flow and fluid compartment changes

Inflammatory agents increase joint tissue blood flow (Najafipour & Ferrell, 1994) and alter vascular tone by agonistic vasoconstrictive and vasodilatory events (Ferrell et al, 1993). These vasoactive responses have been shown to change knee joint microvascular haemodynamics in chronic synovitis, as demonstrated by Hansen and co-workers in a model of carrageenan-induced inflammatory arthritis (Hansen et al, 1992). Increases in blood flow to the injured patellar tendon could, in itself, change the homeostatic osmotic pressure balances and gradients and cause variations in matrix water content. Oedema and altered microvascular haemodynamics are often seen in association with soft-tissue injury, and water content changes in ligament under conditions of injury (Frank et al, 1983), transplantation (Sabiston et al, 1990), or even immobilization (Akeson et al, 1987) have all been reported.

Changes in extra-cellular matrix proteoglycan content could alter fixed charge density (and resultant osmotic pressure) of the ligament, causing variations

in the tendon water content, as is seen in cartilage (Maroudas, 1985). Furthermore, tendon matrix remodelling, in response to altered joint physiology and/or acute injury, may alter the ratio of proteoglycan to collagen and produce changes in tissue hydration (Muller, 1994).

Chimich et al demonstrated that changes in ligament water content in-vitro resulted in increased low-load relaxation in the rabbit MCL (Chimich et al, 1992). Recent studies of ligament by Bray and co-workers have demonstrated that low-load ligament mechanical properties deteriorated as ligament blood flow increased (Doschak et al, 1994; Bray et al, 1997). Thus, matrix remodelling in connective tissues may be mechanically coupled, and may result in altered functional behaviour.

2.7 The Pathophysiology of Patellar Tendinitis

Patellar tendinitis has been described as a condition commonly seen in athletes who have performed repetitive jumping activities (Blazina et al, 1973; Cailliet, 1992; Torstensen et al, 1994). The condition, commonly known as "jumper's knee", seems to result from overuse of the patello-femoral mechanism in repetitive traction overloads, associated with forces of acceleration and deceleration. An overuse injury results to the extensor mechanism.

Cumulative stress on a cadaver tendon will eventually result in tissue failure (Goldstein et al, 1987). Even at lower levels of stress and repetition, microscopic failure and deformation will occur. Tendons, like many other tissues, undergo work

hypertrophy - ie. a gradual increase in collagen fiber diameter (Woo et al, 1980). Synthesis of new matrix elements occurs in an effort to meet the increase in work, as the tendon attempts to maintain its function. However, collagen turnover in tendons is quite slow and as such, work hypertrophy - though present - takes months to years to complete (Neuberger et al, 1951). In-vivo cumulative stress which is found to exceed the capacity for work hypertrophy results in tendon breakdown. Breakdown is usually preceeded by well noted tissue lesions - namely torn collagen fibers in the tendon, with a resultant necrosis and repair by fibroblastic proliferation (Ferretti et al, 1983). These microtears do not initially cause tenderness or pain, and the individual usually continues the injurious activity, causing further tissue damage (Cailliet, 1992). Mucoid degeneration of the tendon and fibrinoid necrosis has been described in surgically treated cases, and these changes are indicative of the normal repair processes failing - perhaps due to the repeated microtearing of the collagen fibers. Associated with these cases are areas of attempted tissue regeneration, with the proliferation of fibroblasts and blood vessels.

2.8 Study Rationale and Significance

The rationale for the present study is based, in part, on work by Henninger et al in race horses (Henninger, 1992). They studied the effects of surgically splitting the equine superficial digitor flexor tendon in cases of tendinitis. Their results suggested that tendon splitting produces a more rapid decrease in lesion

size and superior repair tissue organization when compared to unsplit controls. This was observed in concert with a peritendinous revascularization of the tendon lesions. Thus, a surgically induced neovascularization promoted better tendon healing, suggesting an initial lack of positive healing "factors" associated with blood supply.

Structural lesions seen in acute tendonitis have been shown to be slow to heal (McCullah et al, 1979; Silver et al, 1983), and the repaired tissue is of inferior biomechanical quality. This prolonged repair has been attributed to an inadequate or delayed revascularization of the tendon defect (Fackelman, 1973; Banes et al, 1981). Similarly there appears to be a decreased potential for tendon fibrocytes to become active collagen-producing cells. These observations led Henninger to postulate that although tendon has the ability for exclusively intrinsic repair, the repair process is slower than that seen when an extrinsic blood supply and collagen-producing cells are involved in the repair process (Henninger et al, 1992).

When treating patients with chronic patellar tendinitis or in cases of complete tendon rupture, exploratory surgery often reveals areas of focal tendon degeneration. The procedure of surgical debridement became commonplace, and was progressively increased to include aggressive incision of the remaining tendon (and often invasive drilling into the inferior pole of the patella) in an effort to increase the acute vascular response, and presumably augment the body's natural healing processes. While the outcome is often successful in reducing patient

morbidity, it is limited by the lack of detailed quantitative evaluations of the effects surgical incision has on patellar tendon substance and vasculature.

The study described in this thesis aims to detail the surgical incision of patellar tendon, and in particular, the vascular adaptations which follow. Both morphological and quantitative measures have been combined to evaluate open longitudinal incision, and to provide new and contemporary information regarding the outcome of this procedure. Drilling of the patella was excluded from this study in an effort to limit the measures of vascular adaptation to the patellar tendon alone, without influence from the anatomically distinct patellar blood supply and the added variable of healing bone. The results of this study, though limited to normal tissue, will provide definitive information as to the efficacy, and perhaps consequences, of patellar tendon in the best-case scenario - namely without being complicated by underlying tendinitis pathophysiology.

CHAPTER 3

MATERIALS AND METHODS

3.1 Animal Handling and Experimental Design

Forty-eight outbred, 1-year-old female New Zealand White rabbits (approximately 4.8 kg), were used in this study. Animals were purchased from a single supplier (Riemens Fur Ranche, St.Agathe, Ontario, Canada) and were individually housed in wire bottomed cages (65 x 40 x 45 cm; length x width x height). Unrestricted cage activity was allowed and a 12:12 hour light-dark cycle was simulated in a quiet room at 20°C. Ad libitum access was permitted to water and standard laboratory rabbit chow. The Faculty of Medicine Animal Care Committee reviewed the experimental protocol and approved it, based on the criteria of the Canadian Council on Animal Care (CCAC, 1984).

Following a week of acclimatization to their new surroundings, the animals were randomly allocated into four groups of 12 animals. Group 1,2 and 3 animals underwent unilateral incision surgery of the PT, and were sacrificed following 3 days, 10 days, and 6 weeks post-operative healing respectively. The 3 day interval was chosen to observe vascular responses during the Inflammatory phase of soft-tissue repair, 10 days to the Proliferative Phase and 6 weeks to the Organizational / Remodelling Phase (Ross, 1968). The remaining Group 4 animals were sacrificed at time zero, and provided control PT.

3.2 PT Incision Surgery

All operations were performed only on the right knee. Animals were first sedated with a 0.1 ml intravenous injection of Atravet^{R} (10 mg/ml acepromazine maleate, Ayerst Laboratories, Montreal, PQ) and then anaesthetized (2% halothane/oxygen). The PT was exposed through a medial incision of overlying skin, followed by blunt dissection of underlying fascial tissues. The tendon was isolated by raising the retinacular edges, incising with a scalpel, and inserting a flat spatula under the entire midsubstance of the PT. A series of 3 longitudinal, full-depth incisions were made using a curved #12 scalpel blade. Incisions began inferior to (but not involving direct contact with) the patella, and ran the full length of the PT (Figure 3.1). The incisions were terminated approximately 3mm prior to contacting the tibial insertion. The origin, mid-point and terminus of the 3 midsubstance incisions were demarcated using 6-0 nylon marker sutures. The skin wound was closed using 4-0 nylon suture. The left knee on all animals remained unoperated.

QUALITATIVE MORPHOLOGICAL EVALUATIONS

Three of the 12 animals from each experimental group (Figure 3.2) underwent assessment of microvascular volume and matrix remodelling using a combination of vascular ink-injection and endothelial cell immunohistochemistry utilizing anti-thrombomodulin. Thrombomodulin is expressed on the luminal surface of endothelial cells and has anticoagulative properties (Lager et al, 1995).

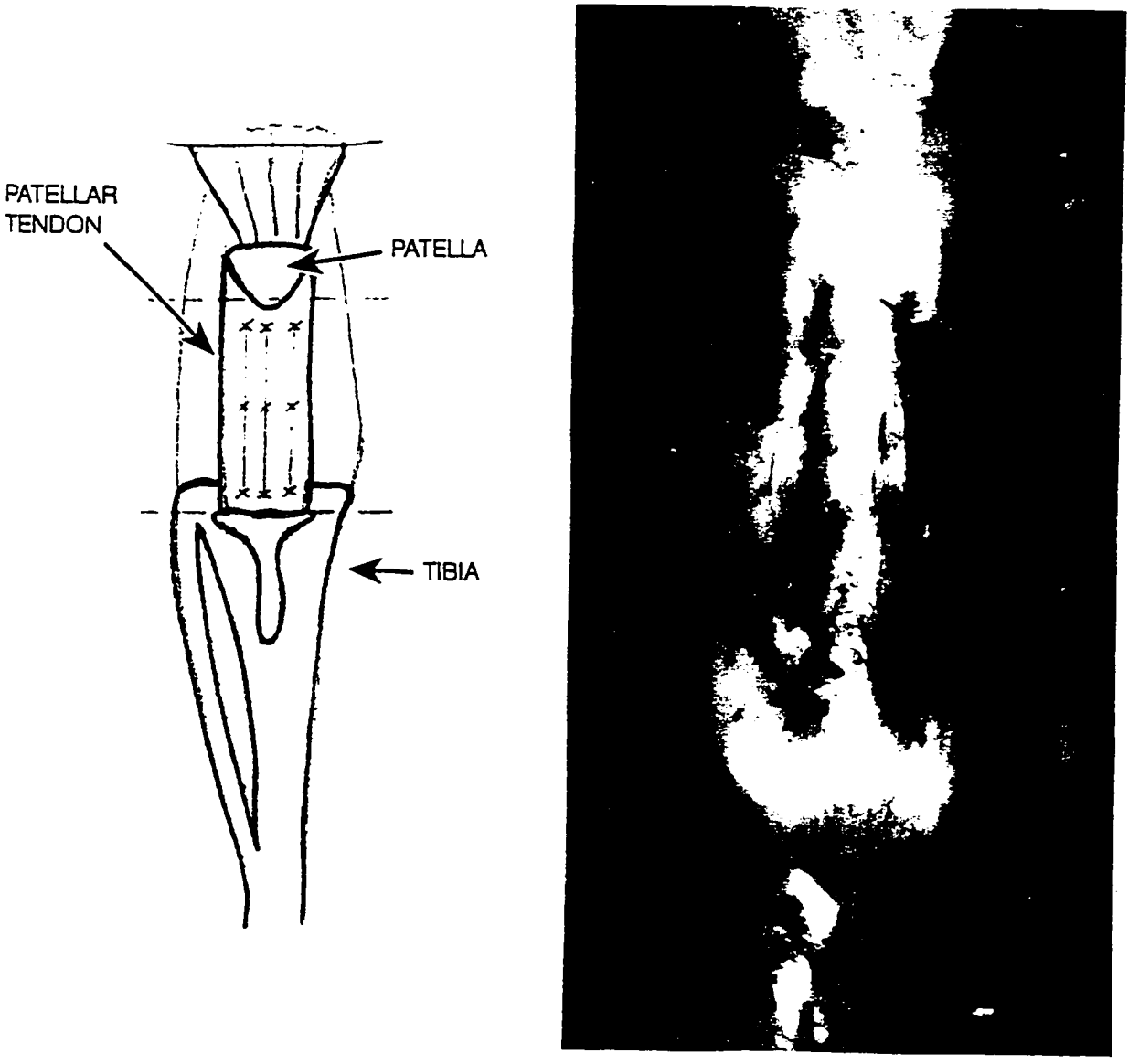

Figure 3.1: Schematic representation (and corresponding macroscopic view) of the rabbit knee, demonstrating the three longitudinal incisions in the patellar tendon midsubstance. Incisions are demarcated at the time of surgery with marker sutures.

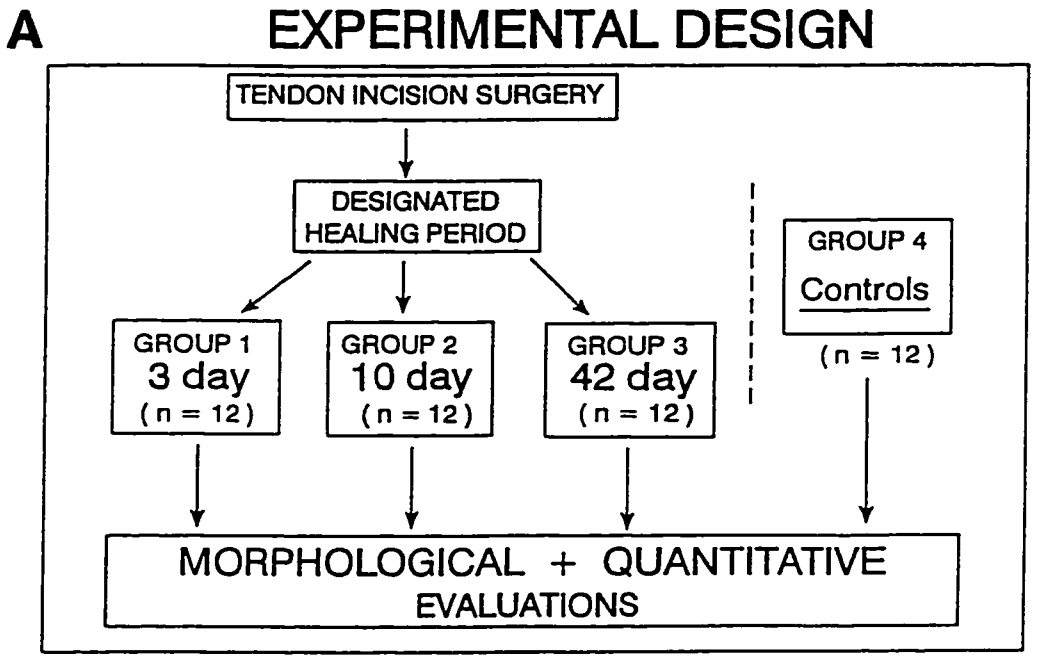

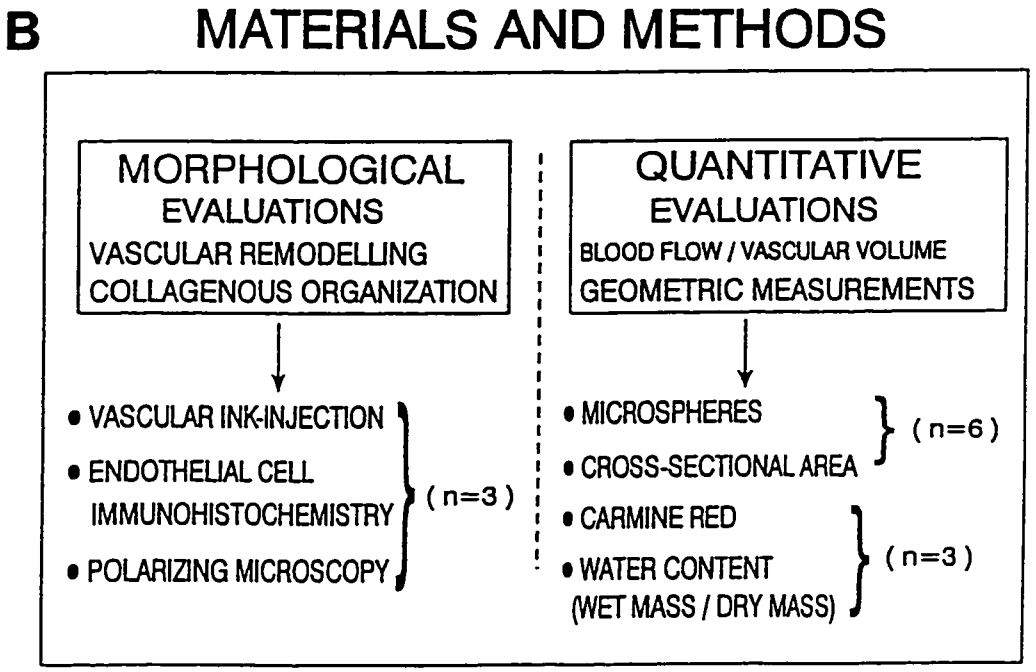

Figure 3.2a: The experimental design of this investigation. Figure 3.2b: Materials and methods used to evaluate both morphological and quantitative aspects of vascular adaptations in the patellar tendon at each interval assessed.

3.3 Vascular Ink-injection with Tissue Clearing (Spalteholz technique).

Animals were anaesthetized, and the femoral artery and vein dissected. The femoral artery was cannulated using PE-90 polyethylene tubing (Clay Adams, Parsippany, NJ, U.S.A.), and the femoral vein transected to permit unrestricted flowthrough of perfused solutions. The animal was sacrificed using a lethal injection of Euthanyl, and the limbs fixed in 90 degrees of flexion using a custom-made thermoplastic hindlimb mould. The limb was flushed with heparinized saline (100 units heparin/ml saline), and fixed by perfusion with a mixture of 4% paraformaldehyde/0.5% saturated picric acid in phosphate buffered saline (pH 7.4). Finally, a solution of filtered india ink (Higgins Black Magic, Faber Castell, Germany) containing 4% gelatin was perfused through the entire hindlimb (Figure 3.3). All solutions were pre-heated to 39°C, and femoral perfusion controlled by means of a Harvard Syringe Pump (Harvard Apparatus, Model 33, St. Laurent, PQ, Canada) at a constant rate of 7.6 ml/min. Perfusion pressures were monitored real-time using a computer-based oscillographic data acquisition system (AT-CODAS System, DataQ Instruments, Akron OH, U.S.A.). Following perfusion, the carcass was stored for 4 hours at 4°C, prior to disarticulating the hindlimb at the hip.

3.4 Vascular Ink-injection, Histology, and Immunohistochemistry.

The PT was dissected in entirety, and quartered into tissue blocks. These blocks were processed through cryoprotectant solutions of DMSO and PBS/10% sucrose, embedded,and serially sectioned at 40μm in entirety using a

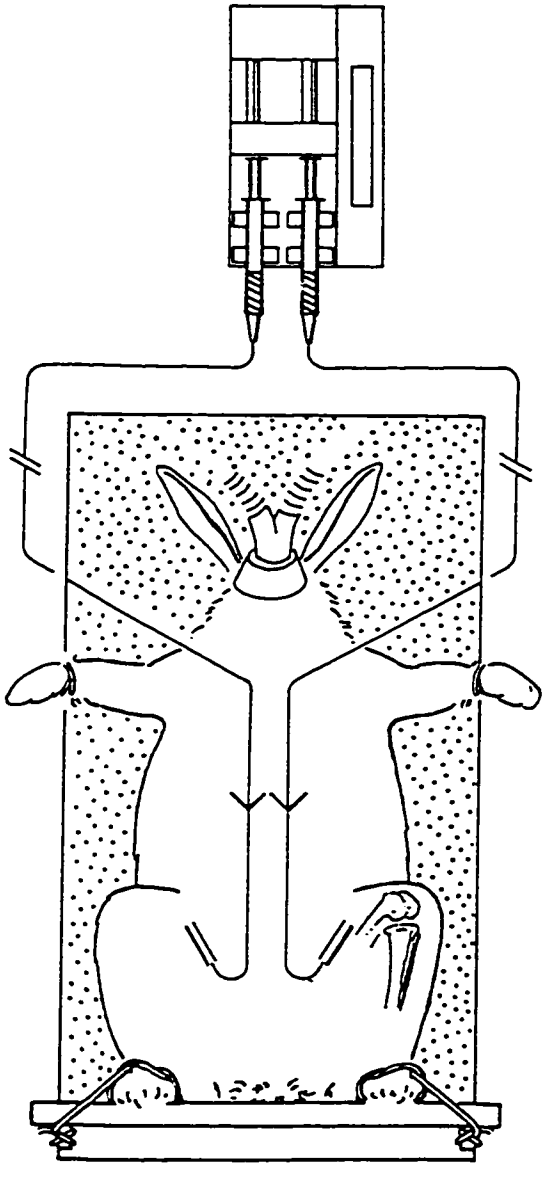

Figure 3.3: The ink-perfusion setup. Both femoral arteries are cannulated and gelatin-ink is infused at a constant rate by means of a syringe pump.

cryomicrotome. Every fourth slide of sectioned tissue was stained using anti-thrombomodulin indirect immunofluorescence, to facilitate colocalization of ink-injected vascular processes. Non-specific background staining was blocked using 5% bovine serum albumin, and pre-incubation with normal rabbit serum. Sections were incubated with goat anti-rabbit thrombomodulin (University of Oklahoma Medical Centre, Oklahoma City, U.S.A.) for 48 hours at 4°C. Following rinses in PBS/0.1% Triton-X 100, the sections were reacted with secondary rabbit anti-goat IgG FITC conjugate for one hour at room temperature in the dark. Following final rinses, sections were mounted and examined using a Leitz Orthoplan microscope under epi-fluorescent illumination (Leica Inc., BC, Canada). Photomicrography was performed using an Orthomat camera housing attachment with high-speed (400 ASA) colour slide film. Colocalization of ink-injected, thrombomodulin-stained blood vessels was achieved by using threshold levels of brightfield illumination in conjunction with epi-fluorescence. All tissue was assessed in a randomized, blinded fashion and graded for vascularization and evidence of angiogenesis at incision and at remote sites. Following these evaluations, the same sections were stained with Haematoxylin and Eosin.

3.5 Evaluation of Matrix Organization and PT Remodelling

A morphological assessment of tendon matrix organization was made by observing the incised slits in sections of PT. The sections were illuminated under polarized light, and organization of the birefringent collagen crimp surrounding the

incised locations observed (Figure 3.4). The term crimp refers to the wave-like pattern collagen exhibits under polarized light (Woo et al, 1994). In particular, the lateral registry of the collagen fibers was noted, and any degree of disruption (due to the incisions) noted.

PT remodelling was assessed by measuring the cross-sectional area of the loaded patella-PT-tibia complex on a separate set of animals, as described in the next section.

QUANTITATIVE PHYSIOLOGICAL EVALUATIONS

A second set of 6 animals from each experimental group underwent tendon blood-flow measurements (using coloured microspheres). Tendon cross-sectional area (CSA) was also measured. The patella-PT-tibia complex was cemented into bone grips, and held at a constant load of 10 Newtons, and the CSA determined (Figure 3.5). The measurement was performed using strain-guaged calipers, and results recorded in square mm. CSA was measured at the PT midsubstance, defined as the midpoint between the patellar and tibial insertions.

3.6 Microsphere Techniques

Coloured microspheres (CMs) were used to assess blood flow to joint tissues in the knee. Dye-Trak^{R} 15.5μm CMs were employed (Triton Technology Inc., San Diego, CA), in the following standard approach (Bray, Butterwick et al, 1996):

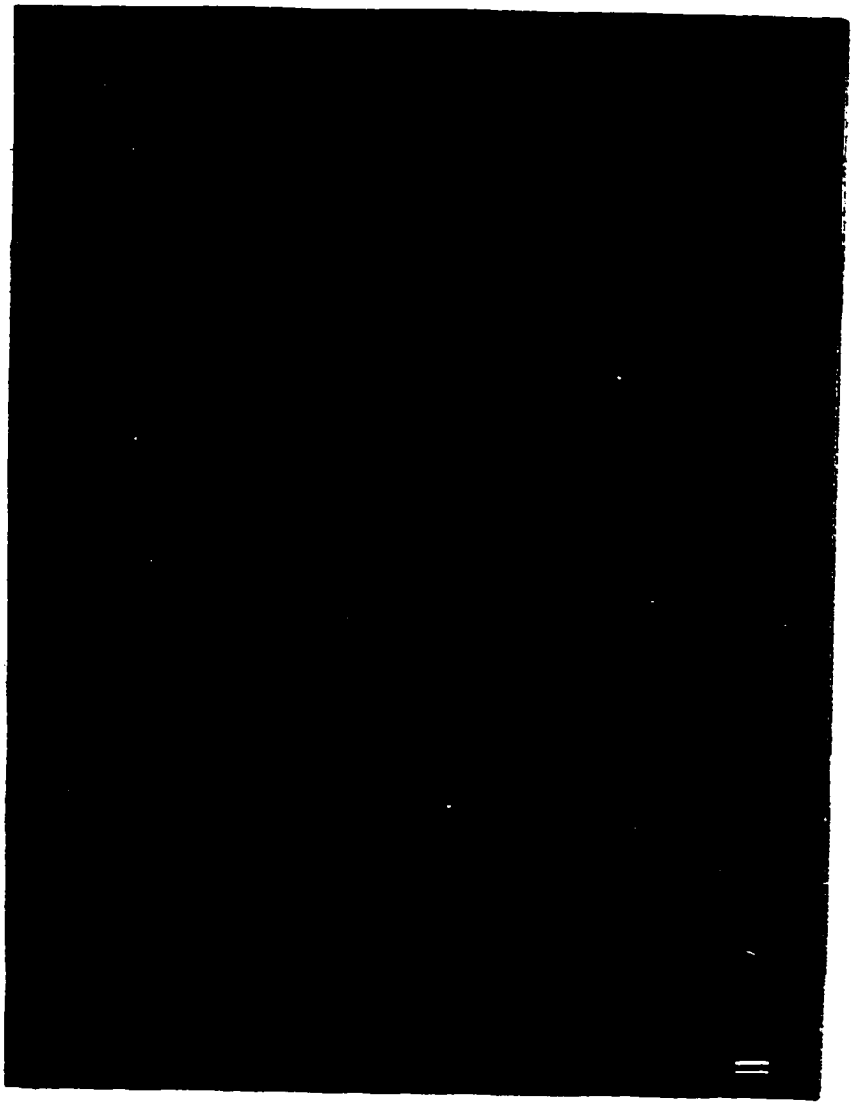

Figure 3.4: Histological photomicrograph of rabbit patellar tendon demonstrating the collagen "crimp" waves. Marker sutures, cut in cross-section, are evident (black arrow)., as are the blood vessels which have been injected with gelatin-ink. Section Thickness = 20 μm. Bar Marker = 50 μm.

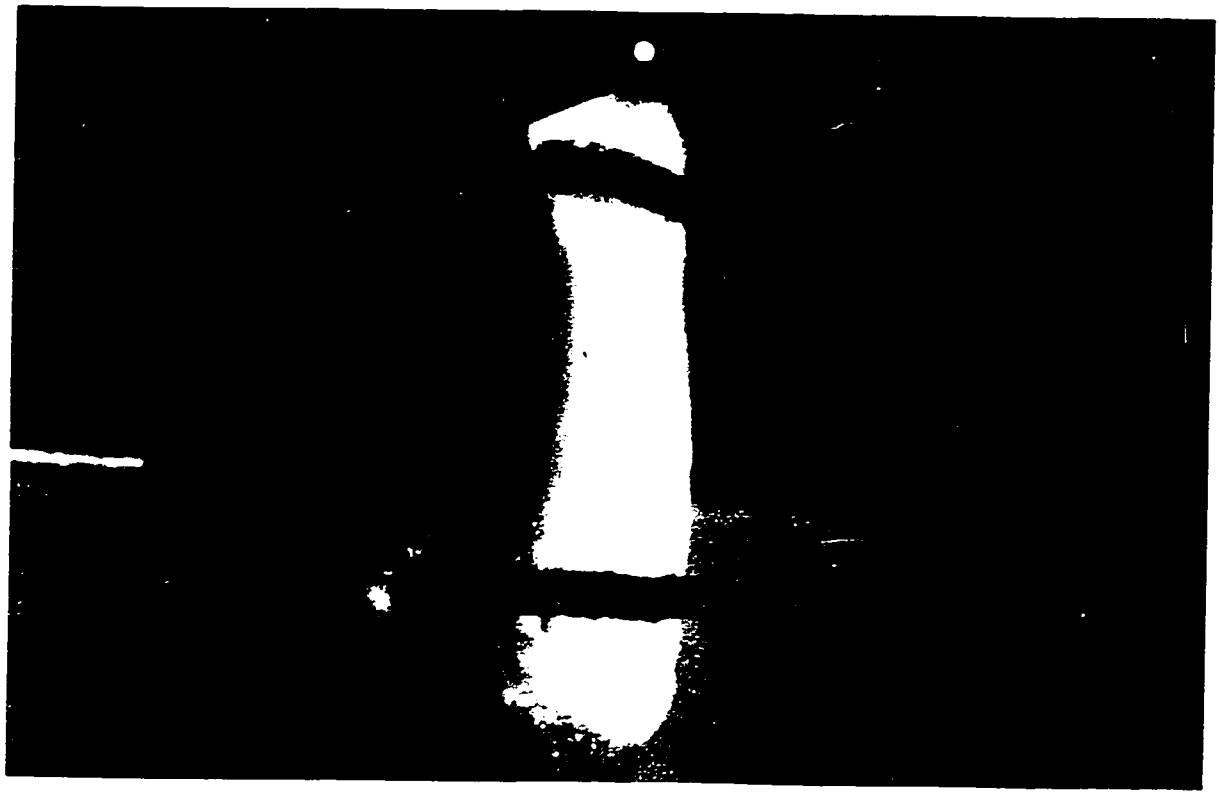

Figure 3.5: A specimen of rabbit patellar tendon clamped vertically in vice grips, awaiting cross-sectional area determination in the midsubstance. The black horizontal marker lines are used to monitor subsequent disruption of the patellar tendon.

Under general anaesthesia, a PE-90 cannula (Clay-Adams, Parsippany, NJ) was inserted retrograde into the left ventricle from the common carotid artery, and placement was confirmed by means of a ventricular pressure waveform from an on-line P23XL pressure transducer (Spectramed, Oxnard, CA)(Figure 3.6). A well-mixed suspension of 10.2 million CMs was infused over a 30 second interval, ultimately becoming trapped in the capillary beds of all tissues (Heyman et al, 1977)(Figure 3.7). Animals were euthanized with a 3ml injection of saturated KCl.

3.7 Coloured Microsphere Processing and Water Content Analyses

After CSA measurement, the PT samples were excised, weighed, desiccated over 48 hours, and dry weights recorded to evaluate water content. Percent water content in the PT samples was determined using the equation:

$$\%WaterContent = \frac{WetMass - DryMass}{WetMass} * 100$$

The kidneys and lungs were removed, quartered, and designated for high blood flow processing, as was the reference blood sample. All tissues were digested to completion in 7ml of 4M KOH at 60°C. The CMs were separated from the hydrolysate by filtration through a 10-μm polyester filter (Spectra-Mesh, Spectrum, Houston, Texas). In high blood flow tissues, CMs were counted by spectrophotometry, using absorbance values provided by the manufacturer's

A

EKG and brachial artery blood pressure readings

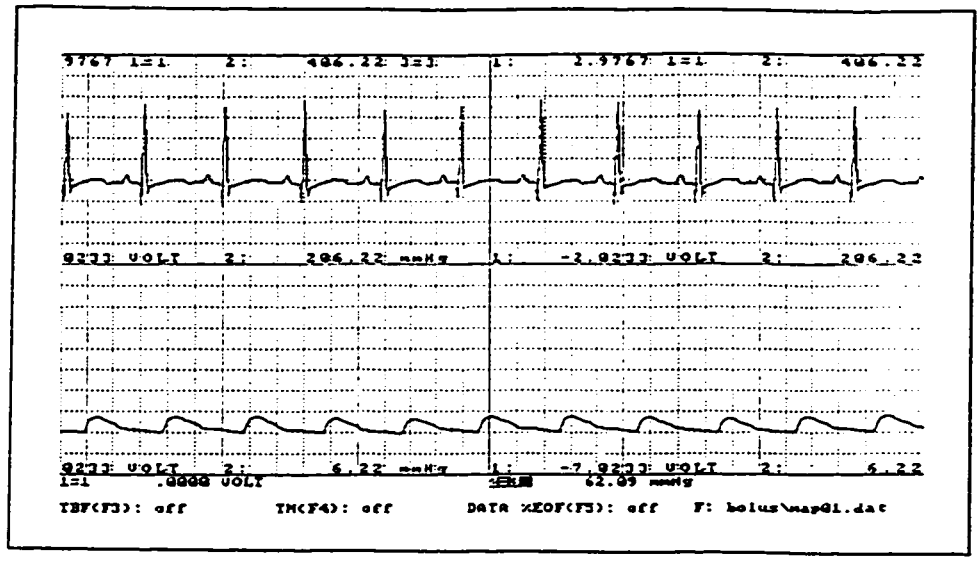

B

Entering the left ventricle of the heart from the carotid artery

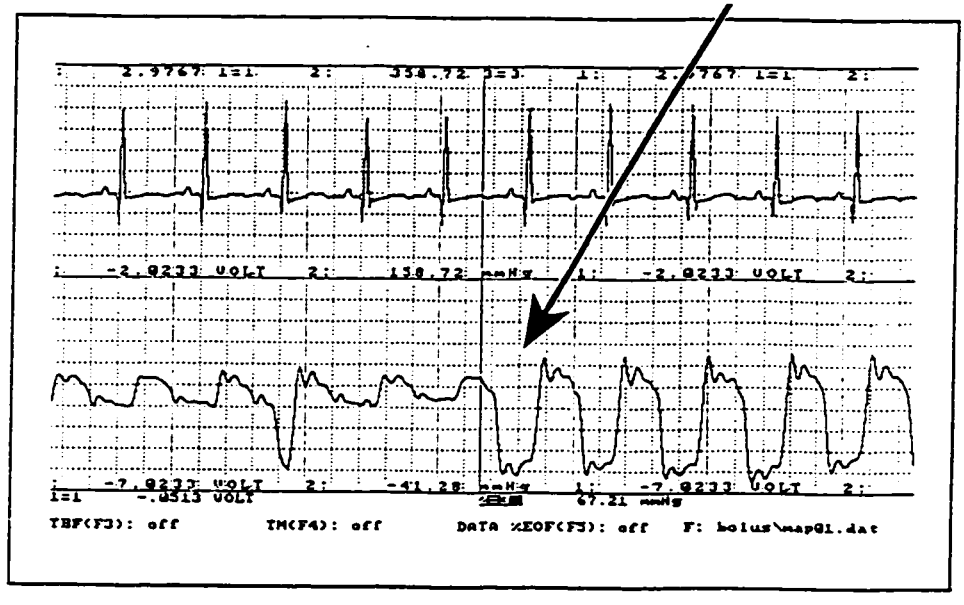

Figure 3.6a: Physiological data acquisition of Electrocardiograph (EKG) and arterial blood pressure in the anaesthetized rabbit, in preparation for microsphere infusion.
Figure 3.6b: Chart recording demonstrating the change in blood pressure waveform (blak arrow) as the infusion cannula enters the heart.

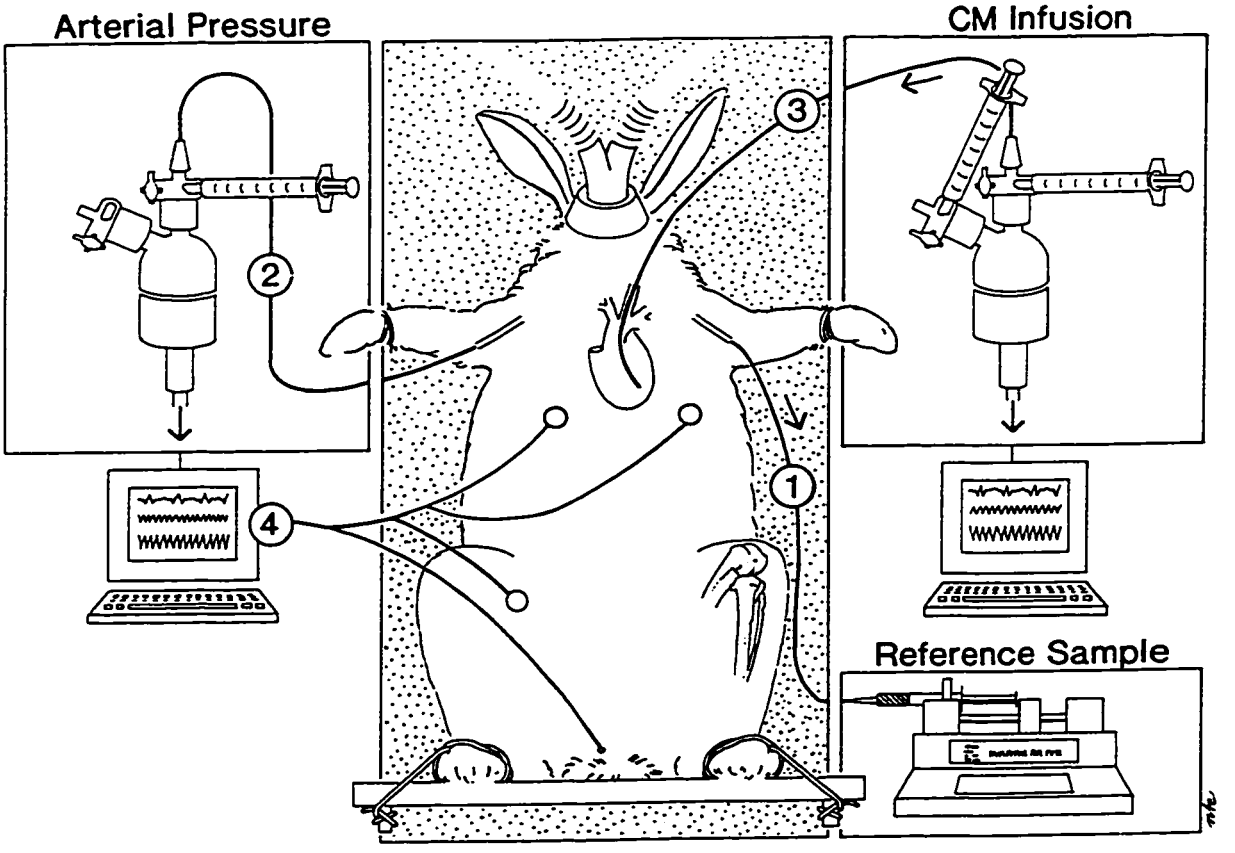

Figure 3.7: Schematic illustrating the protocol for coloured microsphere blood flow evaluation: (1) Brachial artery cannulation for withdrawal of the blood "reference" sample. (2) Transducer monitoring arterial pressure. (3) Transducer confirming placement of the infusion cannula in the left ventricle of the heart. (4) Electrocardiograph (EKG) reading.

standard curve for the particular lot number of CMs used. In low blood flow tissues, CMs were visualized directly on the filter and counted using a Nikon Diaphot-TMD inverted microscope (Nikon Corp., Japan) with epi-fluorescent illumination.

The blood flow to each tissue sample was determined using the following equation (Heyman et al, 1977):

$$Q_t = Q_r \cdot \frac{CM_t}{CM_r}$$

Where Q_t is tissue blood flow, Q_r is the reference sample withdrawal rate (3.0 ml/min), CM_t is the number of CMs in the tissue sample and CM_r is the number of CMs in the reference sample. Standardized blood flow values are reported as *ml/min/100 grams tissue*.

3.8 Vascular Volume Determination

Vascular volume was quantitated in the 3 remaining animals from each experimental group (Figure 3.2) using a standard method (Colville-Nash et al, 1995). Briefly, animals were anaesthetized, and both femoral arteries cannulated and flushed as described above. Animals were sacrificed by lethal injection, and a prewarmed solution of 5% Carmine Red/10% gelatin in water was infused as described above (Figure 3.8). The carcass was chilled for 2 hours at 4°C, and

Figure 3.8a: Anterior view of the rabbit patellar tendon following Gelatin-Carmine Red infusion used to quantify vascular volume. Figure 3.8b: View of the reflected patellar tendon demonstrating the posterior surface of the patella.

both PTs dissected. A central 6mm square of PT midsubstance was resected from the surrounding PT in order to evaluate changes in PT midsubstance vascular volume (Figure 3.9). The resection was standardized using the marker sutures from surgery as reference points. Central PT squares and the remaining PT outer portion were dried for 48 hours, weighed, and enzymatically digested to completion in 0.9ml of buffered papain digestion solution (2mM dithiothreitol, 20mM disodium hydrogen orthophosphate, 1mM EDTA, 12U/ml papain) for 24 hours at 56°C. The Carmine Red dye was eluted by adding 0.1ml of 5M NaOH, and separated using centrifugation (8,000g relative centrifugal force for 3 mins) followed by filtration of the supernatant through a 0.22μm nitrocellulose filter. The dye filtrate was assayed spectrophotometrically for Carmine Red absorbance at 490nm, and dye content was determined by comparison with standard curves. The results were expressed as a Vascular Index (V.I.) of μg dye / mg dry weight of tissue.

3.9 Statistical Analyses

All quantitative values were initially analysed with descriptive statistics. Subsequently, Analysis of Variance (ANOVA test, Statistical Package for the Social Sciences, SPSS) was used to detect "global" significant quantitative differences between experimental and control groups. A 'post-hoc' multiple comparisons test (Tukey's test, SPSS) was used to detect the location of significant differences. A significance level of $p<0.05$ was used for all statistical tests.

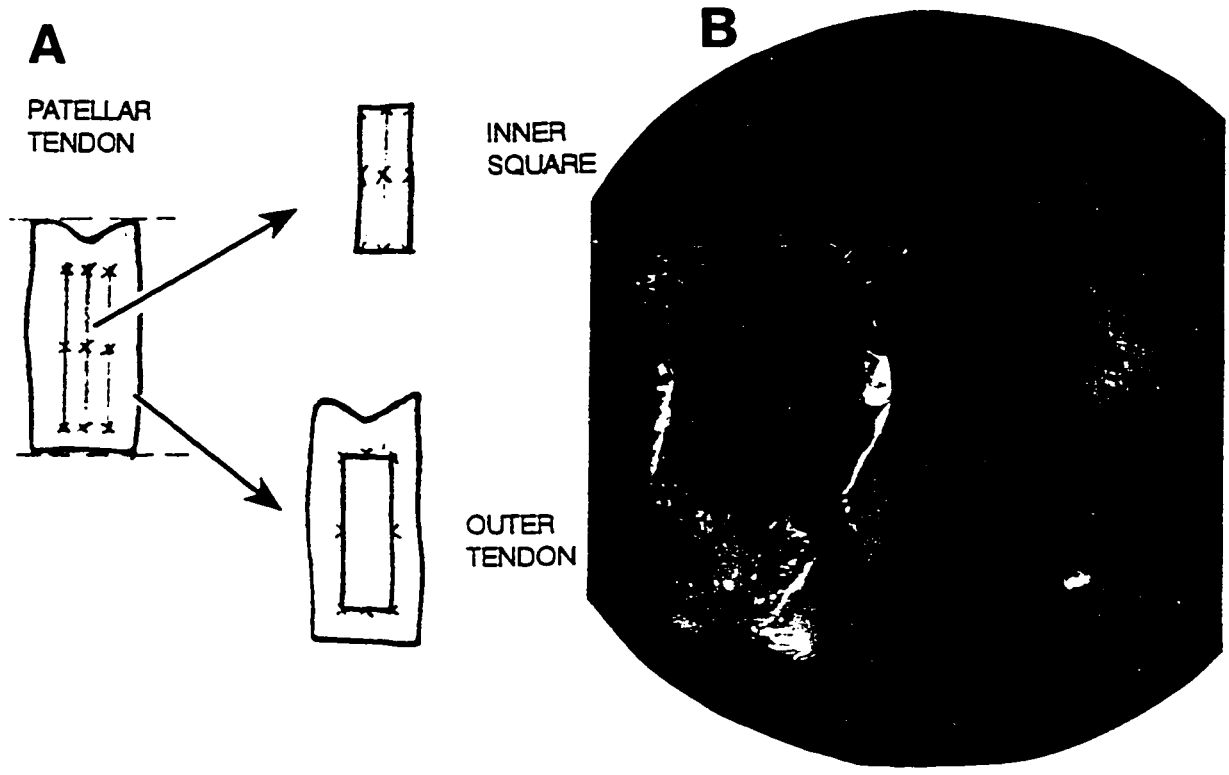

Figure 3.9a: Schematic illustrating the removal of a central square of patellar tendon midsubstance, as demarcated by the marker sutures placed at the time of surgery. Figure 3.9b: Both inner and outer pieces of tissue were subsequently processed to quantify vascular volume by measuring the Carmine Red dye content.

CHAPTER 4

RESULTS

4.1 Morphological Evaluations

Ink-injected normal control PT demonstrated an organized network of fine blood vessels overlying the entire surface, and parts of the posterior surface. Vessels were often seen oriented in a parallel fashion (Figure 4.1a). In contrast, longitudinally incised PT demonstrated greater numbers and larger diameter of blood vessels, with marked disruption of normal vascular organization (Figures 4.1b, 4.1c, 4.1d).

Microscopically, vessels in the controls were organized obliquely, entering from the epitenon towards the tendon proper. Smaller vessels were seen organized longitudinally deep in the tendon, oriented parallel with collagen fibers (Figure 4.2a). The incised tendon, examined 3 days post-surgery, demonstrated large numbers of dilated, engorged blood vessels entering the tendon proper (Figure 4.2b). Angiogenesis was evident morphologically as fingerlike cords of dividing and migrating endothelial cells, especially in the H&E stained sections (Figure 4.3, 4.4). The presence of mast cells was noted in proximity to the leading edge of the angiogenic buds. Co-localization of blood vessels was noted in those specimens stained immunohistochemically, providing a powerful differential analysis of vessels not patently filled with ink-gelatin but staining positively for thrombomodulin (Figures 4.5 - 4.8).

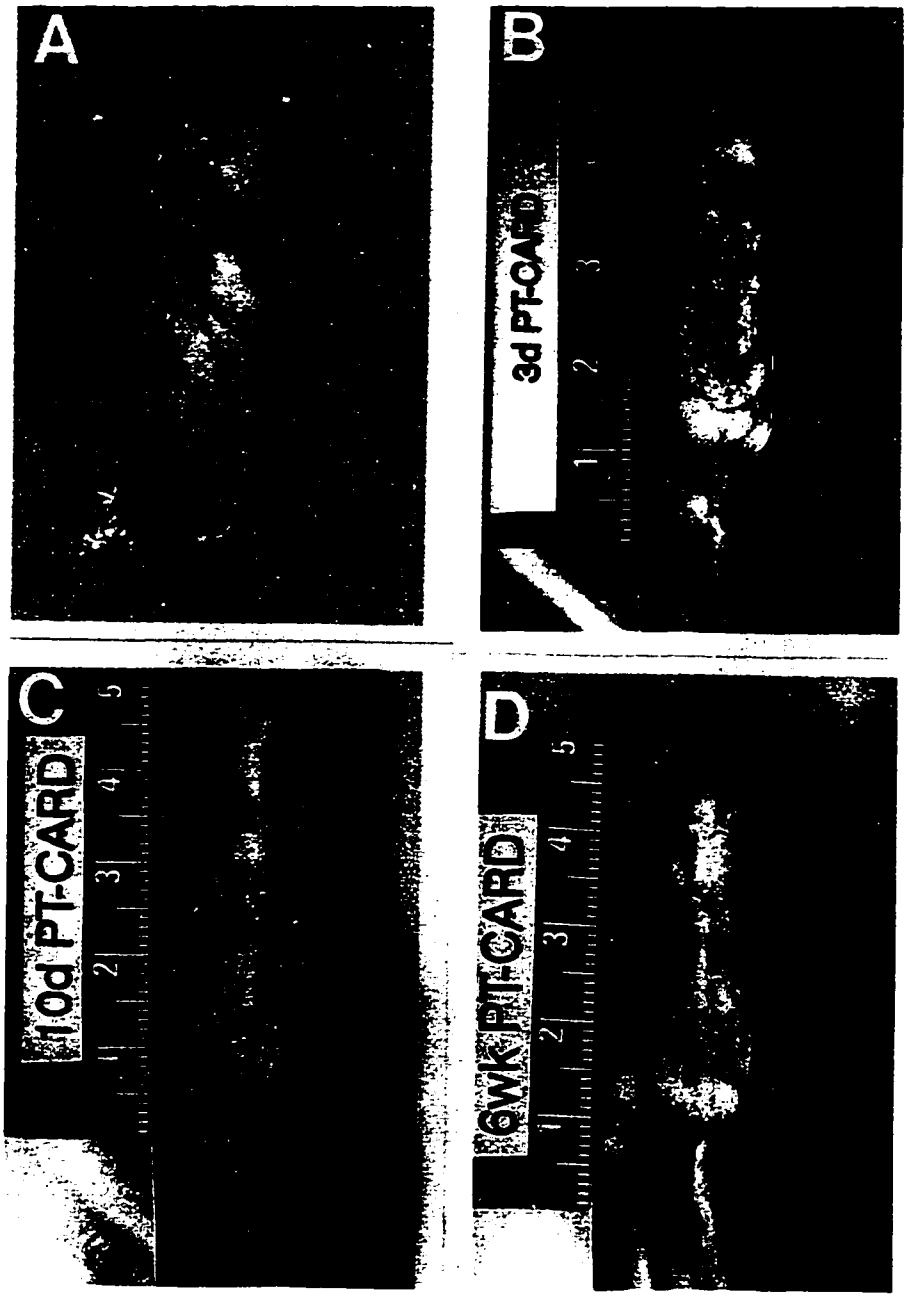

Figure 4.1: Macroscopic photographs of gelatin-ink injected blood vessels in control (A), & longitudinally incised patellar tendon at the indicated intervals (B - D). Rule graduations are in centimetres.

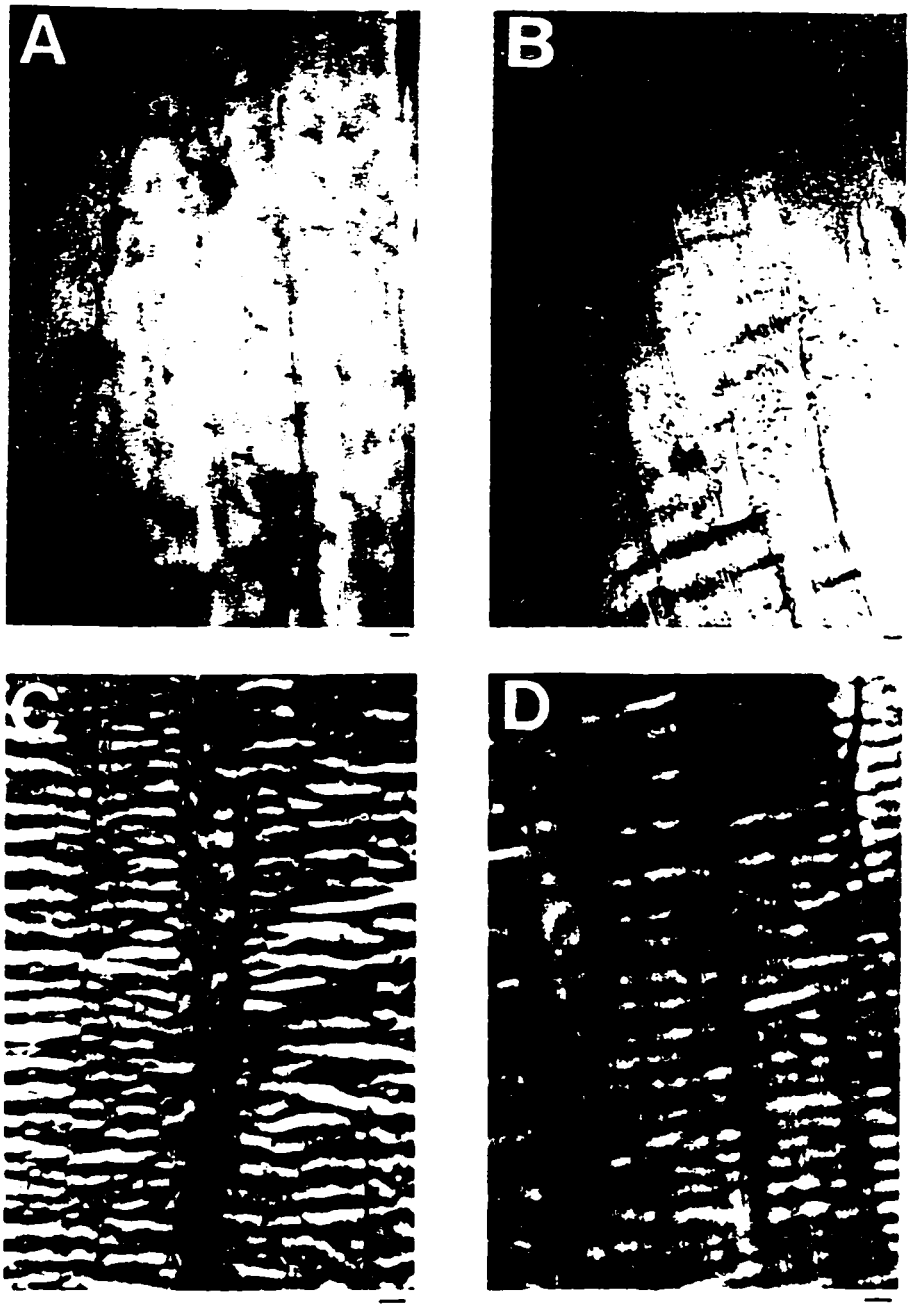

Figure 4.2: Photomicrographs of gelatin-ink injected blood vessels in control (A), and healing patellar tendon 3 days (B), 10 days (C), and 42 days (6 weeks) (D) following longitudinal incision. Section Thickness = 20μm. Bar markers = 50 μm.

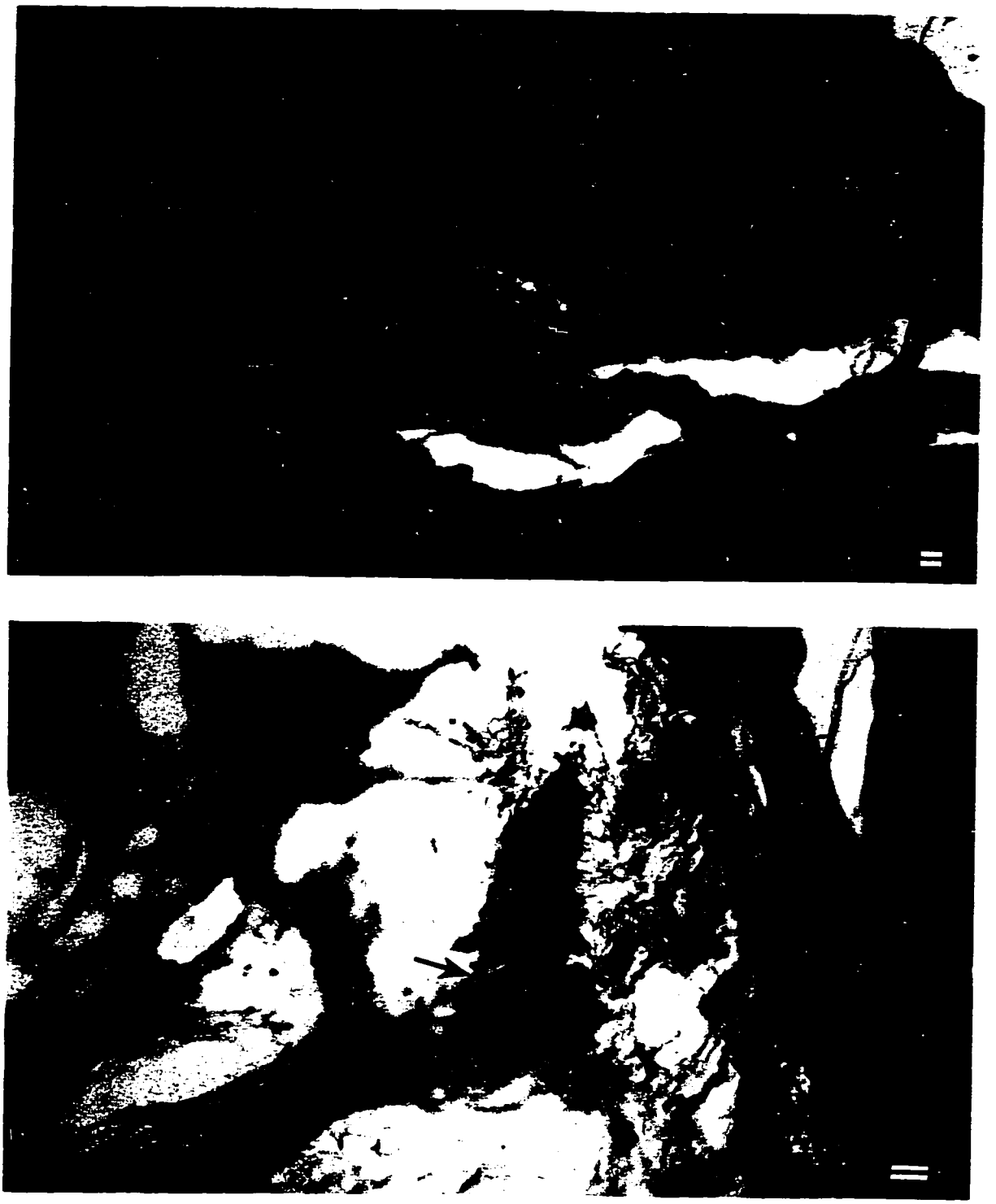

Figure 4.3: Cryomicrotome prepared sections of patellar tendon 3 days following surgical incision. The sections have been stained using Haematoxylin and Eosin, demonstrating cords of migrating endothelial cells (black arrows).
Section Thickness = 20 μm. Bar Marker = 50 μm.

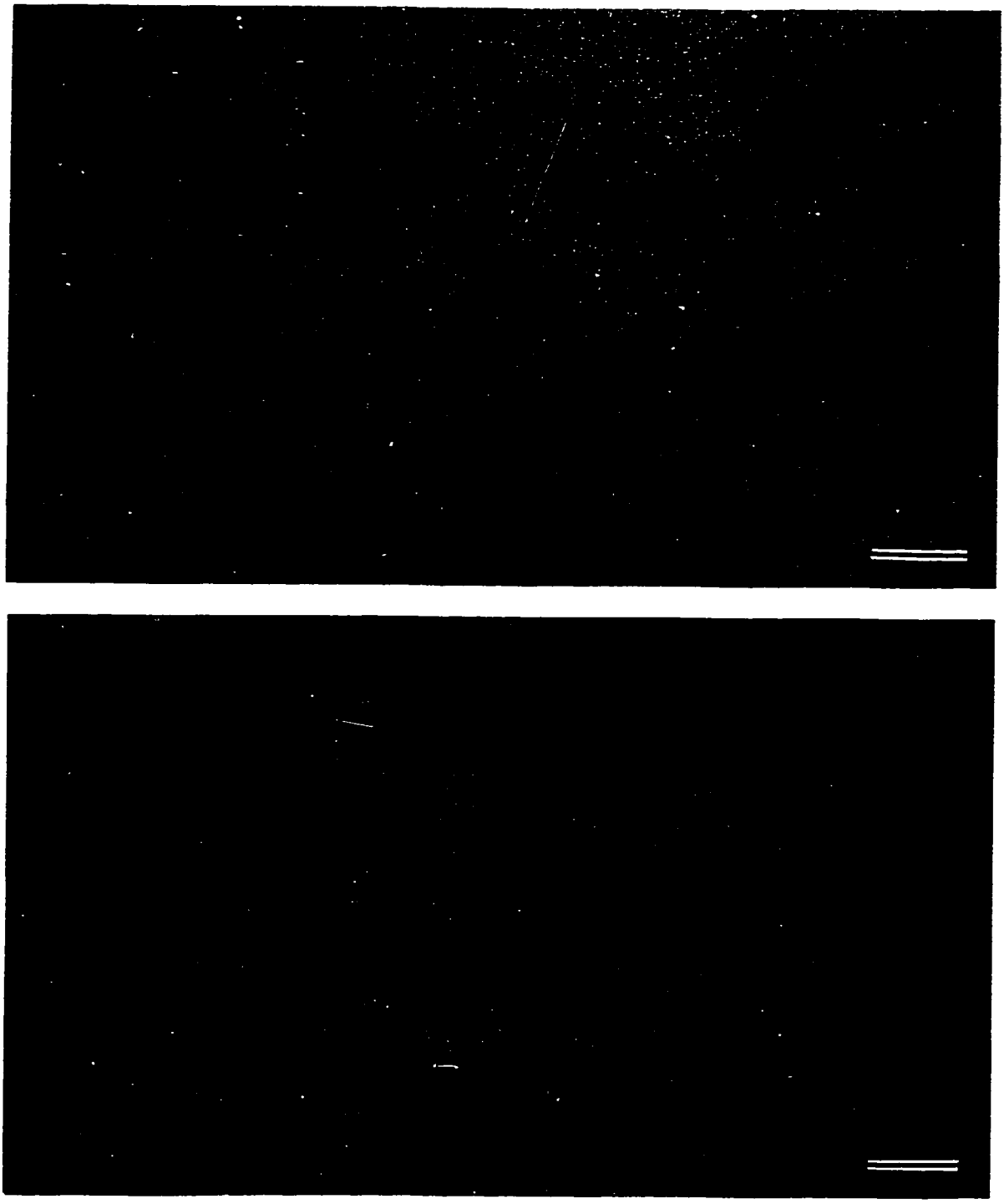

Figure 4.4: Histological photomicrographs of migrating endothelial buds in patellar tendon 3 days following surgical incision. The sections have been stained using the Alcian blue-safranin method to highlight mast cells (black arrows), which promote angiogenesis through the action of heparin and other secreted factors (Whalen & Zetter, 1992). Section Thickness = 20 μm. Bar Marker = 50 μm.

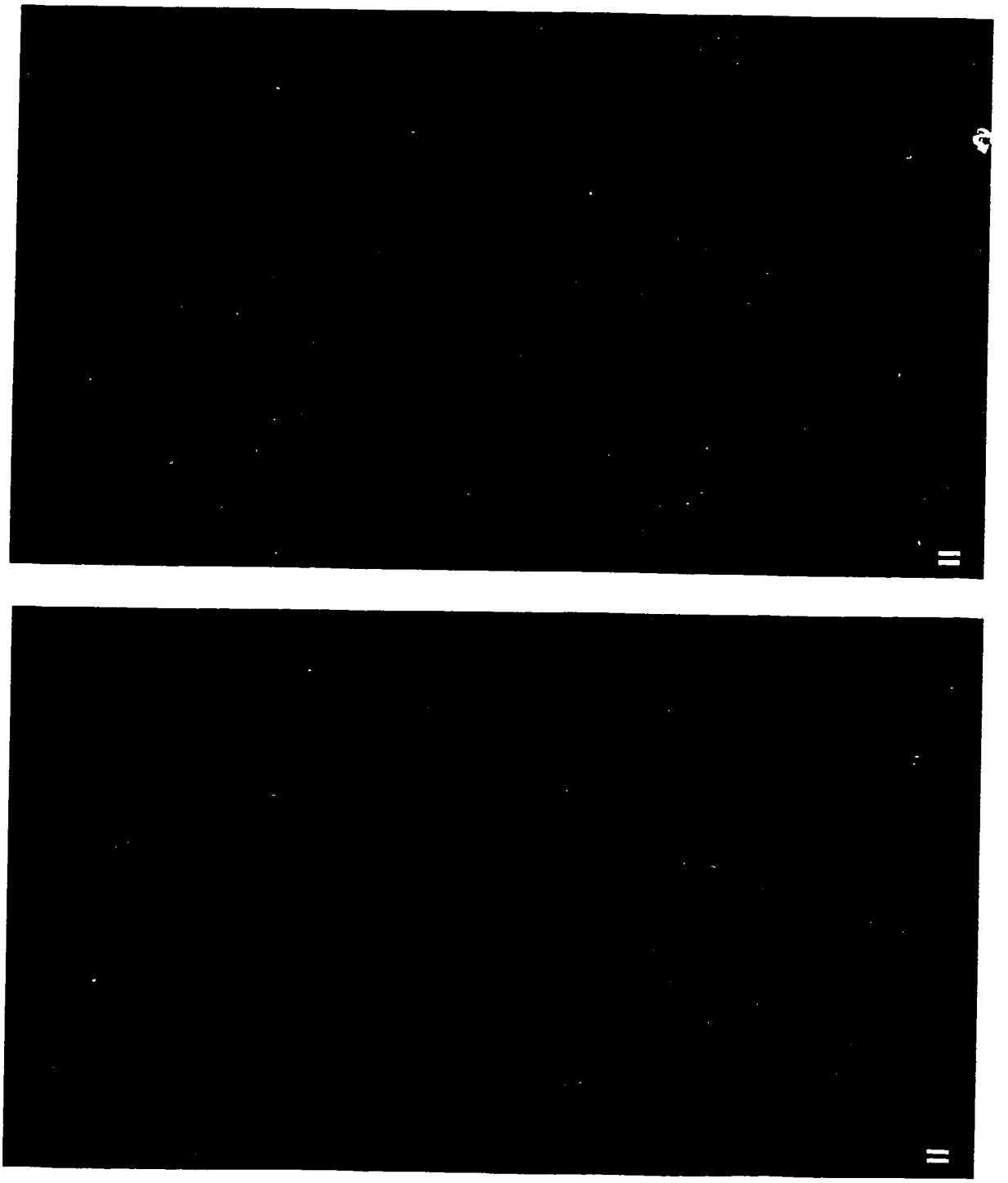

Figure 4.5a: Histological photomicrograph of gelatin-ink injected blood vessels in normal rabbit patellar tendon. Figure 4.5b: The same section co-localized with anti-thrombomodulin immunohistochemistry, demonstrating blood vessels not detected through gelatin-ink injection. Bar Marker = 50 μm.

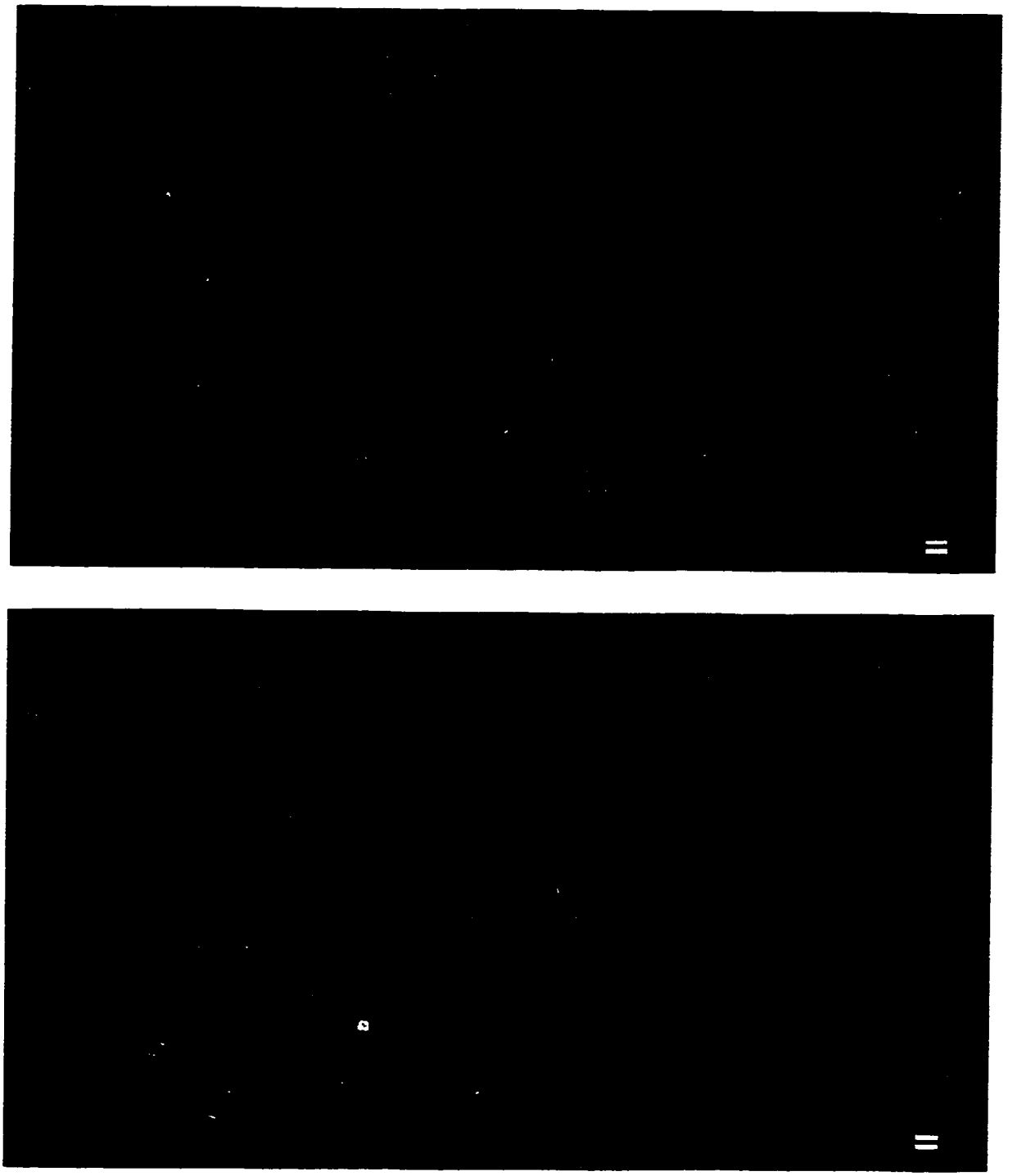

Figure 4.6a: Histological photomicrograph of gelatin-ink injected blood vessels in normal rabbit patellar tendon. Figure 4.6b: The same section co-localized with anti-thrombomodulin immunohistochemistry, demonstrating blood vessels not detected through gelatin-ink injection. Bar Marker = 50 μm.

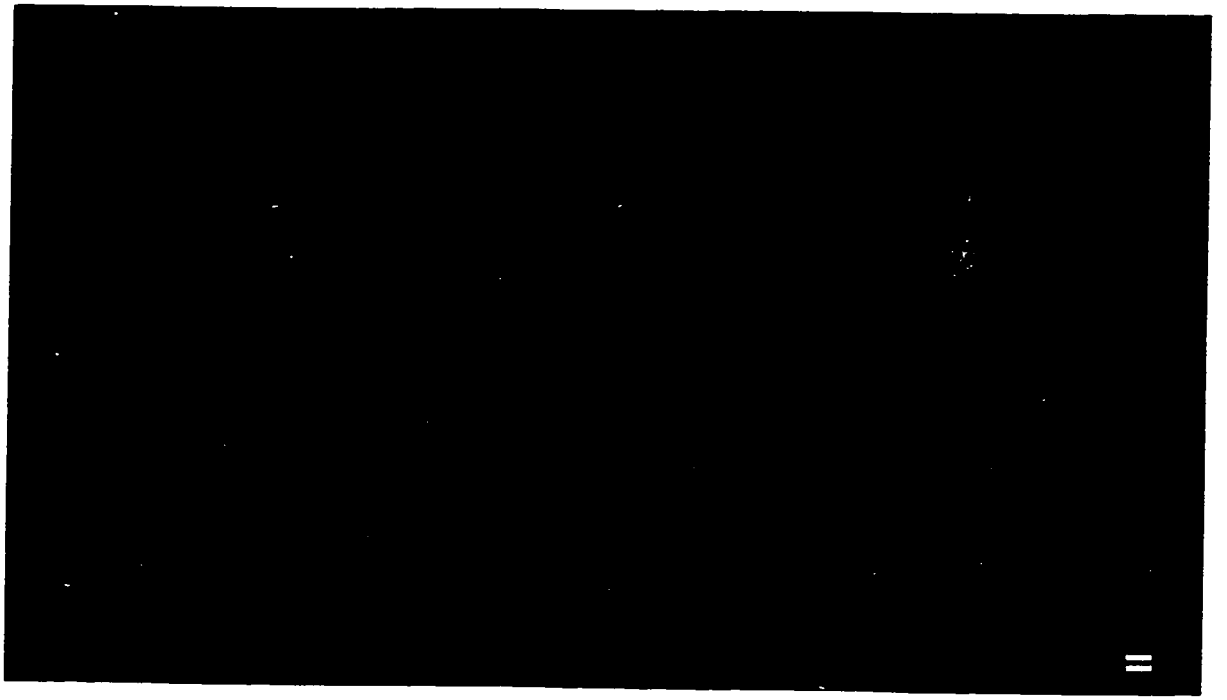

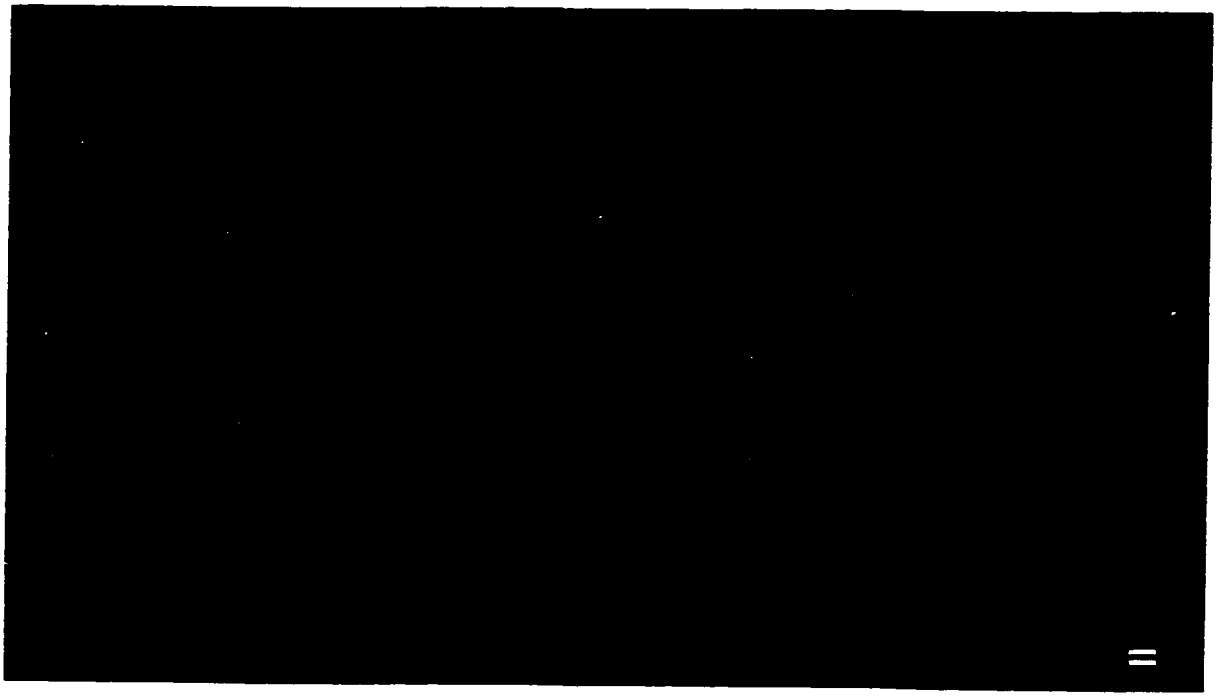

Figure 4.7a: Histological photomicrograph of gelatin-ink injected blood vessels in normal rabbit patellar tendon. Figure 4.7b: The same section co-localized with anti-thrombomodulin immunohistochemistry, demonstrating blood vessels not detected through gelatin-ink injection. Bar Marker = 50 μm.

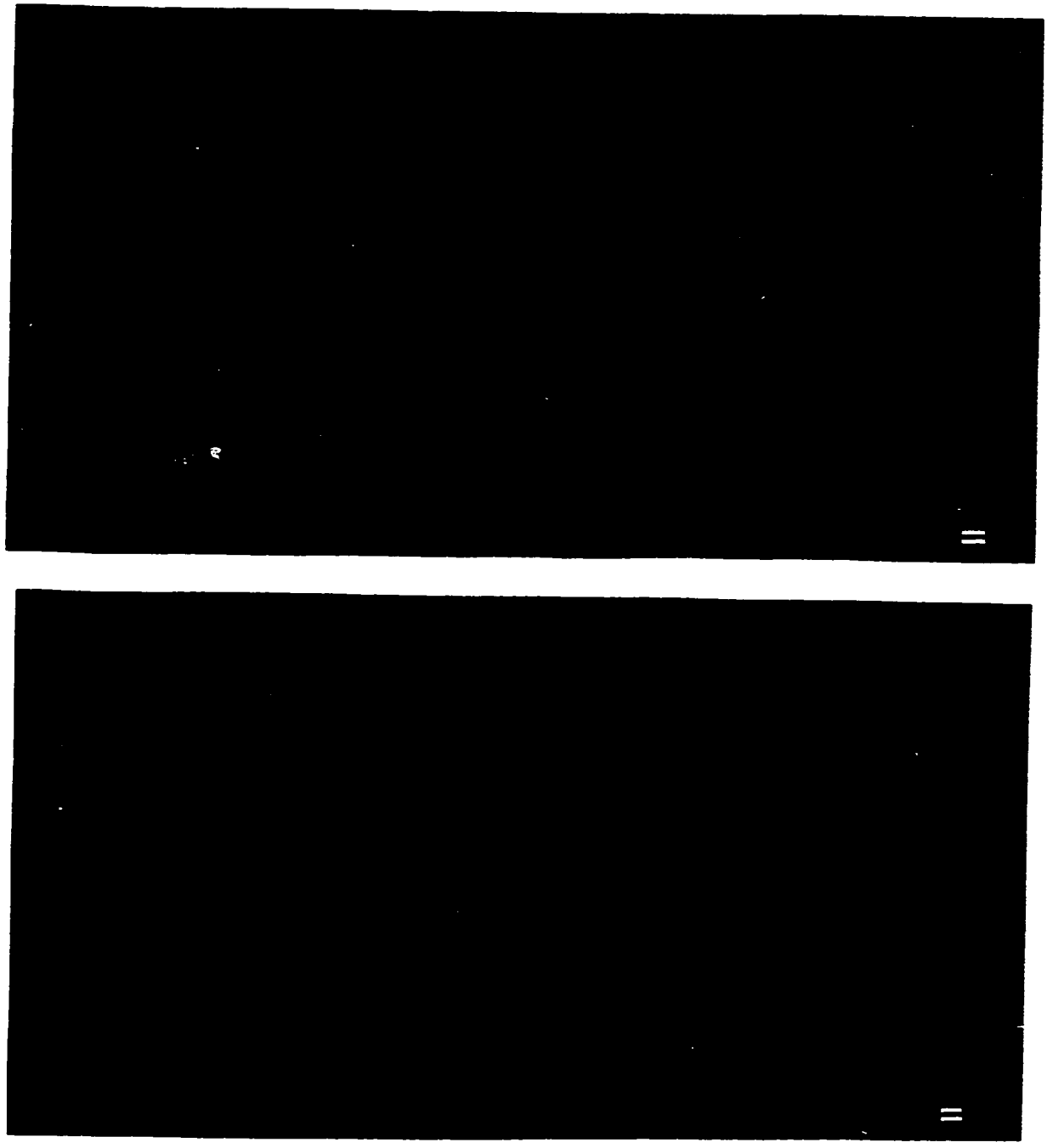

Figure 4.8a: Histological photomicrograph of gelatin-ink injected blood vessels in normal rabbit patellar tendon. Figure 4.8b: The same section stained with anti-thrombomodulin immunohistochemistry, demonstrating blood vessels (black arrows) not detected through gelatin-ink injection. Bar Marker = 50 μm.

By 10 days the tendon incisions were clearly neovaszcularized with longitudinally arranged, thin vessels which were now patently filling with ink. Polarized light revealed the collagen crimp organization, and demonstrated that matrix lateral registry was divided and separated due to the surgical incisions (Figure 4.2c).

At 42 days (6 weeks), the deep tendon and incised locations both remained occupied with an abundant number of branching, longitudinally oriented blood vessels. The incisions had been remodelled with more randomly dispersed collagen bundles (and numerous fibroblasts) which surrounded the blood vessels (Figure 4.2d). The inclusion of other elements, such as fat cells and less densely collagenized regions, was occasionally observed in conjunction with the incised locations (Figure 4.9).

4.2 QUANTITATIVE EVALUATIONS

4.2.1 Blood Flow

Following longitudinal incision, the PT demonstrated a statistically significant elevation in blood flow compared to both time-zero and contralateral controls. Three days following longitudinal incision, PT standardized blood flow was measured to be 13.23 $\pm$ 4.89 (Mean $\pm$ Standard Error of Mean) ml/min/100g, approximately 30-fold greater than time-zero control and contralateral PT values of 0.36 $\pm$ 0.15 ml/min/100g ($p<0.001$) and 0.43 $\pm$ 0.18 ml/min/100

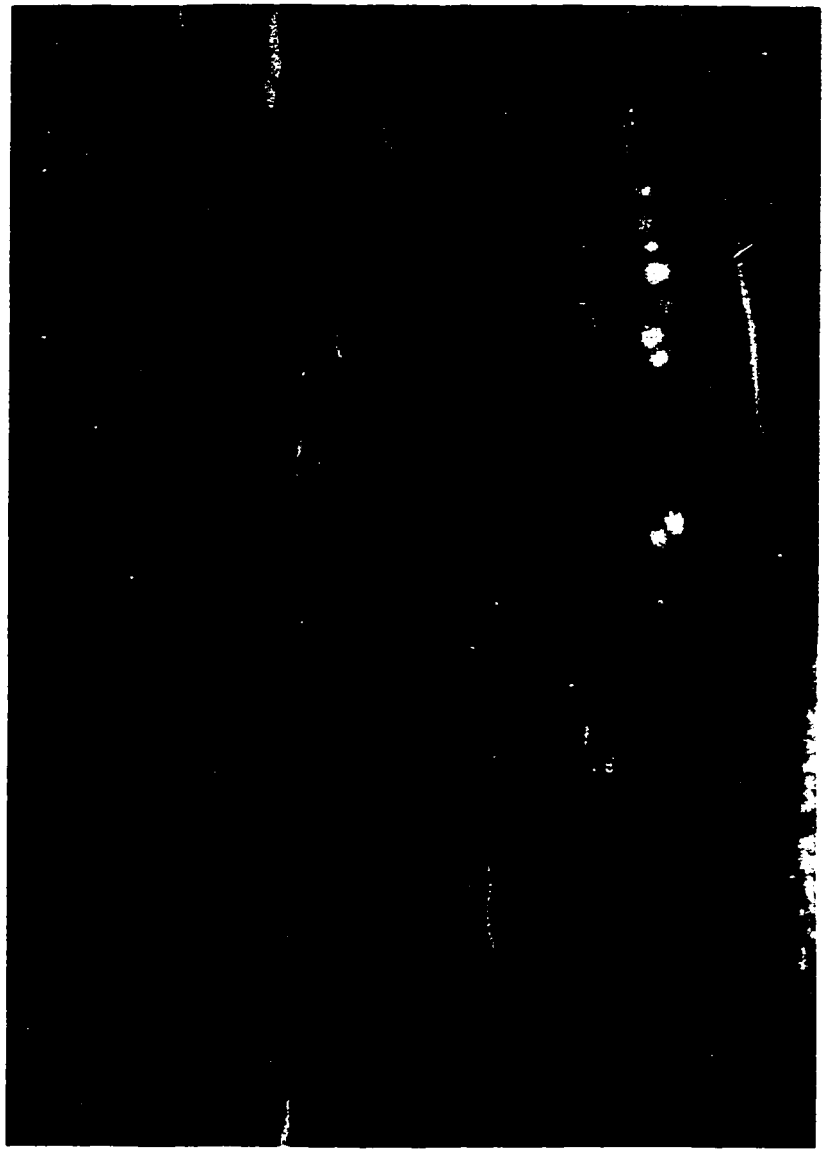

Figure 4.9: Haematoxylin and Eosin stained section of patellar tendon 42 days following surgical incision. The inclusion of a fatty defect (black arrow) at the location of an incised slit is evident.

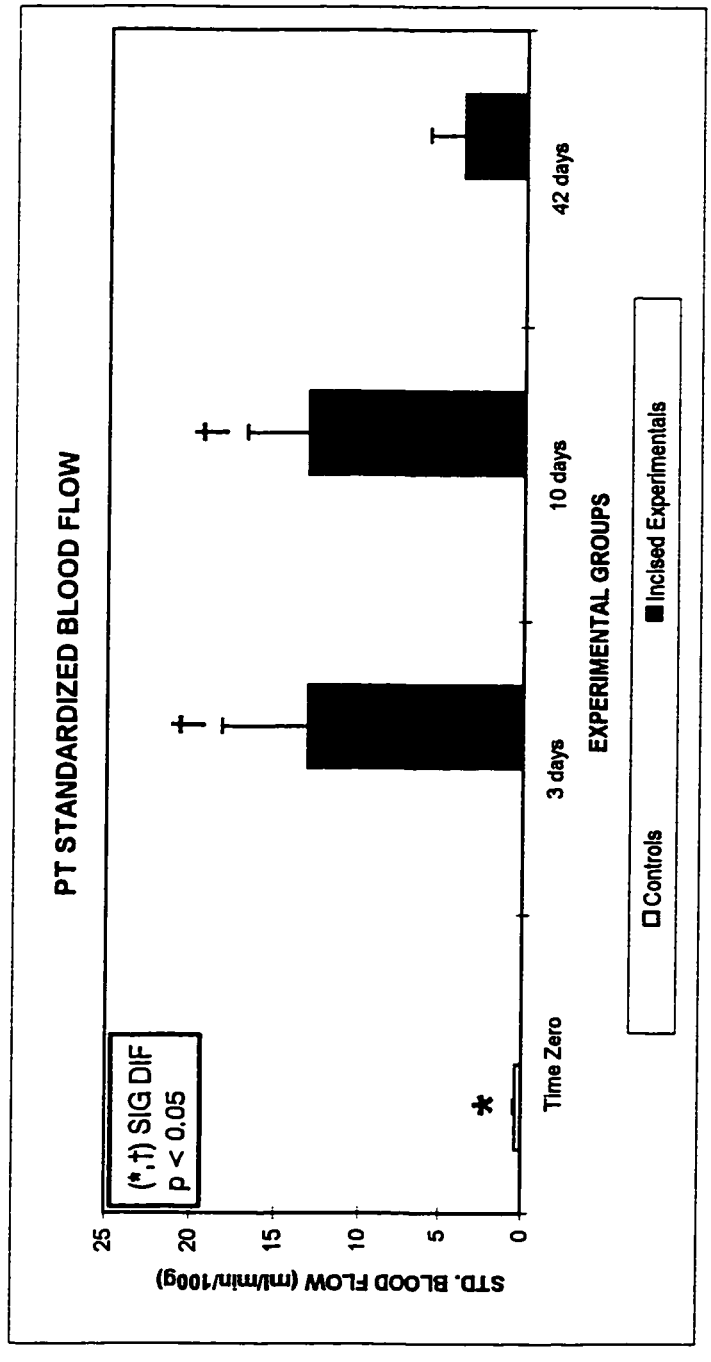

Figure 4.10: Standardized blood flow in control and incised experimental patellar tendon. Values represent the Mean ± Standard Error of Mean. The significances noted are between Time Zero Controls and Incised Experimentals across groups.

grams ($p<0.001$) respectively (Figure 4.10). Ten days following surgery, PT blood flow of 13.26 $\pm$ 3.54 ml/min/100g remained significantly elevated, still being 30-fold greater than that of time-zero controls ($p<0.001$) and 13-times that of the contralateral PT (1.11 $\pm$ 0.44 ml/min/100g; $p<0.01$). However by 42 days, PT blood flow had returned to 3.77 $\pm$ 2.09 ml/min/100g, and was not significantly different to time-zero controls ($p>0.05$) or contralaterals (0.63 $\pm$ 0.20 ml/min/100g; $p>0.05$).

4.2.2 Water Content analyses

The wet mass of the incised PT increased and subsequently diminished over 42 days (Figure 4.11). Similarly, the dry mass of the incised PT increased and subsequently diminished over 42 days (Figure 4.12). However, no significant differences in either parameter were detected, compared to time-zero and contralateral controls. Similarly, the water content for the incised PT did not differ significantly from time-zero controls, and all PT samples maintained an average water content, ranging between 62% to 63.2% water.

4.2.3 Vascular Volume Analyses (Vascular index)

Following longitudinal incision, PT vascular volume significantly increased and subsequently diminished over 42 days (Figure 4.13). At 3 days the incised PT carmine red content increased significantly, providing a vascular index (V.I.) of 2.74 $\pm$ 0.74 μg/mg, compared to time-zero control and contralateral V.I.s of 0.12 $\pm$ 0.10

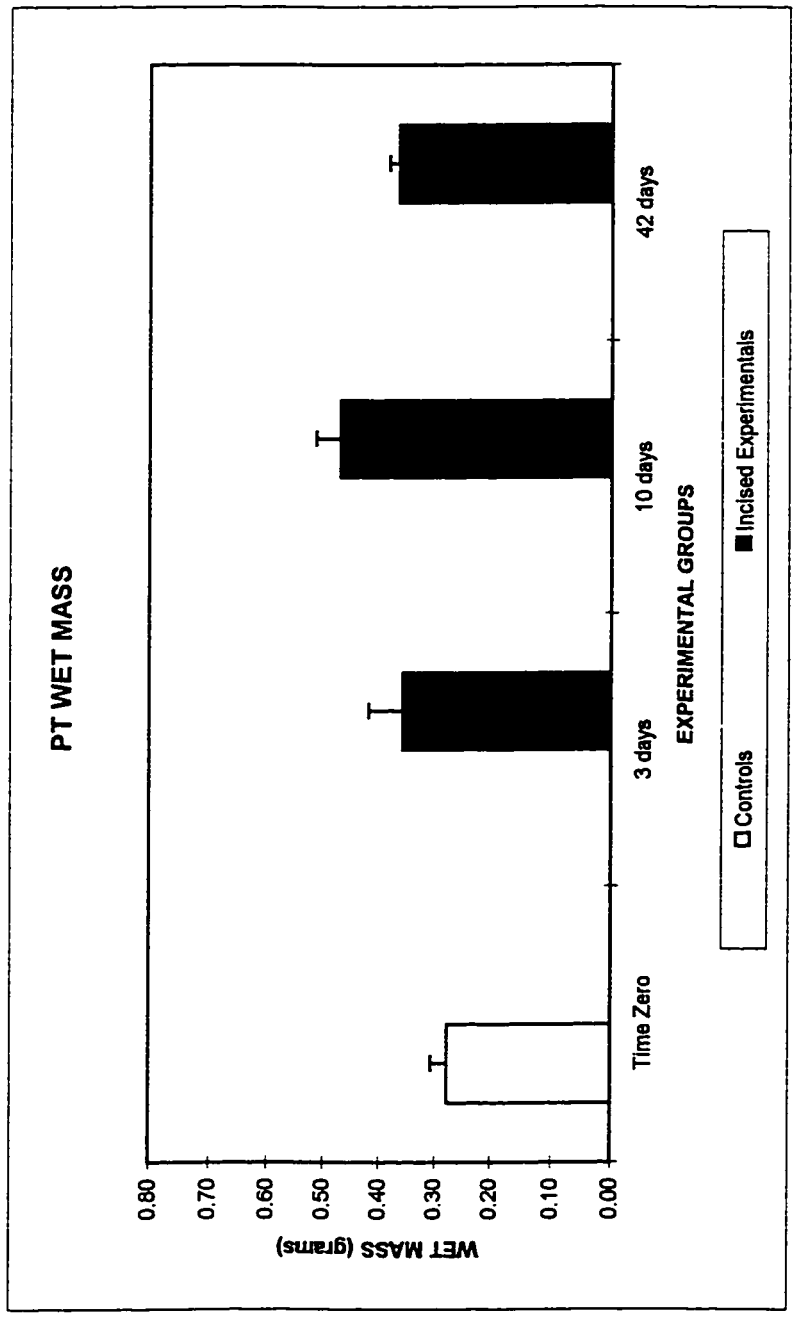

Figure 4.11: Wet mass in control and incised experimental patellar tendon. Values represent the Mean ± Standard Error of Mean.

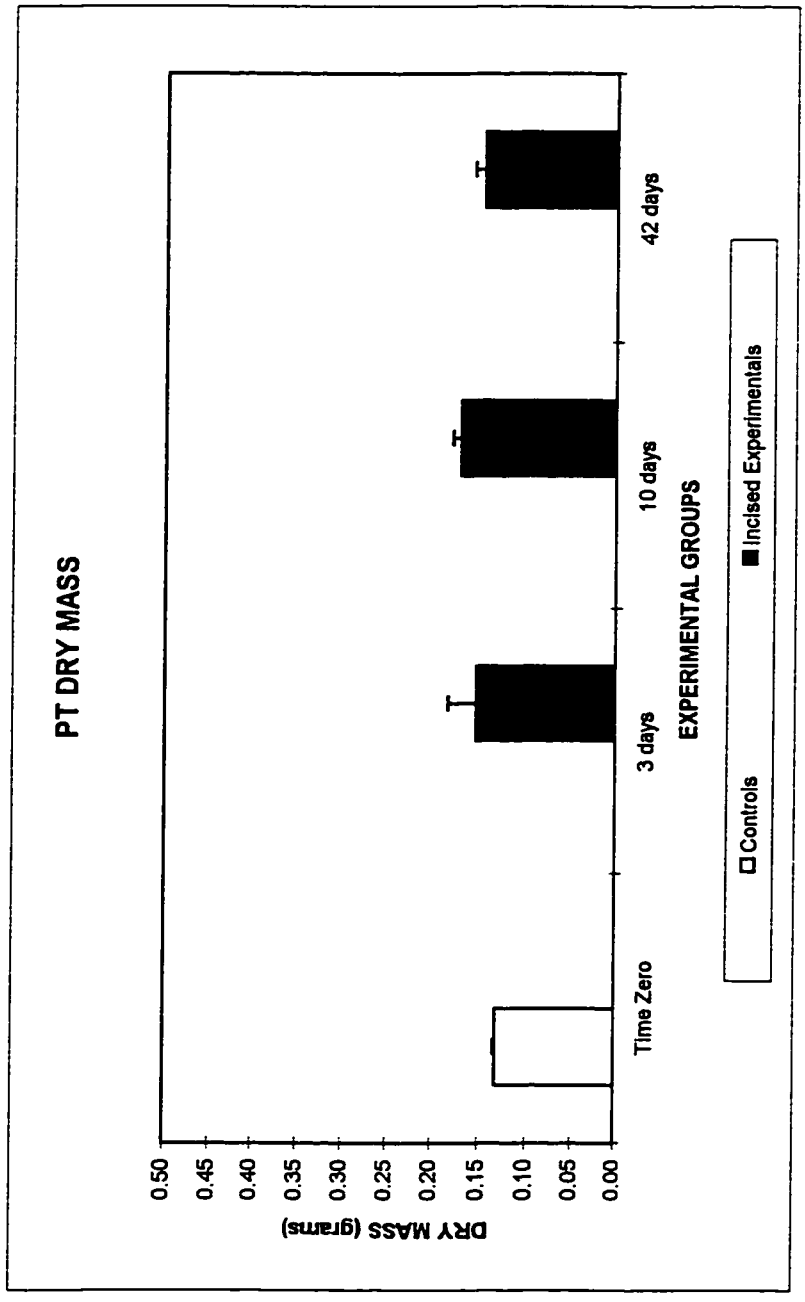

Figure 4.12: Dry mass in control and incised experimental patellar tendon. Values represent the Mean ± Standard Error of Mean.

μg/mg ($p<0.001$) and 0.77 $\pm$ 0.18 μg/mg ($p<0.05$) respectively. By 10 days the incised PT vascular volume (2.37 $\pm$ 0.50 μg/mg) remained significantly elevated compared to time-zero controls ($p<0.01$). However by 42 days PT vascular volume had fallen, with its V.I. of 0.91 $\pm$ 0.50 μg/mg not significantly different from time-zero controls. Of importance, however, was the differential results obtained when analyzing the vascular volume in the central square of PT midsubstance. The PT midsubstance achieved significantly elevated vascular volume only at the 10 day interval with a V.I. of 0.42 $\pm$ 0.18 μg/mg, compared to time-zero and contralateral control values of 0.04 $\pm$ 0.01 μg/mg ($p<0.05$) and 0.07 $\pm$ 0.18 μg/mg ($p<0.05$) respectively (Figure 4.13).

4.2.4 Cross-sectional Area Measurements

There was a rapid and significant increase in PT cross-sectional area (CSA) measured following injury. After longitudinal incision, PT CSA increased significantly, to 15.01 $\pm$ 0.42 mm^2 at 3 days ($p<0.001$) and 15.80 $\pm$ 0.75 mm^2 at 10 days ($p<0.001$) compared with time-zero controls (11.45 $\pm$ 0.45 mm^2) and respective contralateral controls for both intervals. For both 3 and 10 days, this was a 1.3-fold increase over the time-zero control value. At 42 days, CSA for the PT in the longitudinally incised knee was still significantly elevated, with a value of 14.66 $\pm$ 1.31mm^2 compared to contralateral controls (10.72 $\pm$ 0.43 mm^2; $p<0.05$).

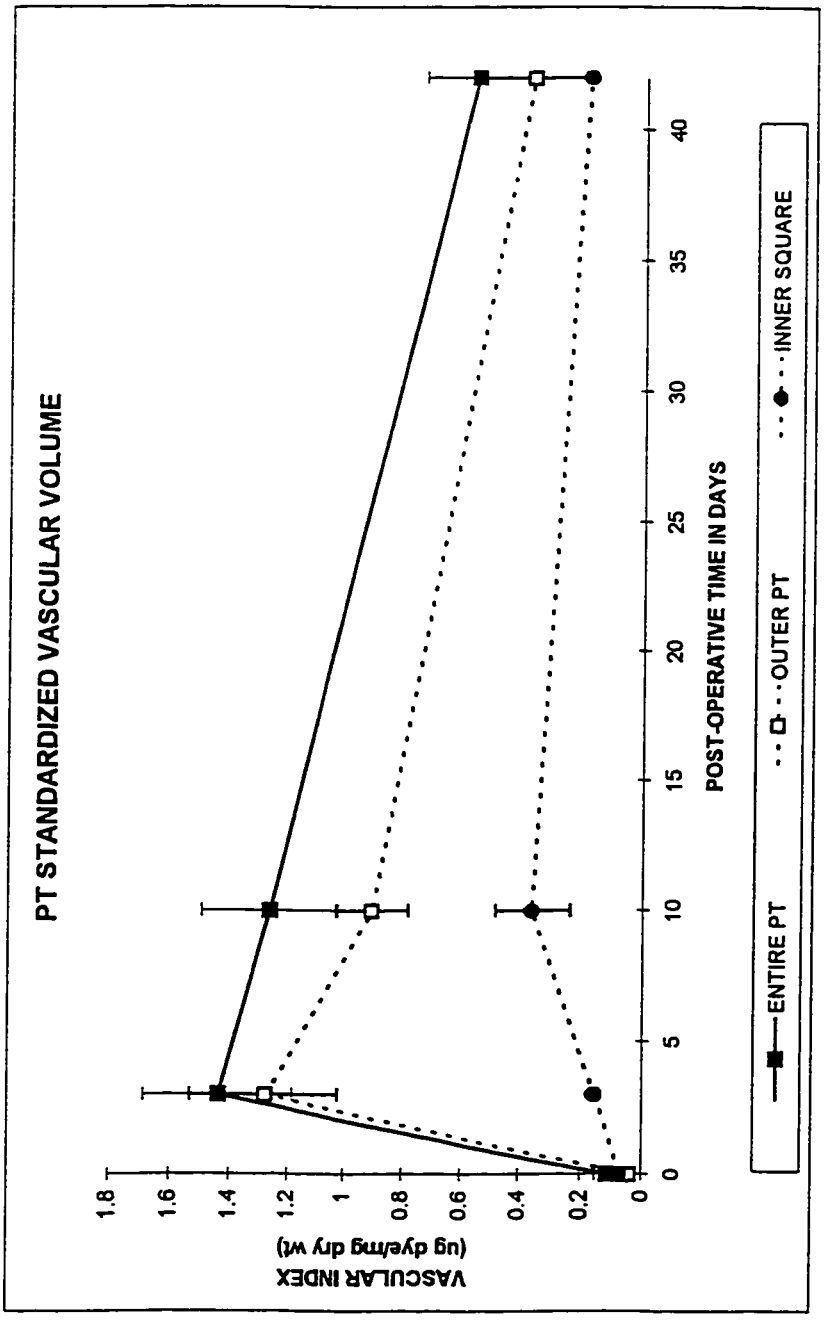

Figure 4.13: The vascular volume for the entire patellar tendon (solid line) sampled at time-zero, 3 days, 10 days, and 42 days post-operatively. The individual components of this vascular volume which supply the outer portions and inner square of patellar tendon substance (as described in Figure 3.9) are represented in the central dotted lines. Values represent the Mean ± Standard Error of Mean.

CHAPTER 5

DISCUSSION

This investigation clearly demonstrates an increase in blood supply to the PT following surgical incision. Quantitative changes in PT blood flow and microvascular volume correspond well with morphological assessments, which demonstrated dilated peripheral vessels and a profuse recruitment of pre-existing blood vessels at 3 days following open incision. Angiogenic buds, observed in proximity to incised locations, were seen to be patently filling with injected dye by the 10 day interval. These morphological findings agree with the quantitative assessments of vascular volume which demonstrated a significant increase in the central square of PT 10 days following longitudinal incision. By the 42 day interval, however, both vascular volume and blood flow of the PT had declined, implying significant/dynamic vascular remodelling (and perhaps the return of normal vasomotor control) occurs after this procedure.

Of potential significance are the data illustrated in Figure 4.13, where the central portion of the PT has a later peak and lower absolute elevation of vascular volume compared to the outer PT. This is possibly related to previous results which have indicated that epiligamentous connective tissues are more vascularized / unit area than deeper ligamentous tissue (Bray, Butterwick et al, 1996; Choudhury and Matyas, 1990). Since outer PT samples likely contained a greater relative proportion of total epitendinous tissue than the central sample, the explanation for

elevated vascular volume in the outer PT might be on that basis. Even more functionally significant is that the peak increase in epitendinous vascular volume preceeds the peak in central PT vascular volume, suggesting sequential steps in the vascular response to injury - first in peritendinous tissues and then into central PT - at the site of the original injury stimulus. This possibility is supported in the histological observations in Figure 4.1, where at 3 days the peritendinous tissue exhibits a striking vasodilation compared to the normal and 10 day intervals.

Although previous investigators have observed changes in vessel number in surgically ruptured and injured tendinous connective tissues, no quantitative measures were undertaken and no studies concerned the PT. Microangiographic and histological studies of the superficial digital flexor tendons of dogs and horses have previously demonstrated a rapid ingrowth of blood vessels into tendon during the early phase (3 days to 17 days) of repair (Gelberman et al, 1991; Stromberg et al, 1974). These morphological evaluations of transected and of "split" (ie. longitudinally incised) tendon suggested increased vascular volume which persists in the short-term (ie. prior to 4 weeks of healing), but declines during the later phases of wound repair (Amadio, 1992; Stromberg et al, 1974). Similarly, increases in blood flow during ligament healing has previously been shown in our laboratory, and confirms that a rapid vascular response (and associated inflammation) follows acute injury of these tissues (Bray, Butterwick et al, 1996).

Studies of PT healing are of particular clinical relevance, as they are commonly predisposed to developing tendinitis, with a poor prognosis for rapid or

effective recovery. Due to the relatively sparse vascular content of the PT, when compared to other connective tissues such as skin and bone, it has often been hypothesized that the poor intrinsic healing of the injured PT is a function of an inadequate blood supply (Torstensen et al, 1994).

An important issue which arose during the analysis of vascular quantity was the fact that it was difficult to unequivocaly discern new vasculature over pre-existing blood vessels. Vascular ink-injection studies, using gelatin-ink or gelatin-carmine red, highlighted all blood vessels within the sample, and as such did not discern new growth. Thus, the reported measures gained significance only when compared to controls, or to several temporal healing points. Similarly, the quantitative measures (ie. vascular volume and blood flow) could not discern between vasomotor changes in vessel diameter or an increase in new vessel numbers as the defining event which results in increased PT blood supply.

Temporal morphological observations, however, clearly suggest that the increase results through a combination of both processes. Peripheral blood vessels in the epitendon are morphologically larger in surgically incised PT than in the control PT. This is suggestive of an immediate vasomotor response, as the angiogenic process would not have had sufficient time to have developed into such large, and patently flowing, blood vessels by the early 3 day interval. This statement is supported by the wound healing literature which places the earliest angiogenic events at the 3 day interval, and demonstrates these vessels are small in size and limited to a short migration distance from the parent vessel (Whalen and

Zetter, 1992). Perhaps the most definitive indicator of angiogenesis discerned in this study has been the increased degree of branching in newly angiogenic vessels, such as that witnessed surrounding the locations of PT incision. As such, histomorphometric measures of vascular branching or vascular entropy (dispersion) may indeed prove to be quantitative measures of angiogenesis.

It was hoped that anti-thrombomodulin staining would highlight non-patent angiogenic buds, and provide a definitive tool for identifying angiogenesis in any given sample. Such a marker of angiogenesis could then be used in concert with vascular injection techniques to morphologically contrast new vascular growth over pre-existing blood vessels. Thrombomodulin is an endothelial cell surface receptor which displays various anticoagulant functions, by activating the protein C/thrombin pathway (Bourin, 1991). Preliminary evidence is emerging that thrombomodulin is down-regulated in patients and animals with inflammation (Esmon et al, 1991). As such, the anti-thrombomodulin-ink colocalization technique, used in this study, did not provide the expected clarity for any such interpretation of new vascular growth, particularly in the inflammatory environment of open PT incision. There were examples where anti-thrombomodulin staining successfully highlighted blood vessels which had not taken on any injected ink (Figures 4.5 - 4.8). These vessels likely represent the artefactual incomplete filling of the resident vessels. This was easily discernible when a blood vessel was half-filled with ink and half empty (Figure 4.6). However some vasculature in normal control PT was preferentially highlighted by the anti-thrombomodulin staining (Figure 4.8), and may indeed

represent non-patent blood vessels (such as dormant capillaries awaiting vasomotor recruitment) or even lymphatics which presumably require a non-thrombogenic lumen. However, in this study, H&E staining of PT sections provided the best means to discern new capillary buds through morphological means.

Following open surgical incision of the normal PT, many elements of the acute inflammatory response are observed (ie. redness, swelling). Blood flow to the PT was measured to increase rapidly and significantly, as was vascular volume. In an acute inflammatory response, dilated vessels are known to become "leaky" as cells and plasma proteins extravasate. Furthermore, as fluid flow between the intravascular and extravascular fluid compartments is known to be controlled by differences in partial pressures on either side of the vascular walls, it was hypothesized that increased PT water content would result following open incision. This was based on the premise that an increased blood supply and flow rate within the blood vessels, in combination with leaky vascular junctions, may lead to an extravasation of fluid resulting in swelling of the injured tissue.

Surprisingly, quantitative measures of PT water content did not demonstrate any significant increases. Although the PT wet mass gradually increased following open incision, so did the PT dry mass. When percent water content was calculated, standardized to the dry mass of tissue in the sample, the PT was remarkably constant, ranging between 62% to 63.2% water content. This measure was the same for normal PT, and all healing intervals assessed.

One can conclude, in this model of PT injury, that although oedema is often associated with soft-tissue injury, the increased production of connective tissue matrix is concurrent. When fluid finds the capacity to pool within bursae, or within joint space, oedema is rapid and readily discerned. However, it may be that within the tissue matrix itself, a homeostatic balance of water content is maintained by upregulated expression of matrix components, particularly with the preponderance of recruited fibrocytic cells witnessed in the acute inflammatory response. Therefore, it can be stated that increases in blood flow to acutely injured patellar tendon, in this model, do not necessarily result in increased tissue water content.

This study also demonstrated that open surgical incision of the PT resulted in significant increases in PT cross-sectional area, when compared to normal control PT. Similarly, morphological assessments clearly confirmed the disruption and separation of collagen crimp organization, particularly when vascular and loose connective tissue elements were incorporated within the incised locations (Figure 4.9). These indicators of tissue remodelling, which likely persist beyond the measured 42 day interval, may alter the material composition of these mechanically load-bearing structures. Such changes may predispose the tissue to altered mechanical functioning, particularly with respect to low-load viscoelastic measures, which are known to be compromised by elevations of blood flow (Bray et al, 1997). Tissue remodelling likely persists well beyond the 42 day post-operative interval.

Other investigations into ligament healing by Shrive and co-workers demonstrated that material 'flaws' in scar tissue of ligament predicted inferior

biomechanical properties (Shrive et al, 1995). They noted that soft-tissue flaws (consisting of blood vessels, fat cells, and disorganized matrix) correlated with losses in tensile strength and structural stiffness in a transection model of injury. In our current investigation, it was noted that longitudinal incision of the PT, on occasion, introduced vascular and fatty soft-tissue defects which remained evident 6 weeks post-surgically. Thus, questions arise as to the functional consequences of neovascular channels traversing (and increasing in volume) in load-bearing tissues (Doschak et al, 1995; Bray et al, 1997).

Therefore, it seems reasonable to conclude from this study that: i) PT vascular volume increases rapidly following longitudinal incision; ii) PT blood flow similarly increases, iii) PT water content does not change when standardized to the dry mass of tissue, and iv) PT remodelling occurs as documented by changes in PT CSA, and matrix organization over time.

The major limitations of this study include that the incision surgery is performed in samples of normal tendon. Therefore, it constitutes only a pre-baseline normal model for the further evaluation of tendinitis pathophysiology. A further limitation is that sham-operated, surgical controls were not included. However, as the debridement of PT requires the surgical incision of overlying skin and tissues, this study mimics the procedure. Furthermore, morphological evaluations concentrated on the sites of PT incision, and the conclusions are therefore representative of the incised PT.

FUTURE DIRECTIONS

This study has important clinical relevance in providing a detailed analysis of direct vascular adaptation induced by the open surgical incision of the normal PT. If vascular adaptations are responsible for changes in normal PT composition, structure and function, then such changes may also be linked to clinical outcomes.

Future studies will examine the newly developed vascular endothelial cell population, and its long-term fate in the central portions of the PT. How these cells function and communicate with the surrounding matrix, as the tendon transmits tensile biomechanical loads, is of great interest. The newly formed vasculature may remodel in response to the biomechanical loading, or the vessels may resorb (perhaps through apoptotic mechanisms), requiring the surrounding matrix to remodel further and absorb the spaces left behind. In either situation, the molecular signals (from resident cells), and their interaction with the proteoglycan extracellular matrix, play a pivotal role in the regulation of vascular adaptation, and resulting tendon physiology. It is known, for example, that angiogenesis is often initiated through the mechanism of proteoglycan (heparan sulfate, in particular) mediated binding of angiogenic molecules, such as the basic fibroblast growth factor family.

Thus, further evaluation of the mechanisms underlying the vascular adaptations seen in the healing PT may provide an important link between vasculature and tendon function. If, in the future, the molecular mechanisms of vascular adaptation are better understood, they may prove useful in mediating desired therapeutic endpoints following tendon injury.

CHAPTER 6

REFERENCES

Akeson WH, Amiel D, La Violette D: The connective tissue response to immobility. A study of the chondroitin-4 and -6 sulfate and dermatan sulfate changes in periarticular connective tissue of control and immobilized knees of dogs. *Clin Orthop* 51:183-197, 1967

Amadio PC: Tendon and ligament. In: *Wound Healing*, pp 384-395. Ed by IK Cohen, RF Diegelmann, WJ Lindblad, Toronto, W.B.Saunders, 1992

Arnoczky SP, Rubin RM, Marshall JL: Microvasculature of the cruciate ligaments and its response to injury. *J Bone Joint Surg* 61A:1221-1229, 1979

Arnoczky SP: Blood supply to the anterior cruciate ligament and supporting structures. *Orthop Clin N Amer* 16/1:15-29, 1985

Arsenault AL: Microvascular organization at the epiphyseal-metaphyseal junction of growing rats. *J Bone Mineral Res* 2/2, 143-149, 1987

Auerbach R, Kubai L, Knighton D: A simple procedure for the long term cultivation of chicken embryos. *Dev Biol* 41:391-394, 1974

Ausprunk DH, Folkman J: Migration and proliferation of endothelial cells in preformed and newly formed blood vessels during tumour angiogenesis. *Microvasc Res* 14:53-65, 1977

Banes AJ, Enterline D, Bevin AG, Salisbury RE: Effects of trauma and partial devascularization on protein synthesis in the avian flexor profundus tendon. *J Trauma* 21:505-512, 1981

Blazina ME, Kerlan RK, Jobe FW, Carter VS, Carlson GJ: Jumper's Knee. *Orthop Clin N. America* 4/3:665-678, 1973

Bourin MC: [Thrombomodulin: a new proteoglycan. Structure-function relation.][French]. *Annales de Biologie Clinique* 49:199-207, 1991

Bray RC, Fisher AWF, Frank CB: Fine vascular anatomy of adult rabbit knee ligaments. *J Anat* 172:69-79, 1990

Bray R, Butterwick D, Doschak M, Tyberg J: Coloured microsphere assessment of blood flow to knee ligaments in adult rabbits. Effects of injury. *J Orthop Res*, 14:618-625, 1996

Bray RC, Rangayyan RM, Frank CB: Normal and healing ligament vascularity: a quantitative histological assessment in the adult rabbit medial collateral ligament. *J Anat* 188:87-95, 1996

Bray RC, Doschak MR, Gross TS, Zernicke RF: Physiological and mechanical adaptations of rabbit medial collateral ligament after anterior cruciate ligament transection. *J Orthop Res* 15:830-836, 1997

Brookes M, Harrison RG: The vascularization of the rabbit femur and tibiofibula. *J Anat* 91/1:61-74, 1967

Brown RA, Weiss JB: Neovascularization and its role in the osteoarthritic process. *Ann Rheum Dis* 47:881-885, 1988

Butler DL, Grood ES, Noyes FR, Zernicke RF: Biomechanics of ligaments and tendons. In: *Exercise and Sports Sciences Review* , pp 125-181. Ed by RS Hutton, Washington, Franklin Institute Press, 1978

Cailliet R: *Knee Pain and Disability*, FA Davis, Philadelphia, 1992

CCAC: Canadian Council on Animal Care. Guide to the care and use of experimental animals. Volumes 1 and 2, Ottawa, Ontario, 1984

Chimich D, Shrive N, Frank C, Marchuk L, Bray R:Water content alters viscoelastic behaviour of the normal adolescent rabbit medial collateral ligament. *J Biomechanics*, 25:831-837, 1992

Chowdhury P, Matyas JR, Frank CB: The "epiligament" of the rabbit medial collateral ligament: a quantitative morphological study. *Conn Tiss Res* 27:33-50, 1991

Colville-Nash PR, Scott DL: Angiogenesis and rheumatoid arthritis: pathogenic and therapeutic implications. *Ann Rheum Dis* 51:919-925, 1992

Colville-Nash PR, Alam CAS, Appleton I, Brown JR, Seed MP, Willoughby DA: The pharmacological modulation of angiogenesis in chronic granulomatous inflammation. *J Pharmac Exp Therapeutics* 274:1463-1472, 1995

Davies DV, Edwards DAW: The blood supply of the synovial membrane and intra-articular structures, *Ann Royal College Surg England* 2:142-156, 1948

Doschak MR, Bray RC, Tyberg JV: Elevation of blood flow correlates with degradation of MCL mechanical behaviour in ACL-deficient joints. *Proc Can Orthop Res Soc* 28:39, 1994

Esmon CT, Johnson AE, Esmon NL: Initiation of the protein-C pathway. *Ann NY Acad Sci* 614:30-43, 1991

Fackelman GE: The nature of tendon damage and its repair. *Equine Vet J* 5:141-149, 1973

Ferrell WR, Khoshbaten A, Angerson WJ, Najafipour H: Localized neural control of blood flow in the posterior region of the knee joint in anaesthetized rabbits. *Exp Physiol* 78:105-108, 1993

Ferretti A, Ippolito E, Mariani P, Puddu G: Jumper's knee. *Am J Sports Med* 11/2:58-62, 1983

Floyd WE, Zaleske DJ, Schiller AL, Trahan C, Mankin HJ: Vascular events associated with the appearance of the secondary centre of ossification in the murine distal femoral epiphysis. *J Bone Joint Surg* A69:185-190, 1987

Folkman J: How is blood vessel growth regulated in normal and neoplastic tissue?-G.H.A. Clowes memorial award lecture. *Cancer Res* 46:467-473, 1986

Frank CB, Woo SL-Y, Amiel D, Harwood F, Gomez M, Akeson W: Medial collateral ligament healing; a multi-disciplinary assessment in rabbits. *Am J Sports Med* 11:379-389, 1983

Ganey TM, Love SM, Ogden JA: Development of vascularization in the chondroepiphysis of the rabbit. *J Orthop Res* 10:496-510, 1992

Gelberman RH, Khabie V, Cahill CJ: The revascularization of healing flexor tendons in the digital sheath. *J Bone Joint Surg* 73A:868-881, 1991

Goldstein SA, Armstrong TJ, Chaffin DB, et al: Analysis of cumulative strain in tendons and tendon sheaths. *J Biomech* 20:1-6, 1987

Gross JL, Moscatelli D, Rifkin DB: Increased capillary endothelial cell protease activity in response to angiogenic stimuli in vitro. *PNAS* 80:2623-2627, 1983

Gross TS, Doschak MR, Zernicke RF, Bray RC: Vascular adaptation may mediate subchondral bone degradation induced by joint laxity. *Proc Can Orthop Res Soc* 28:51, 1994

Hansen ES, Soballe K, Henriksen TB, Hjortdal VE, Bunger C: [99mTc] diphosphonate uptake and hemodynamics in arthritis of the immature dog knee. *J Orthop Res* 9:191-202, 1991

Hardy J, Bertone AL, Muir WW: Determination of synovial membrane blood flow in equine joints using colored microspheres. *Am College Vet Surg* 28:383, 1993

Henninger RW, Bramlage LR, Bailey M, Bertone AL, Weisbrode SE: Effects of tendon splitting on experimentally-induced acute equine tendinitis. *V.C.O.T.* 5:1-9, 1992

Heyman MA, Payne BD, Hoffman JIE and Rudolph AM: Blood flow measurements with radionuclide-labeled particles. *Progress Cardiovas Dis* 20:55-79, 1977

Hooper G, Davies R, Tothill P: Blood flow and clearance in tendons. *J Bone Joint Surg* 66B/3:441-443, 1984

Hunter W: Of the structure and diseases of articulating cartilages *Philos Trans Royal Soc London* 42:1941-1943, 1743

Kai K, Takagi K, Iyama K-I, Kitaoka M, Yoshioka H, Mizuta H, Usuku G: Immunohistochemical localization of basal lamina components in the developing rat epiphyseal cartilage canals. *Clin Orthop Rel Res* 279:292-298, 1992

Khoshbaten A, Ferrell WR: Nerve-mediated responses of blood vessels in the rabbit knee joint. *J Vasc Res* 30:102-107, 1993

Lager DJ, Callaghan EJ, Worth SF, Raife TJ, Lentz SR: Cellular localization of thrombomodulin in human epithelium and squamous malignancies, *Am J Path*, 146/4:933-43, 1995

Langham ME: Observations on the growth of blood veessels into the cornea, *Br J Ophthalmol* 37:210-222, 1953

Le Douarin N, Dieterlen-Lievre F, Teillet M-A: Quail-chick transplantations. In: *Methods in Cell Biology*, pp 23-59. Ed by M Bronner-Fraser. Toronto, Academic Press, 1996

Leeson TS, Leeson CR: *Histology*, W.B.Saunders, [2nd Ed], Toronto, 1970

Levene C: The patterns of cartilage canals. *J Anat* 98:515-538, 1964

Li G, Bronk JT, Kelly PJ: Canine bone blood flow estimated with microspheres. *J Orthop Res* 7:61-67, 1989

Liew M, Carson-Dick W: The anatomy and physiology of blood flow in a diarthrodial joint. *Clinics Rheum Diseases* 7/1: 131-148, 1981

Maroudas A, Ziv I, Weisman N, Venn M: Studies of hydration and swelling pressure in normal and osteoarthritic cartilage. *Biorheology* 22:159-169, 1985

McCullah KG: Tendon injuries and their treatment in the horse. *Vet Rec* 105:54-57, 1979

McFarland EG, Wood MB, Morrey BF, An KN: Canine cruciate and patellar tendon blood flow estimates with high and low dose microspheres. *Trans Orthop Res Soc* 34:202, 1988

Moss-Salentijn AGM: *The Epiphyseal Vascularization of Growth Plates: A developmental study in the rabbit.* PhD Thesis, University of Utrecht, Amsterdam, in the Netherlands, 1975

Muller FJ, Setton LA, Manicourt DH, Mow VC, Howell DS, Pita JC: Centrifugal and biochemical comparison of proteoglycan aggregates from articular cartilage in experimental joint disuse and joint instability. *J Orthop Res* 12:498-508, 1994

Najafipour H, Ferrell WR: Role of prostaglandins in regulation of blood flow and modulation of sympathetic vasoconstriction in normal and acutely inflamed rabbit knee joints. *Exp Physiol* 79:93-101, 1994

Neuberger A, Perrone JC, Slack HGB: The relative metabolic inertia of tendon collagen in the rat. *Biochem J* 49:199-204, 1951

Parker RD, Calabrese GJ: Anterior knee pain. In *Knee Surgery*, Ed by FH Fu, CD Harner, and KG Vince, Baltimore, Williams and Wilkins, 1994

Peacock DJ, Banquerigo ML, Brahn E: A novel angiogenesis inhibitor suppresses rat adjuvant arthritis. *Cellular Immunol* 160:178-184, 1995

Rifkin DB, Klagsbrun M: *Angiogenesis: Mechanisms and Pathobiology*, Cold Spring Harbour, New York, 1987

Riggi K, Wood MB, Ilstrup DM: Dose-dependent variations in blood flow evaluation of canine nerve, nerve graft, tendon, and ligament tissue by the radiolabelled - microsphere technique. *J Orthop Res* 8:909-916, 1990

Ross R: The fibroblast and wound repair. *Biol Rev* 43:51-96, 1968

Sabiston P, Frank CB, Lam TC, Shrive NG: Allograft ligament transplantation: a morphological and biochemical evaluation of a medial collateral complex in a rabbit model. *Am J Sports Med* 18:160-168, 1990

Sandison JC: Observations on the growth of blood vessels as seen inn the transparent chamber introduced in the rabbit's ear. *Am J Anat* 41:475-496, 1928

Scapinelli R: Studies on the vasculature of human knee joint. *Acta Anatomica* 70: 305-331, 1968

Schepsis AA, Leach RE: Surgical management of achilles tendinitis. *Am J Sports Med* 15/4:308-315, 1987

Schlehr FJ, Limbird TA, Swiontkowski MF, KellerTS: The use of laser doppler flowmetry to evaluate anterior cruciate blood flow. *J Orthop Res* 5:150-153, 1987

Schmidt D, von Hochstetter AR: The use of CD31 and collagen IV as vascular arkers. A study of 56 vascular lesions. *Path Res Prac* 191:410-414, 1995

Shim S, Leung G: Blood supply of the knee joint. *Clin Orthop Rel Res* 208: 119-125, 1986

Shrive N, Chimich D, Marchuk L, Wilson J, Brant R, Frank C: Soft-tissue flaws are associated with the material properties of the healing rabbit medial collateral ligament. *J Orthop Res* 13:923-929, 1995

Silver IA, Brown PM, Goodship AE: A clinical and experimental study of tendon injury, healing and treatment in the horse. *Equine Vet J* 1(Suppl):5-32, 1983

Simkin P, Huang A, Benedict R: Effects of exercise on blood flow to canine articular tissues. *J Orthop Res* 8:297-303, 1990

Stromberg B, Tufvesson G, Nilsson G: Effect of surgical splitting on vascular reactions in the superficial flexor tendon in the horse. *J Am Vet Med Assoc* 164:57-60, 1974

Torstensen ET, Bray RC, Wiley JP: Patellar tendinitis: A review of current concepts and treatment. *Clin J Sports Med* 4:77-82, 1994

Trifitt PD, Cieslak CA, Gregg PJ: Cast immobilization and tibial diaphyseal blood flow: An initial study. *J Orthop Res* 10:784-788, 1992

Vignon E, Arlot M, Hartmann D, Moyen B, Ville G: Hypertrophic repair of articular cartilage in experimental osteoarthritis. *Ann Rheum Dis* 42:82-88, 1983

Weidman KA, Simonet WT, Wood MB, Cooney WP, Ilstrup DM: Quantification of regional blood flow to canine flexor tendons, *J Orthop Res* 2:257-261, 1984

Whalen GF, Zetter BR: Angiogenesis. In: *Wound Healing*, pp 384-395. Ed by IK Cohen, RF Diegelmann, WJ Lindblad, Toronto, W.B.Saunders, 1992

Whiteside LA, Sweeney RE: Nutrient pathways of the cruciate ligaments: An experimental study using the hydrogen wash-out technique *J Bone Joint Surg* 62A: 1176-1180, 1980

Woo SL-Y, An K-N, Arnoczky SP, Wayne JS, Fithian DC, Myers BS: Anatomy, biology and biomechanics of tendon, ligament, and meniscus. In: *Orthopaedic Basic Science*, pp 45-87. Ed by SR Simon, Rosemont, AAOS: Port City Press, 1994

Woo SL-Y, Gomez MA, Woo Y-K, et al: Mechanical properties of tendons and ligaments. The relationships of immobilization and exercise on tissue remodelling. *Biorheology* 19:397-408, 1982

Woo SL-Y, Smith BA, Johnson GA: Biomechanics of knee ligaments. In: *Knee Surgery*, pp155-172. Ed by FH Fu, Philadelphia, Williams & Wilkins, 1994

APPENDIX A

SURGICAL INCISION OF THE NORMAL RABBIT PATELLAR TENDON CAUSES SIGNIFICANT VASCULAR ADAPTATIONS

M.R. DOSCHAK, J.R. MATYAS, D.A. HART, R.C. BRAY

McCaig Centre for Joint Injury and Arthritis Research
Faculty of Medicine
University of Calgary
Calgary, Alberta, Canada

Running Title: Vascular Adaptations after Tendon Incision

Address all correspondence to:

Michael R. Doschak
The University of Calgary
3330 Hospital Drive N.W.
Calgary, Alberta, Canada T2N 4N1
Phone: (403) 220-4244
Fax: (403) 270-0617
Email: doschak@acs.ucalgary.ca

SUMMARY

Open incision of the patellar tendon (PT) is thought to promote acute vascular responses, which ultimately results in an enhanced degree of tendon repair. Such a clinical procedure has been applied to patients with tendinitis. The objective of this study was to investigate and quantify the vascular adaptations (both anatomical and physiological) to longitudinal incision of the PT, and the resultant effects on tendon organization. Forty-eight New Zealand White rabbits were separated into three experimental groups and one control group. Experimental groups underwent surgical incision of the right PT, and were assessed 3 days, 10 days and 42 days following injury; normal, unoperated controls were evaluated at time-zero. At 3 days the healing responses characterized the inflammatory phase of soft-tissue repair, at 10 days the proliferative phase, and at 42 days the organizational / remodelling Phase. Histomorphology was assessed to evaluate vascular remodelling and matrix organization in the healing PT. Quantitative measures of PT blood supply (blood flow, microvascular volume) and geometric properties of PT substance were also obtained for each PT. Longitudinal open incision surgery of the PT led to rapid increases in blood flow and vascular volume. Substantial changes in matrix organization persisted at 42 days after surgery. PT blood flow increased an average of 30-fold by 3 days and remained significantly elevated at the 10 day interval compared to time-zero controls. Similarly, vascular volume of the incised PT increased on average 10-fold at 3 days compared to time-zero controls. At the 10 day interval, the increase in vascular volume was greatest

in the central PT substance. Augmentation of PT blood supply appears to result from a combination of vasomotor regulation (resulting in an early and substantial vasodilatation), and newly formed angiogenic vessels in the centrally incised PT. By 42 days both blood flow and vascular volume of the incised tendon had diminished, and were not significantly different from controls. With respect to PT geometric properties, a larger PT results as the tendon matrix and blood vessels remodel. PT cross-sectional area increased rapidly by 3 days to 1.3-times control values, and remained significantly elevated at 42 days post-injury. Morphological assessments demonstrated the disruption of normal matrix organization by vascular and soft-tissue components associated with the longitudinal incisions. These findings suggest that open longitudinal incision of the PT increases the vascular supply to deep tendon early after injury. These changes arise through both vasomotor and angiogenic activity in the tissue. Since PT blood flow and vascular volume return to control levels after 42 days, but structural features remain disorganized, we propose that vascular remodelling is more rapid and complete than matrix remodelling after surgical incision of the PT.

Index terms: Blood Flow, Patellar Tendon, Vascular Volume, Surgery

INTRODUCTION

The surgical debridement of patellar tendon (PT) is routinely performed to treat refractory cases of tendinitis (Blazina et al, 1973; Henninger et al, 1992; Parker et al, 1994; Schepsis et al, 1987; Torstensen et al, 1994). In this procedure, a number of longitudinal incisions are randomly introduced in the tendon midsubstance in an effort to stimulate the healing process. The healing of tendon injuries has been well described, and occurs through haematoma organization, cellular recruitment and scar formation (Amadio, 1992; Ross, 1968). However, the microvascular events associated with tendon healing have not been as clearly delineated. It has been postulated that longitudinal incision of normal tendons increases tendon vascularity (Stromberg et al, 1974), but no studies have quantified the microvascular adaptations during tendon healing.

This study is based on the rationale that surgical incision of tendons stimulates acute vascular and matrix remodelling responses to injury. Vascular responses include increases in vessel numbers (through angiogenesis), and increases in blood supply (vasomotor changes in vessel diameter and rate of blood flow). Previous investigators have shown that following tendon injury, blood vessels divide and vascularize the repair site (Gelberman et al, 1991; Henninger et al, 1992; Stromberg et al, 1974). This necessitates a direct alteration of the tendon structural organization and material composition, and may also alter normal vasomotor physiology in the tissue (Shrive et al, 1995). Furthermore, vasoactive changes in blood supply during the acute phase following injury is paramount in

defining the classical inflammatory responses of redness, swelling, and heat. Often the immediate outcome of acute inflammation is "loss of function", and in the healing tendon, this process may possibly be mediated by the degree in which vascular adaptation alters normal tendon physiology.

The objectives of this study were to: i) describe the adaptive changes and time course of vascular events in the incised, healing PT; ii) quantify changes in PT blood flow and vascular volume; and iii) assess the effects of longitudinal (non-transecting) incision on PT matrix remodelling and geometric properties. This investigation details a surgical model for studying PT vascular supply, and demonstrates experimental evidence that open incision of the PT stimulates vascular and matrix adaptations in the PT.

METHODS

Animal Handling and Experimental Design

Forty-eight outbred, 1-year-old, female New Zealand White rabbits (mean of 4.8 kg body mass), were used in this study. Animals were purchased from a single supplier (Riemens Fur Ranche, St. Agathe, Ontario, Canada) and were housed individually in wire bottomed cages (65 x 40 x 45 cm; length x width x height). Unrestricted cage activity was allowed and a 12:12 hour light-dark cycle was simulated in a quiet room at 20°C. Ad libitum access was permitted to water and standard laboratory rabbit chow. The Faculty of Medicine Animal Care

Committee reviewed and approved the experimental protocol based on the criteria of the Canadian Council on Animal Care (CCAC, 1984).

Following a week of acclimatization, animals were randomly allocated into four groups of 12 animals. Group 1,2 and 3 animals underwent unilateral incision surgery of the PT (described below and in Figure 3.2), and were sacrificed following 3 days, 10 days, and 42 days post-operatively. The remaining Group 4 animals were sacrificed at time zero, and provided control PT.

PT Incision Surgery

All operations were performed on the right knee. Animals were first sedated with a 0.1 ml intravenous injection of Atravet^{R} (10 mg/ml acepromazine maleate, Ayerst Laboratories, Montreal, PQ) and then anaesthetized with a metred gaseous mixture of 2% halothane/oxygen. The PT was exposed medially through an open incision of overlying skin, followed by blunt dissection of underlying fascial tissues. The tendon was isolated by raising the retinacular edges, incising with a scalpel, and inserting a flat spatula under the entire midsubstance of the PT. A series of 3 longitudinal, full-depth incisions were made using a curved #12 scalpel blade. Incisions extended from the inferior pole of (but not involving direct contact with) the patella, and ran the full length of the PT. The incisions were terminated approximately 3mm prior to contacting the tibial insertion. The origin, mid-point and terminus of the 3 midsubstance incisions were demarcated using 6-0 nylon marker sutures to ensure precise relocation of the incised sites during subsequent

analyses. The skin wound was closed using 4-0 nylon suture. The left knee on all animals remained unoperated.

QUALITATIVE MORPHOLOGICAL EVALUATIONS

Three animals from each experimental group (Figure 3.2) underwent assessment of microvascular volume and matrix remodelling using a combination of vascular ink-injection and immunolocalization of thrombomodulin. Thrombomodulin, a molecule with anticoagulative properties, is expressed on the luminal surface of endothelial cells and was used to positively identify blood vessels. The antibody to thrombomodulin was a gift from Dr. Naomi Esmon (University of Oklahoma Medical centre, Oklahoma City, OK) and has been used in previous investigations (Lager et al, 1995).

Just prior to euthanasia, animals were deeply anaesthetized, and the femoral artery and vein were isolated. The femoral artery was cannulated using PE-90 polyethylene tubing (Clay Adams, Parsippany, NJ, U.S.A.), and the femoral vein was transected to permit uninhibited drainage of perfused solutions. The animal was euthanized with an intra-venous injection of Euthanyl (240 mg/ml sodium pentobarbital), and the hind limbs were held in 90 degrees of flexion using a custom-made thermoplastic mould. Each hind limb was flushed with heparinized saline (100 units heparin/ml saline), and fixed by perfusion with Zamboni's mixture (4% paraformaldehyde / saturated picric acid). Finally, a solution of filtered India ink (Higgins Black Magic, Faber Castell, Germany) containing 4% gelatin was

perfused through the entire hindlimb. All solutions were pre-heated to 39°C, and perfusion controlled by means of a Harvard Syringe Pump (Harvard Apparatus, Model 33, St. Laurent, PQ, Canada). Real-time perfusion pressures were monitored using a computer-based oscillographic data acquisition system (AT-CODAS System, DataQ Instruments, Akron OH, U.S.A.). Immediately following perfusion, the carcass was stored for a minimum of four hours at 4°C to ensure solidification, prior to disarticulating the hindlimb at the hip.

Histology and Immunohistochemistry

The PT was dissected free from its bony insertions and fatty attachments. Overlying fascial layers of connective tissue were removed until no free movement of overlying translucent fascia could be discerned against the opaque white tendon. This resulted in a PT specimen encapsulated with its immediate epitendinous layer. The PT was bisected in the saggital plane, and each block further halved transversely. These blocks were processed through cryoprotectant solutions of DMSO and PBS/10% sucrose, embedded, serially sectioned at 40μm (in the coronal plane) using a cryomicrotome, and mounted 3 sections / slide. Every fourth slide was stained using anti-thrombomodulin indirect immunofluorescence, and colocalization of ink-injected vascular processes examined. Briefly, sections were blocked with 5% bovine serum albumin, and pre-incubated with normal rabbit serum. Sections were incubated with goat anti-rabbit thrombomodulin for 48 hours at 4°C. Following rinses in PBS/0.1% Triton-X 100, the sections were reacted with

secondary rabbit anti-goat IgG FITC conjugate for one hour at room temperature in the dark. Following final rinses, sections were mounted and examined using a Leitz Orthoplan microscope under epi-fluorescent illumination (Leica Inc., BC, Canada). Colocalization of ink-injected, thrombomodulin-stained blood vessels was achieved by using threshold levels of brightfield illumination in conjunction with epi-fluorescence. All sections were assessed in a randomized, blinded fashion by a single observer, and graded for vascularization and evidence of angiogenesis at incision and at remote sites. These same sections were then stained with haematoxylin and eosin for complete morphological assessment. Photomicrography was performed using an Orthomat camera housing attachment (Leica Inc., BC, Canada) with high-speed (400 ASA) colour slide film.

Evaluation of PT Remodelling

Morphological assessments of tendon matrix organization were made by observing the incised slits on sections of PT. The coronal sections were illuminated with transmitted plane-polarized light, and organization of the birefringent collagen crimp surrounding the incised locations was assessed. In particular, the lateral registry of the collagen fibers was noted, and any degree of disruption (due to the incisions) noted as a potential indicator of functional compromise in tendon composition over the healing intervals.

QUANTITATIVE EVALUATIONS

A second set of 6 animals from each experimental group underwent PT blood flow measurements using coloured microspheres (Figure 3.2). Following infusion of microspheres, geometric assessment of PT cross-sectional area was performed as a gross but quantitative measure of PT remodelling. The wet mass of the PT was recorded, and following dessication, the dry mass was recorded to determine PT water content. Details of these procedures are provided below.

Blood Flow: Microsphere Technique

Coloured microspheres (CMs) were used to measure blood flow to the PT. Dye-Trak^{R} 15.5μm CMs were employed (Triton Technology Inc., San Diego, CA), in the following standard approach (Bray, Butterwick et al, 1996). Under general anaesthesia, a PE-90 cannula (Clay-Adams, Parsippany, NJ) was inserted retrograde into the left ventricle from the common carotid artery, and placement was confirmed by means of a ventricular pressure waveform from an on-line P23XL pressure transducer (Spectramed, Oxnard, CA). A well mixed suspension of 10.2 million CMs were infused over a 30 second interval, ultimately becoming trapped in the capillary beds of all tissues (Heyman et al, 1977). Animals were euthanized with a 3ml intra-cardiac injection of saturated KCL.

After sacrifice, the patella-PT-tibia complex was dissected, clamped, held at a constant load (in an MTS materials testing device) of 10 Newtons while cemented into bone grips, and the cross-sectional area determined according to a

standardized protocol (Shrive et al, 1995). The measurement was performed using strain-guaged calipers, and results recorded in square mm. Cross-sectional area was measured at the PT midsubstance.

Coloured Microsphere Processing and Water Content Analyses

After geometric testing, the PT samples were excised, weighed, dessicated overnight, and dry weights recorded to evaluate water content. The percentage of water in the PT samples was determined using the equation:

$$\%WaterContent = \frac{WetMass - DryMass}{WetMass} * 100$$

All tissues were digested to completion in 7ml of 4M KOH at 60°C. The CMs were separated from the hydrolysate by filtration through a 10-μm polyester filter (Spectra-Mesh, Spectrum, Houston, Texas). In high blood flow tissues (kidneys, lungs, reference blood sample) CMs were counted by spectrophotometry, using absorbance values provided by the manufacturer's standard curve for the particular lot number of CMs used. In tissues with low blood flow, CMs were visualized directly on the filter and counted using a Nikon Diaphot-TMD inverted microscope (Nikon Corp., Japan) with epi-fluorescent illumination. The blood flow to each tissue sample was calculated, and standardized blood flow values reported as *ml/min/100 grams tissue.*

Vascular Volume Determination

Vascular volume was quantified in the three remaining animals from each experimental group (Figure 3.2) by the method of Colville-Nash et al (Colville-Nash et al, 1995). Briefly, animals were anaesthetized, and both femoral arteries cannulated and flushed as described above. Animals were sacrificed by lethal injection, and a prewarmed solution of 5% Carmine Red in 10% gelatin was infused as described above. The carcass was chilled for 2 hours at 4°C, and both PTs dissected. A central 6mm square of PT midsubstance was resected from the surrounding PT in order to evaluate changes in PT midsubstance vascular volume (Figures 3.9). The resection was standardized using the marker sutures from surgery as reference points. Central PT squares and the remaining PT outer portion were dried for 48 hours, weighed, and enzymatically digested to completion in 0.9 ml of buffered papain digestion solution (2mM dithiothreitol, 20mM disodium hydrogen orthophosphate, 1mM EDTA, 12U/ml papain) for 24 hours at 56°C. The Carmine Red dye was eluted by adding 0.1ml of 5M NaOH, and separated using centrifugation (8,000g for 3 mins) followed by filtration of the supernatant through a 0.22μm nitrocellulose filter. The dye filtrate was assayed spectrophotometrically for Carmine Red absorbance at 490nm, dye content determined by comparisson with standard curves, and results expressed as a Vascular Index (V.I.) of μg dye/mg dry weight of tissue.

STATISTICAL ANALYSES

Analysis of Variance (ANOVA, Statistical Package for the Social Sciences, SPSS) was used to detect significant quantitative differences between experimental and control groups. A 'post-hoc' multiple comparisons test (Tukeys test, SPSS) was used to localize significant differences. A significance level of $p=0.05$ was used for all statistical tests.

RESULTS

Morphological Evaluations

Ink-injected normal control PT demonstrated an organized network of fine blood vessels overlying the entire surface, and parts of the posterior surface. Vessels were often seen oriented in tandem to each other in a parallel fashion (Figure 4.1a). In contrast, longitudinally incised PT demonstrated greater numbers and larger diameter of blood vessels, with marked disruption of normal vascular organization (Figures 4.1b, 4.1c, 4.1d).

Microscopically, vessels in the controls were organized obliquely, entering from the epitenon towards the tendon proper. Smaller vessels were seen organized longitudinally deep in tendon, oriented parallel with collagen fibers (Figure 4.2a). The incised tendon, examined 3 days post-surgery, demonstrated large numbers of dilated, engorged blood vessels entering the tendon proper (Figure 4.2b). Co-localization of blood vessels was noted in those specimens stained

immunohistochemically, providing a powerful differential analysis of vessels not patently filled with ink-gelatin but staining positively for thrombomodulin.

By 10 days the tendon incisions were clearly neovaszcularized with longitudinally arranged, thin vessels which were now patently filling with ink. Polarized light revealed the collagen crimp organization, and demonstrated that matrix lateral registry was divided and separated due to the surgical incisions (Figure 4.2c).

At 42 days (6 weeks), the deep tendon and incised locations both remained occupied with an abundant number of branching, longitudinally oriented blood vessels. The incisions had been remodelled with more randomly dispersed collagen bundles (and numerous fibroblasts) which surrounded the blood vessels (Figure 4.2d). The inclusion of other elements, such as fat cells and less densely collagenized regions, was occaisionally observed in conjunction with the incised locations.

QUANTITATIVE EVALUATIONS

Blood Flow

Following longitudinal incision, the PT demonstrated a statistically significant elevation in blood flow compared to both time-zero and contralateral controls. Three days following longitudinal incision, PT standardized blood flow was measured to be 13.23 $\pm$ 4.89 (Mean $\pm$ Standard Error of Mean) ml/min/100g, 30-fold greater than time-zero control and contralateral PT values of 0.36 $\pm$ 0.15

ml/min/100g ($p<0.001$) and 0.43 $\pm$ 0.18 ml/min/100g ($p<0.001$) respectively (Figure 4.10). Ten days following surgery, PT blood flow of 13.26 $\pm$ 3.54 ml/min/100g remained significantly elevated, still being 30-fold greater than that of time-zero controls ($p<0.001$) and 13-times that of the contralateral PT (1.11 $\pm$ 0.44 ml/min/100g; $p<0.01$). However by 42 days, PT blood flow had returned to 3.77 $\pm$ 2.09 ml/min/100g, and was not significantly different to time-zero controls ($p>0.05$) or contralaterals (0.63 $\pm$ 0.20 ml/min/100g; $p>0.05$).

Standardized Vascular Volume (Vascular index)

Following longitudinal incision, PT vascular volume significantly increased and subsequently diminished over 42 days (Figure 4.13). At 3 days the incised PT carmine red content increased significantly providing a vascular index (V.I.) of 2.74 $\pm$ 0.74 μg/mg, compared to time-zero control and contralateral V.I.s of 0.12 $\pm$ 0.10 μg/mg ($p<0.001$) and 0.77 $\pm$ 0.18 μg/mg ($p<0.05$) respectively. By 10 days the incised PT vascular volume (2.37 $\pm$ 0.50 μg/mg) remained significantly elevated compared to time-zero controls ($p<0.01$). However by 42 days PT vascular volume had fallen, with its V.I. of 0.91 $\pm$ 0.50 μg/mg not significantly different to time-zero controls. Of importance, however, was the differential results obtained when analyzing the vascular volume in the central square of PT midsubstance. The PT midsubstance achieved significantly elevated vascular volume only at the 10 day interval with a V.I. of 0.42 $\pm$ 0.18 μg/mg, compared to time-zero and contralateral

control values of 0.04 ± 0.01 μg/mg ($p<0.05$) and 0.07 ± 0.18 μg/mg ($p<0.05$) respectively (Figure 4.13).

When analyzing the geometric properties of the PT, a rapid and significant increase in tendon cross-sectional area (CSA) was detected following injury. After longitudinal incision, PT CSA increased significantly, to 15.01 ± 0.42 mm^2 at 3 days ($p<0.001$) and 15.80 ± 0.75 mm^2 at 10 days ($p<0.001$) compared with time-zero controls (11.45 ± 0.45 mm^2) and respective contralateral controls for both intervals. For both 3 and 10 days, this was a 1.3-fold increase over the time-zero control value. At 42 days, CSA for the PT in the longitudinally incised knee was still significantly elevated, with a value of 14.66 ± 1.31mm^2 compared to contralateral controls (10.72 ± 0.43 mm^2; $p<0.05$).

The wet mass of the incised PT increased and subsequently diminished over 42 days. Similarly, the dry mass of the incised PT increased and subsequently diminished over 42 days. However, no significant differences in either parameter were measured, compared to time-zero and contralateral controls. Similarly, the water content for the incised PT did not differ significantly from time-zero controls, and all PT samples maintained an average water content of 63%.

DISCUSSION

This investigation demonstrates that open incision of the PT increases the blood supply to PT, both in terms of greater blood vessel volume, and increased tendon blood flow. Quantitative changes in blood flow and microvascular volume

correspond well with our temporal morphological assessments, which demonstrated dilated peripheral vessels and a profuse recruitment of pre-existing blood vessels at 3 days. Angiogenic buds, observed in proximity to incised locations, were seen to be patently filling with injected dye by the 10 day interval. These morphological findings agree with the quantitative assessments of vascular volume which demonstrated a significant increase in the central square of PT 10 days following longitudinal incision. By the 42 day interval, however, both vascular volume and blood flow of the PT had declined, implying significant / dynamic vascular remodelling and return of normal vasomotor control occurs after this procedure. Of potential significance is the data illustrated in Figure 4.13, where the central portion of the PT has a later peak and lower absolute elevation of vascular volume compared to the outer PT. This is possibly related to previous results which have indicated that epiligamentous connective tissues are more vascularized / unit area than deeper ligamentous tissue (Bray, Butterwick et al, 1996). Since outer PT samples likely contained a greater relative proportion of total epitendinous tissue than the central sample, the explanation for elevated vascular volume in the outer PT might be on that basis. Even more functionally significant is that the peak increase in epitendinous vascular volume preceeds the peak in central PT vascular volume, suggesting sequential steps in the vascular response to injury - first in peritendinous tissues and then into central PT - at the site of the original injury stimulus. This possibility is supported in the histological observations in Figure 4.1,

where at 3 days the peritendinous tissue exhibits a striking vasodilation compared to the normal and 10 day intervals.

This study also demonstrated that open longitudinal incision of the PT leads to increases in tendon cross-sectional area, as the blood vessels and tendon matrix remodel. PT CSA increases rapidly by 3 days to 1.3-times control values, and remains significantly elevated beyond 42 days post-surgically. Our morphological assessments confirmed the disruption of collagenous organization by the longitudinal incisions, particularly when vascular material and fatty soft-tissue elements were incorporated. Thus, the PT undergoes significant geometric changes through tissue remodelling as a result of longitudinal incision. Tissue remodelling likely persists well beyond the 42 day post-operative interval.

Microangiographic and histological studies in the superficial digital flexor tendons of dogs and horses have previously demonstrated a rapid ingrowth of blood vessels into tendon during the early phase (3 days to 17 days) of repair (Gelberman et al, 1991; Stromberg et al, 1974). These morphological evaluations of transected and of "split" (ie. longitudinally incised) tendon suggested increased vascular volume which persists in the short-term (ie. prior to 4 weeks of healing), but declines during the later phases of wound repair (Amadio, 1992; Stromberg et al, 1974). Similarly, increases in blood flow during ligament healing has previously been shown in our laboratory, and confirms that a rapid vascular response (and associated inflammation) follows acute injury of these tissues (Bray, Butterwick et al, 1996).

Other investigations into ligament healing by Shrive and co-workers demonstrated that material 'flaws' in scar tissue of ligament predicted inferior biomechanical properties (Shrive et al, 1995). They noted that soft-tissue flaws (consisting of blood vessels, fat cells, and disorganized matrix) correlated with losses in tensile strength and structural stiffness in a transection model of injury. In our current investigation, it was noted that longitudinal incision of the PT, on occasion, introduced vascular and fatty soft-tissue defects which remained evident 6 weeks post-surgically. Thus, questions arise as to the functional consequences of neovascular channels traversing (and increasing in volume) in load-bearing tissues (Doschak et al, 1995; Bray et al, 1997).

From our results, it is reasonable to conclude that: i) PT vascular content increases rapidly following longitudinal incision; ii) PT blood flow similarly increases, and iii) PT remodelling occurs as documented by changes in vascular volume, PT CSA, and matrix organization over time. This study has important clinical relevance in providing a detailed analysis of direct vascular adaptation induced by the surgical incision of the normal PT. Furthermore, if early vascular adaptations mediate even some changes in tendon composition, structure and function, then such physiological changes may also be linked to clinical outcomes. Studies are currently underway to probe fundamental questions related to the functional consequences of altered PT physiology in terms of mechanical behaviour.

APPENDIX B

ANGIOGENESIS IN THE DISTAL FEMORAL CHONDROEPIPHYSIS OF THE RABBIT DURING DEVELOPMENT

M.R. DOSCHAK, J.R. MATYAS, D.A. HART, R.C. BRAY

McCaig Centre for Joint Injury and Arthritis Research
Faculty of Medicine
University of Calgary
Calgary, Alberta, Canada

Running Title: Angiogenesis in the Femoral Chondroepiphysis

Address all correspondence to:

Michael R. Doschak
The University of Calgary
3330 Hospital Drive N.W.
Calgary, Alberta, Canada T2N 4N1
Phone: (403) 220-4244
Fax: (403) 270-0617
Email: doschak@acs.ucalgary.ca

SUMMARY

New blood vessels which result from the process of angiogenesis are often difficult to discern histologically from pre-existing vasculature. The objective of this study was to assess the developmental neovascularization of the rabbit distal femoral chondroepiphysis for use as a model to study angiogenesis. Fifteen pregnant New Zealand White rabbits were euthanized and an average of 7 kits / litter delivered. The time-course of chondroepiphyseal vascular invasion was determined by standardizing measures of kit body mass against Crown-Rump length. Histological analyses confirmed the classical steps of angiogenesis from elongating endothelial sprouts to the formation of patent new blood vessels. To confirm the angiogenic nature of the chondroepiphysis itself, samples was assayed on the chick Chorio-allantoic membrane (CAM). Neovascular outgrowths from the CAM were apparent 48 hours following introduction of the chondroepiphyseal sample. This investigation confirms the usefulness of studying chondroepiphyseal development as a model for evaluating angiogenesis, particularly in articular connective tissues. As this angiogenic process occurs without injury, and in a defined tissue environment initially devoid of blood vessels, it provides a unique opportunity to study the new vessels without the complication of underlying inflammation or background vasculature. Furthermore, the discovery of angiogenic or angiostatic molecules specific to a developing connective tissue may one day be applied to analyses of regulation of angiogenesis in articular tissues.

INTRODUCTION

Adult articular cartilage is generally considered to be avascular. However, during embryological development, blood vessels invade and vascularize the epiphyseal cartilage of long bones. The development of these vessels (found in cartilage erosions known as canals) has been described morphologically, and involves a stepwise neovascularization of the epiphysis which terminates with the establishment of a centrally located secondary centre of ossification (Ganey et al, 1992; Floyd et al, 1987; Moss-Salentijn, 1975). Blood vessels which meet in the centre expand to form a cavitation, by eroding surrounding cartilaginous matrix, and calcification begins centrally and radiates out towards the periphery.

Angiogenesis proceeds in a series of distinct events from endothelial cell activation and migration, to the formation of patent new blood vessels (Folkman, 1986; Ausprunk & Folkman, 1977; Colville-Nash & Scott, 1992). The process is initiated and regulated by an exquisite controlling mechanism which, once activated, will continue to completion, whereupon it will shut-down completely. When the regulatory control of angiogenesis is lost, pathology may result, such as the destructive angiogenesis-dependant growth of pannus into the joint cartilage of rheumatoid arthritis patients. Angiogenesis is often present amidst the inflammatory mediators of arthritic conditions, and thus the regulatory molecules of angiogenesis are difficult to discern from those of the inflammatory response.

As the general features of capillary growth are similar regardless of the source of the angiogenic stimulus (Folkman, 1986), the developmental process of

angiogenesis in the cartilage canals of the fetal NZW rabbit provide the unique opportunity to observe the angiogenic process in joint connective tissues clearly, without the presence of underlying inflammation or injury.

The objectives of this study were to: i) accurately determine the time-course of vascular invasion into the epiphyseal cartilage of the NZW rabbit knee joint; ii) evaluate if developing cartilage canals are a suitable model for studying angiogenesis in joint connective tissues; and iii) confirm the expression of powerful angiogenic factor(s) resident within the local environment of the epiphysis itself. This investigation details the angiogenic process in epiphyseal cartilage during development, and demonstrates experimental evidence that a locally produced angiogenic factor stimulates vascular and matrix adaptations in the developing epiphysis.

METHODS

Animal Handling and Experimental Design

Fifteen, 6-month-old, pregnant female New Zealand White rabbits were used in this study. A total of 102 kits (from these rabbits) were evaluated between 18 days gestation through to birth. Animals were purchased from a single supplier (Riemens Fur Ranche, St. Agathe, Ontario, Canada) and were housed individually in wire bottomed cages (65 x 40 x 45 cm; length x width x height). Unrestricted cage activity was allowed and a 12:12 hour light-dark cycle was simulated in a quiet room at 20°C. Ad libitum access was permitted to water and standard laboratory

rabbit chow. The Faculty of Medicine Animal Care Committee reviewed and approved the experimental protocol based on the criteria of the Canadian Council on Animal Care (CCAC, 1984).

Pregnant rabbits were timed from the suspected hour of insemination, which occured through the regular mating of 6 month old virgin females with a male breeder. The pregnant rabbits were sacrificed, by intra-venous injection of Euthanyl, at 14 intervals between 18 days to 31 days post-insemination (Figure B.1). Litters were delivered through an abdominal dissection, and placed on a covered warming mat set at 39°C.

Measures of temporal staging

The kits, which numbered from 4 to 11 per litter, were initially weighed after which the Crown-Rump (C-R) length was measured. This was performed using a piece of thread, which was subsequently referenced against a graduated ruler. These measures were compared against the age, namely the timed "number of days" post-insemination. Results were graphed and the gestational age for subsequent evaluations determined from the graph as a function of mass versus C-R length.

The kits were anaesthetized in an ether chamber and killed by decapitation. The hind limbs were severed at the hip with a scalpel, and fixed in a mixture of 4% paraformaldehyde/0.5% saturated picric acid in phosphate buffered saline (pH 7.4).

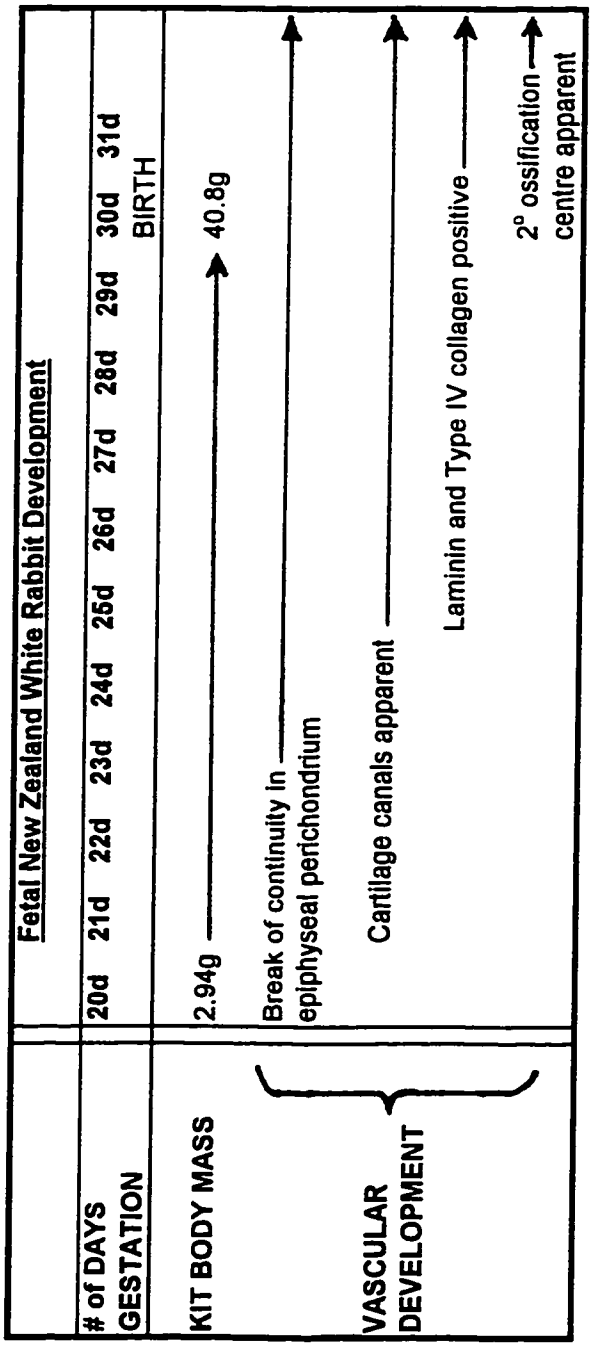

Figure B.1: Time-course of cartilage canal development in the distal femoral epiphysis of the fetal New Zealand White rabbit.

QUALITATIVE MORPHOLOGICAL EVALUATIONS

Histology and Immunohistochemistry

The entire hind-limb from one kit, at each developmental time point, was serially sectioned at 20 μm using a cryomicrotome. The mounted, dried sections were imaged under an image analysis system and sequential images of the epiphyses in entirety digitized. Every fifth slide was subsequently stained using anti-thrombomodulin immunohistochemistry.

Briefly, sections were blocked with 5% bovine serum albumin, and pre-incubated with normal rabbit serum. Sections were incubated with goat anti-rabbit thrombomodulin (Oklahoma Medical Research Foundation, Oklahoma City, OK) for 48 hours at 4°C. Following rinses in PBS/0.1% Triton-X 100, the sections were reacted with secondary rabbit anti-goat IgG FITC conjugate for one hour at room temperature in the dark. Following final rinses, sections were mounted and examined using a Leitz Orthoplan microscope under epi-fluorescent illumination (Leica Inc., BC, Canada). These same sections were then stained with haematoxylin and eosin for complete morphological assessment. Photomicrography was performed using an Orthomat camera housing attachment (Leica Inc., BC, Canada) with high-speed (400 ASA) colour slide film.

Evaluation of Cartilage Canals

A full-depth assessment of cartilage canal erosion was made by sequential observation of digitized images for all samples (Appendix C). Temporal

assessments of cartilage canal progression was noted with respect to the formation of the secondary ossification centre centrally in the epiphysis, in conjunction with evidence of calcification - visible as dense granules in the cellular cartilaginous matrix.

TRANSPLANTATION EXPERIMENTS

Four fertilized chicken eggs were obtained, and prepared at 13 days post-fertilization to accept fetal rabbit epiphyseal transplants 1 day prior to vascular invasion.

Egg preparation

The blunt-end of each egg was presented and swabbed with 70% alcohol and air-dried. Scotch Magic-tape (3M brand) was applied and pressed flat. Using a #12 hooked scalpel blade, the shell was scored and pierced, after which fine curved scissors were used to cut a 5cm diameter hole in the blunt-end of the egg. The hole exposed the air sac of the egg, and a dry white, fibrous membrane was now exposed. A few drops of sterile Chick Ringers Solution was dripped onto the exposed fibrous membrane to wet it, and the excess liquid removed using a pasteur pipette. A pair of fine, curved forceps were used to tease at the membrane gently. Once broken, the fibrous membrane could be easily peeled back to expose the patent Chorio-Allantoic Membrane (CAM) with abundantly branching vasculature. The chick could easily be seen moving within the shell under the protection of the

CAM. The eggshell hole was covered loosely with electrical tape, while the donor epiphyseal samples were prepared.

Chondroepiphyseal dissection

Four kits, at 19 days post-insemination, were isolated aseptically and delivered into sterile petri-dishes lined with sterilized filter paper. The kits were weighed, and the C-R length measured, prior to decapitation. The femur was dissected free under a dissecting scope by teasing the sample over the dry filter paper. Once clearly isolated, the distal femoral epiphysis was severed with a scalpel blade just below the condylar curvature, close to or through the growth plate region. The sample was moistened with chick ringers solution, and transplanted onto the CAM.

TRANSPLANTATION

The donor egg was uncovered and the CAM exposed. The chondroepiphyseal sample was placed in a mostly clear region of the CAM equidistant from pre-existing large vessels (Figure B.2). The white fibrous membrane from the egg air-chamber was reapposed to snugly overlay and cover the epiphyseal sample and press it directly against the CAM. The eggshell hole was covered tightly with the electrical tape, and the eggs incubated in a rotating dry-air 37°C egg incubator (Petersime Incubator Company, Gettysburg, OH). Following incubation from 1 to 4 days post-implantation, the samples were exposed

by removal of overlying air-sac membrane and photographed. The epiphyseal plug and surrounding CAM was dissected free from the egg, fixed in a mixture of 4% paraformaldehyde/0.5% saturated picric acid in phosphate buffered saline (pH 7.4), and subsequently serially sectioned at 20 μm, as described above.

RESULTS

Gross Observations

A large degree of variance was measured in the masses of kits delivered from the same litter, and presumably at the same gestational age. Similarly, C-R lengths varied accordingly. However, when kit mass was plotted as a function of C-R length, an exponential curve was obtained. When rendered linear by plotting on log-log axes, the ensuing straight line could be used to accurately stage development (Figure B.3). The exponential growth of kit body mass was evident grossly, as kit size increased visibly from day-to-day.

Morphological Evaluations

Cartilage canal formation begins when vascular erosions penetrate the periphery of the chonroepiphysis. This process begins at around day 20 post-insemination. Erosions are seen to occur simultaneously at multiple sites around the epiphysis, but commonly in the metaphyseal region of the epiphysis (Figure B.4; Appendix C). The vascular components of the canal are seen centrally, and the

Figure B.2: A view of the freshly transplanted chondroepiphysis on the chorio-allantoic membrane. Magnification x10.

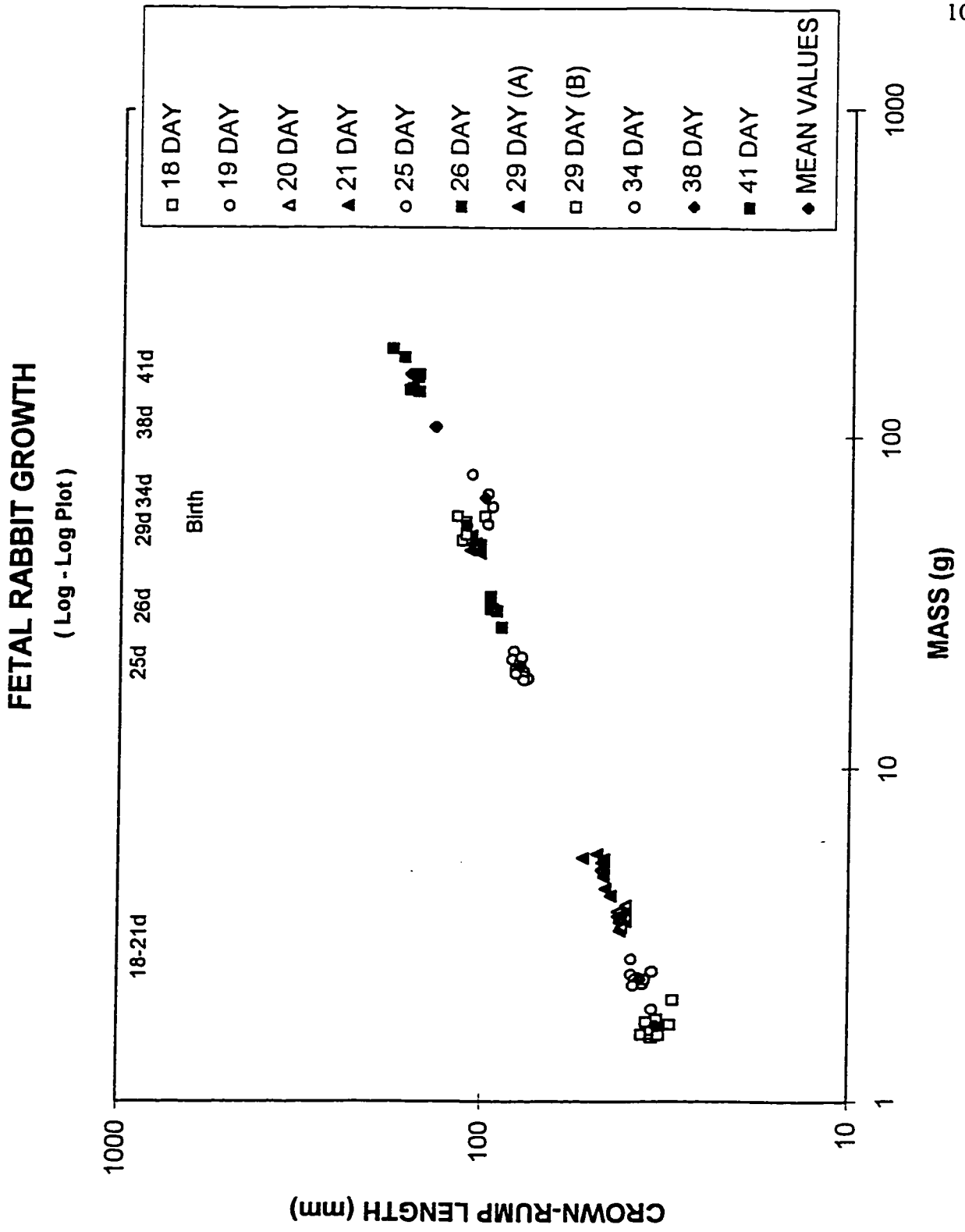

Figure B.3: Time-course of fetal New Zealand White rabbit growth, from 18 to 41 days post-conception (Log-Log plot).

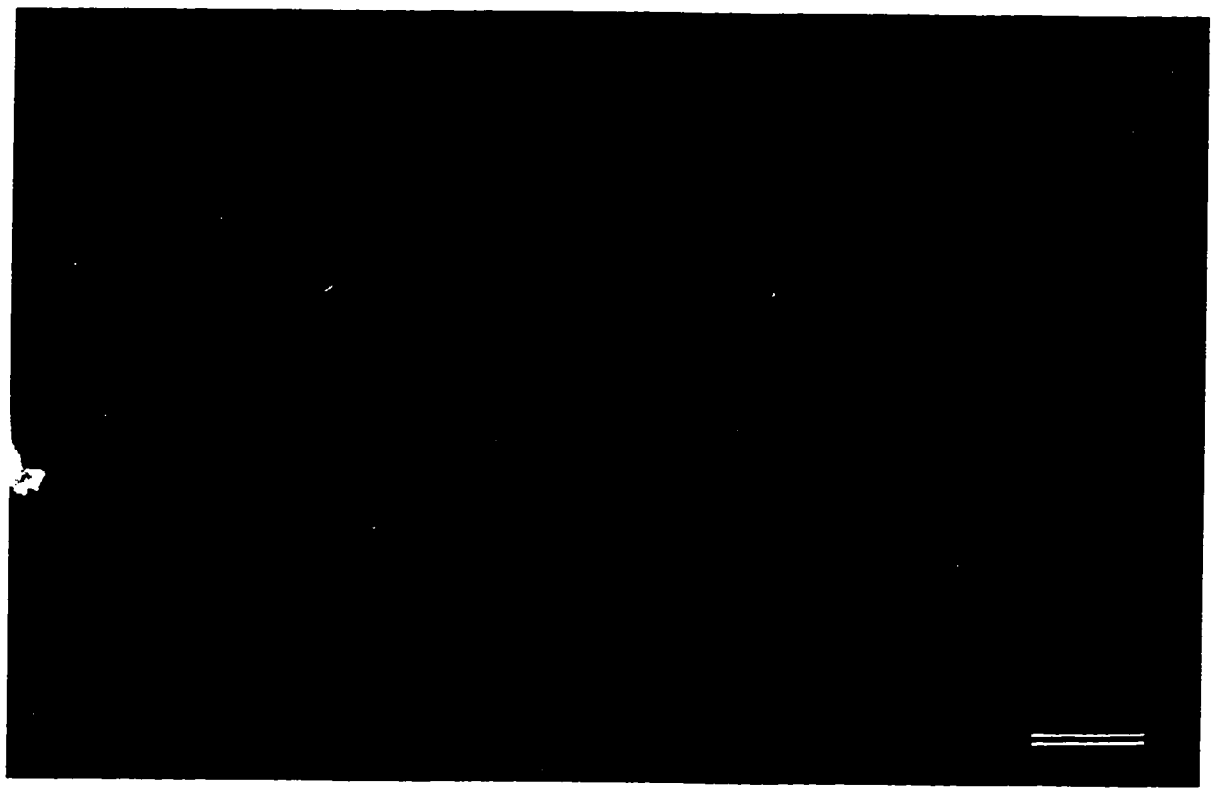

Figure B.4: A metaphyseal vascular erosion of the 21 day chondroepiphysis stained with anti-thrombomodulin and viewed under epi-fluorescent illumination. Bar Marker = 50 μm.

advancing edge of vasculature appears as a capillary glomus which burrows into the cartilaginous anlage proceeding towards the centre of the epiphysis. Canals are often mushroom-shaped at their blind-ends, confirming a broad front of degradative enzymatic action at the glomus-shaped, angiogenic capillary bed. Anti-thrombomodulin immunofluorescence highlights the endothelial cells, not only in the epiphysis, but in the surrounding adjacent joint connective tissues such as ligament, tendon and bone. Subsequent haematoxylin and eosin staining confirmed the surrounding environment of hypertrophic chondrocytes in relation to the onset of cartilaginous erosion by the canals.

Cartilage canals are apparent by day 21, and progress in number and distance from the epiphyseal periphery through to 28 days (Appendix C). The majority enter the epiphysis radially, and extend linearly towards the centre. Deep within the centre of the epiphysis, canals are often seen entering through the intercondylar notch, and at times communicating between the epiphysis and the shaft of the long bone, namely through the growth plate (Appendix C).

At this point in time, vessels begin to meet in the epiphyseal centre, and the first signs of calcification are evidenced as dark granules under light microscopy, originating centrally. From days 29 through to birth (approximately day 30), and for a number of days beyond, the secondary ossification centre forms as a cavitating process of central epiphyseal cartilage erosion and extensive calcification.

Transplantation Experiments

Four donor rabbit chondroepiphyses at 19 days post-insemination were overlayed onto the CAM of four donor eggs. They were subsequently removed and examined after 12 hours (ie. 19.5 days), 48 hours (21 days), 72 hours (22 days), and 120 hours (24 days).

The first chondroepiphysis remained avascular after 12 hours of contact with the CAM. No alterations in surrounding CAM vasculature or cartilaginous anlage of the chondroepiphysis could be discerned under the dissecting microscope, and later during histological examination.

When the second chondroepiphysis was examined 48 hours after introduction, it macroscopically appeared to be vascularized and angiostimulatory in nature (Figure B.5). Blood vessels from the surrounding CAM had sprouted new branches which grew directly towards the chondroepiphysis and surrounded it . The chondroepiphysis itself had grown somewhat, and had become embedded within the collagenous matrix of the CAM, resulting in a living chimaeric construct. Microscopically, neovascularization was seen to be contained around the periphery of the chondroepiphysis (Appendix C). No vascular erosions could be evidenced into the matrix of the chonroepiphysis itself, as witnessed in the embryological development in the fetal rabbit. Many nucleated chick blood cells could be seen in proximity to the chondroepiphysis, and chick leukocytes were amassed in areas of vasculature surrounding the chondroepiphysis, suggesting some form of immune response against the donor rabbit tissue. The chondroepiphysis appeared healthy,

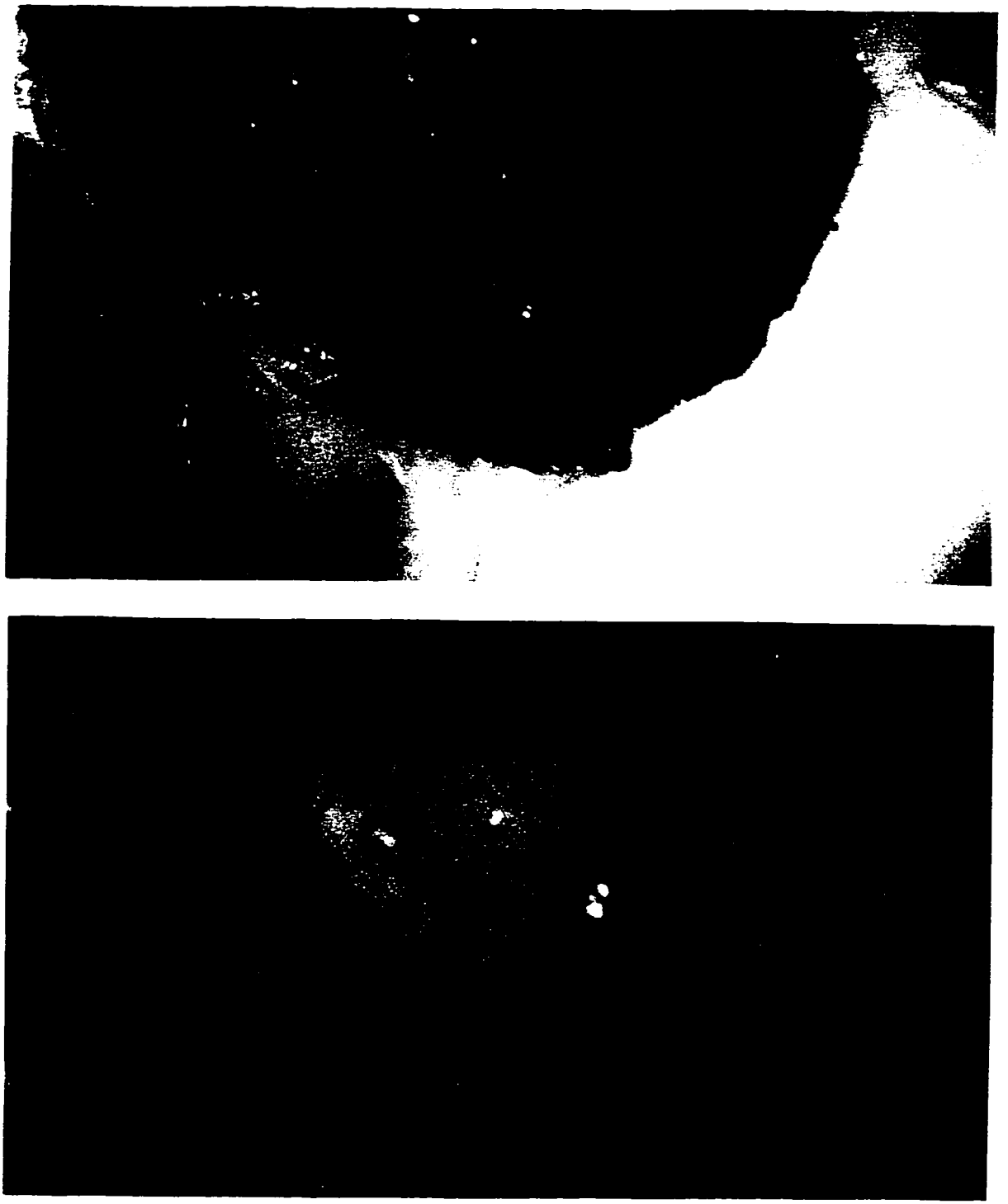

Figure B.5: Angiogenesis from the chorio-allantoic membrane directed towards a 48 hour implant of 20 day chondroepiphysis. Magnifications x6.5 and x20 respectively.

with patently staining chondrocytic nuclei and some chondrocytic growth around the periphery. This growth, however, was not tightly regulated, and some disintegration of epiphyseal structure could be discerned at the edges. Cartilaginous growth appeared in patches, and merged with the collagenous matrix of the surrounding chick CAM.

The third chondroepiphysis, examined at 72 hours post-introduction, presented a very similar picture to that seen at 48 hours. A definite angiostimulatory response had occured, with the chondroepiphysis becoming surrounded by neovascular growths from the surrounding CAM (Figure B.6). Microscopically, no vascular erosions were evidenced into the chondroepiphysis itself, however many small capillaries looped around and butted into the chonroepiphysis. Chick leukocytes could be seen in association with the chondroepiphysis, and disintegration of epiphyseal structure was apparent.

The final chondroepiphysis, examined 120 hours post-introduction, had begun to fragment. Angiostimulatory growth surrounded the remnant chondroepiphyseal plugs, which had become incorporated into the chick CAM. No great increase in epiphyseal size was noted, indicating cessation of regulated developmental growth of the implant. Microscopically, viable chondrocytic nuclei were evident, however were surrounded by empty spaces and an evident decrease in chondrocyte numbers. Chick leukocytes were seen surrounding the periphery of the plugs, but were not readily observed in the remnant chondroepiphyseal implants.

Figure B.6: Angiogenesis from the chorio-allantoic membrane directed towards a 72 hour implant of 20 day chondroepiphysis. Magnifications x6.5 and x20 respectively.

DISCUSSION

This investigation confirms the time-course of developmental angiogenesis in the chondroepiphysis of the fetal NZW rabbit. At 20 days post-insemination, breaks in the continuity of the perichondrium are evident in the distal femoral head of the fetal rabbit as blood vessels invade the chondroepiphysis in response to some angiogenic stimulus. Previous investigations have timed this event to a fetal body mass of 2.94g, and our investigation further defines this event at a C-R length of 22mm. By 21 days, cartilage canals are apparent and the vascular substance within these erosions stain positively with anti-thrombomodulin immunofluorescence. It is evident, histologically, that the leading edge of angiogenesis within the canal is an expanding glomus-shaped capillary bed, which serves as the turn-around point for blood flow within the blind-ended canal.

Fetal growth is exponential, and by 30 days the fetus weighs 40.8g with an average C-R length of 44mm. The cartilage canals, with centrally placed blood vessels, have progressed towards the centre of the chondroepiphysis and met, forming an erosive cavern. Calcification is apparent, as the secondary ossification centre forms, and the blood vessels lie freely in the ossification centre once the cartilage has been resorbed.

Previous investigators have stressed the importance of a critical epiphyseal size, which triggers the vascular invasion. As blood vessels are a major source of nutrients, oxygen, and waste removal, they may well be required on purely metabolic grounds to facilitate the 25-fold increase in volume of hyaline cartilage

seen after vascular invasion. Vascular invasion of the chondroepiphysis is always associated with maturation of the chondrocytes. Therefore, it is reasonable to hypothesize that some angiostimulatory molecule(s) are secreted by these cells once they have reached a certain state of differentiation. Previous studies by Levene involved the implantation of rat chondroepiphyses into an incised flap of the rat kidney capsule (Levene, 1964). Results suggested an angiogenic response towards the implant with vascular invasion of the chondroepiphysis in one instance. In our study, we introduced chondroepiphyseal implants onto the CAM of an egg, a classical angiogenesis assay. Coinciding with the time-course for vascular invasion in the fetal rabbit chondroepiphysis, an angiostimulatory phenomenon was exerted by the implanted chondroepiphysis, and directed angiogenesis occured in the CAM. This phenomenon strongly supports the presence of a powerful angiogenic molecule(s) originating from the chondroepiphysis during development.

This study confirms the usefulness of developmental chondroepiphyseal angiogenesis for studying the angiogenic process in joint connective tissues. The cartilaginous anlage is initially devoid of blood vessels, and gradually becomes vascularized through the classical process of angiogenesis - from initiation, through division and elongation, to complete vascular patency and blood flow. The observations are not compromised by underlying inflammation or injury, and associated regulators of these processes. As such, the use of this angiogenic model may assist in the search for regulatory molecules to curb destructive

angiogenesis, such as that seen in rheumatoid arthritis, which physically destroys joint connective tissue structures.

Although transplantation experiments of rabbit tissues onto the chick CAM proved useful in detecting the presence and expressed time-course of an angiostimulatory molecule(s) being produced within the chondroepiphysis, there was clearly many compromising factors to preclude immediate use of this chimaeric construct for further conclusions regarding angiogenesis. Firstly, chondroepiphyseal development once removed from its original environment was clearly retarded, as evidenced by the lack of exponential growth within the chick egg. Secondly, although a clear angiostimulatory event had occurred, with chick blood vessels dividing and growing towards the chondroepiphyseal implant, no vascular erosion or cartilage canal formation was witnessed. This differs dramatically from the developmental model, and from the rat chondroepiphyseal implants into rat hosts (Levene, 1964), and implies incompatability between the genetic complement of the chicken and the rabbit. The failure of avian-mammalian chimaeric constructs has previously been reported in the literature, and there are obvious limitations to the scope of experimental use for this model (Le Douarin et al, 1996). On a similar note, evidence of an immune response was suggested by the preponderance and directed accumulation of chick leukocytes around the rabbit implant, and by the loss of cell number and disintegration of the chondroepiphysis itself. Of interest would be to determine the mechanisms involved in loss of

chondroepiphyseal cell number, as the chimaeric construct may prove a useful model to further study processes such as apoptosis in articular cartilage.

Thus, in conclusion, angiogenic events in the developing articular chondroepiphysis are coordinated in a stepwise manner, and occur in response to the expression of a resident angiostimulatory event. Developing cartilage canals provide a unique opportunity to observe the classical steps involved in angiogenesis, without the complication of background pre-existing vessels, or underlying pathophysiology. It may therefore prove useful for studying the angiogenic process in joint connective tissues, and in elucidating natural mechanisms for exerting regulatory control in cases of disease.

APPENDIX C.1

DIGITIZED SLIDES OF CARTILAGE CANALS TRAVERSING A SERIALLY SECTIONED DISTAL FEMORAL EPIPHYSIS FROM A 29 DAY KIT

The purpose of this appendix is to provide a visual insight into the three-dimensional nature of cartilage canal erosions. The following slides represent digitized microscopic "fields-of-view" from transilluminated 20 μm serial sections of the distal femoral epiphysis in a 29 day kit. At this time-point, developing blood vessels have eroded through to the centre of the epiphysis, and the secondary centre of ossification has begun to form.

Cartilage canals appear as "holes" within the dense cartilaginous matrix, and appear white due to the transmitted brightfield illumination. As the slides progress towards the epiphyseal centre, it is evident how comprehensive the canal system is deep within the epiphysis at this early developmental time-point.

All slides have been digitized at a magnification of x15.

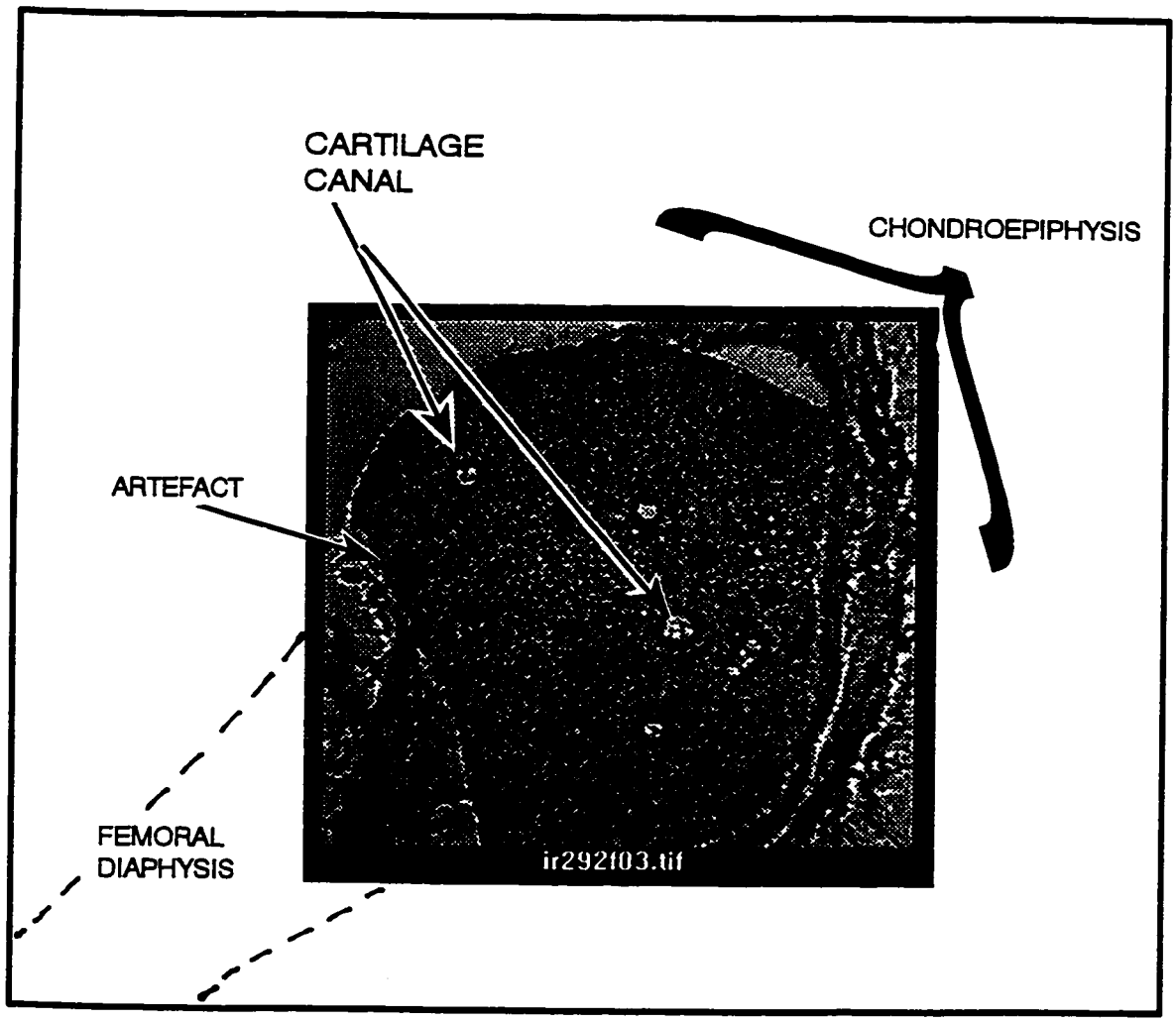
CARTILAGE
CANAL
CHONDROEPIPHYSIS
ARTEFACT
FEMORAL
DIAPHYSIS
ir292f03.tif

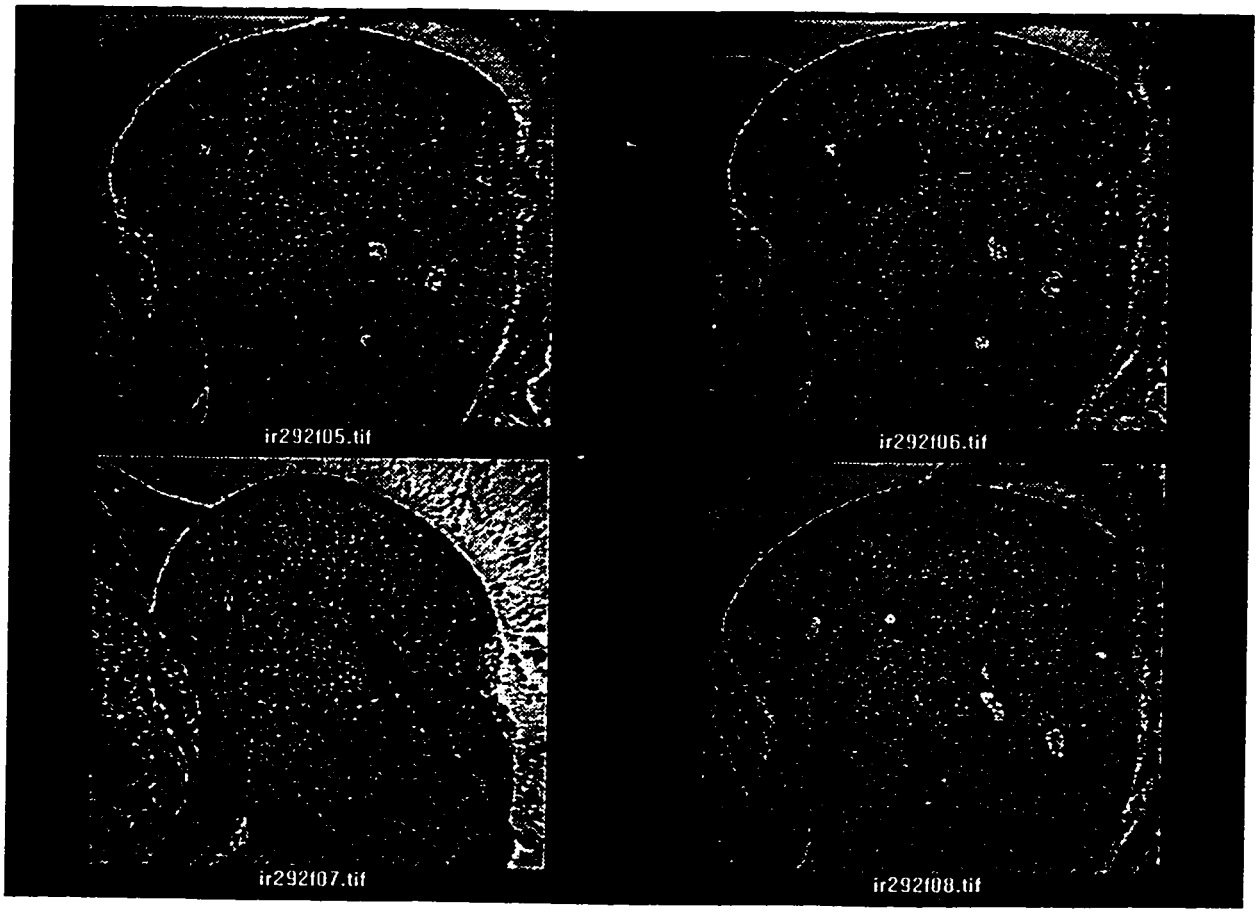
ir292105.tif
ir292106.tif
ir292107.tif
ir292108.tif

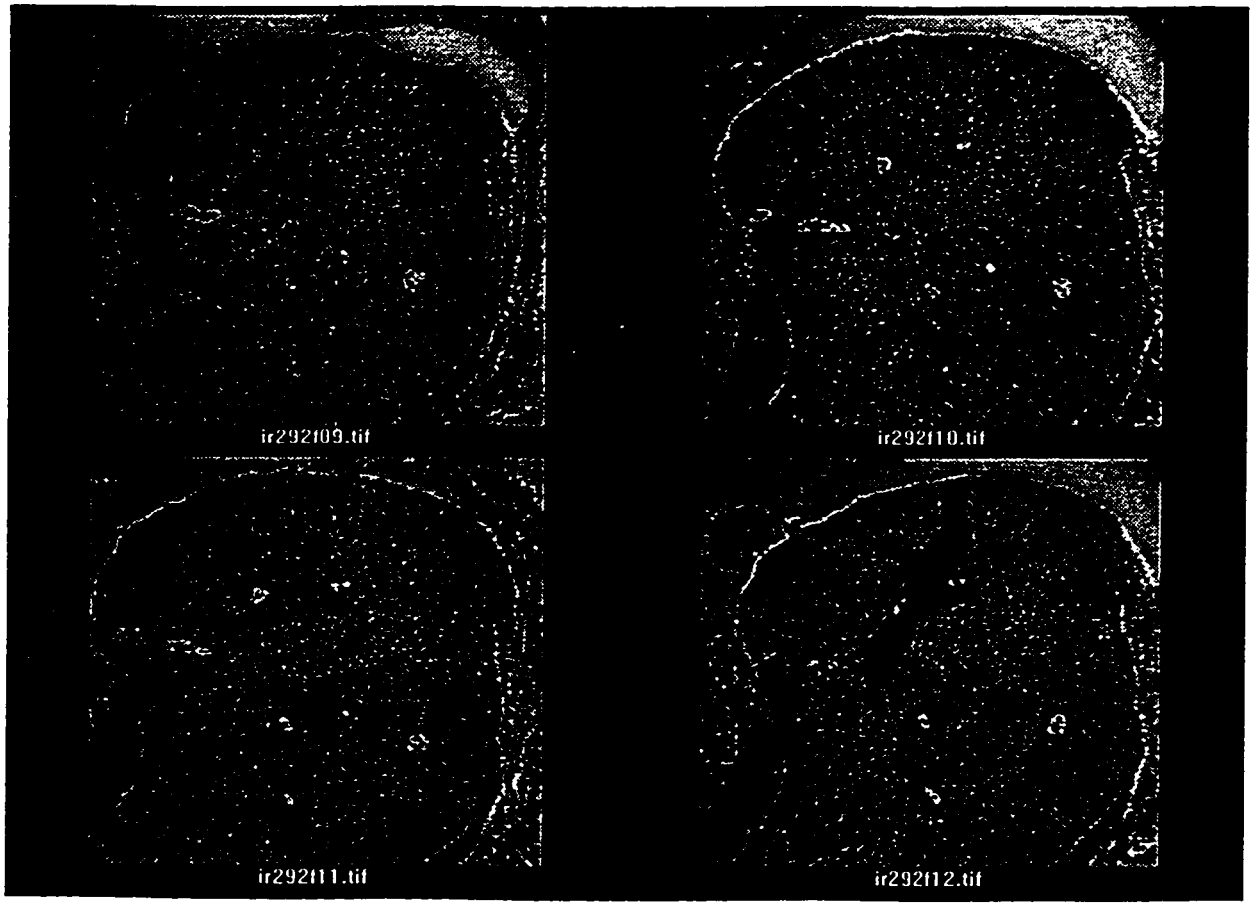
ir292f09.tif
ir292f10.tif
ir292f11.tif
ir292f12.tif

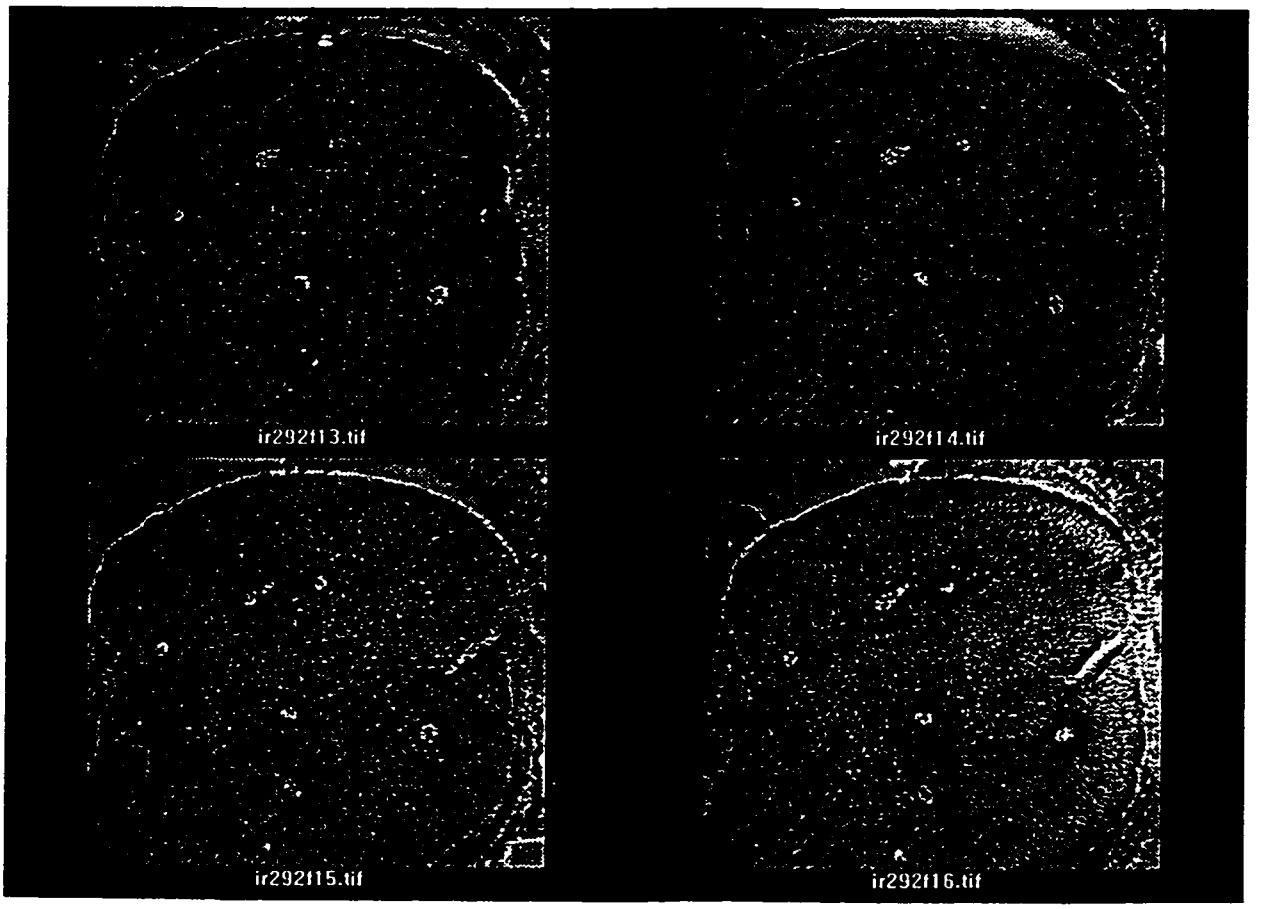
ir292f13.tif
ir292f14.tif
ir292f15.tif
ir292f16.tif

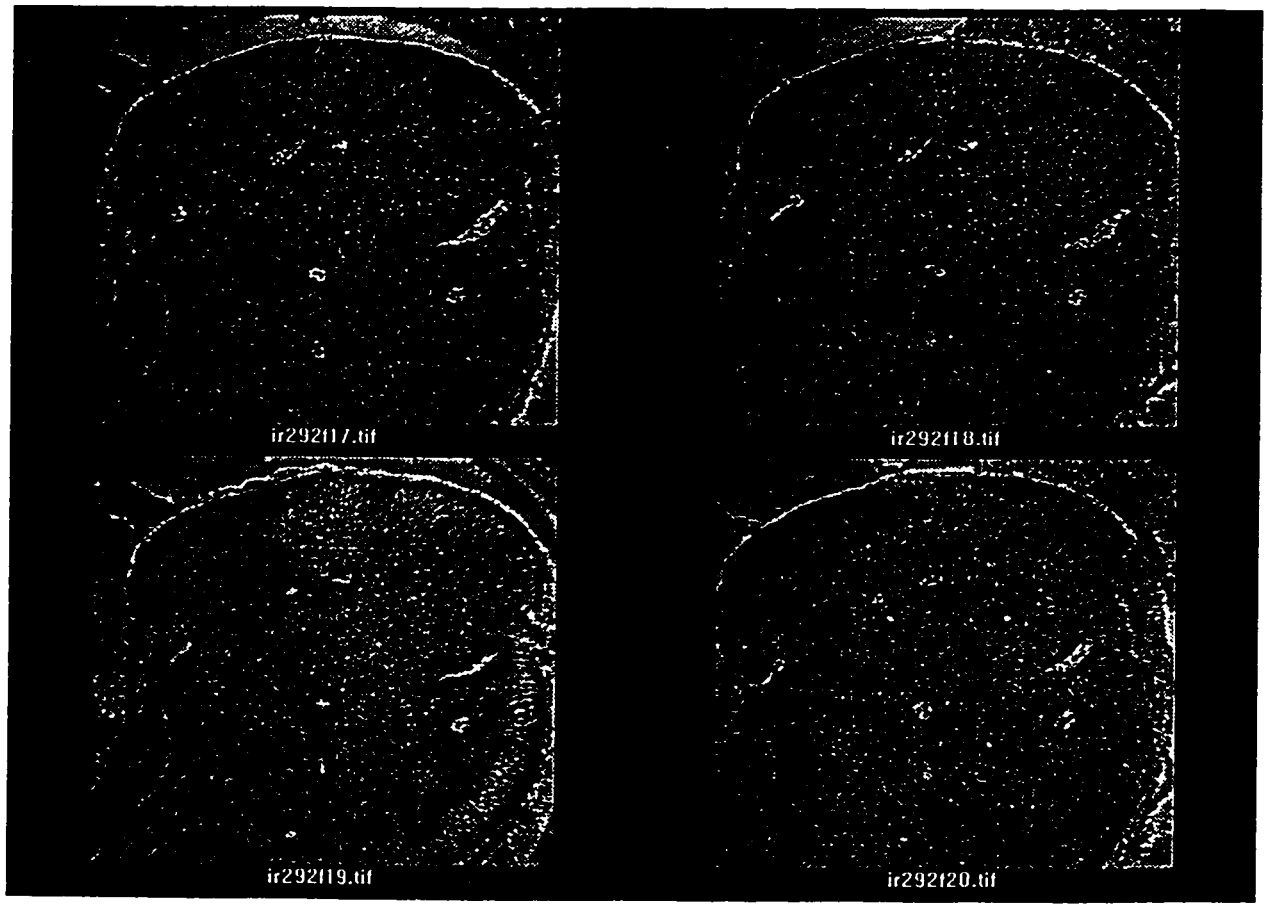
ir292f17.tif
ir292f18.tif
ir292f19.tif
ir292f20.tif

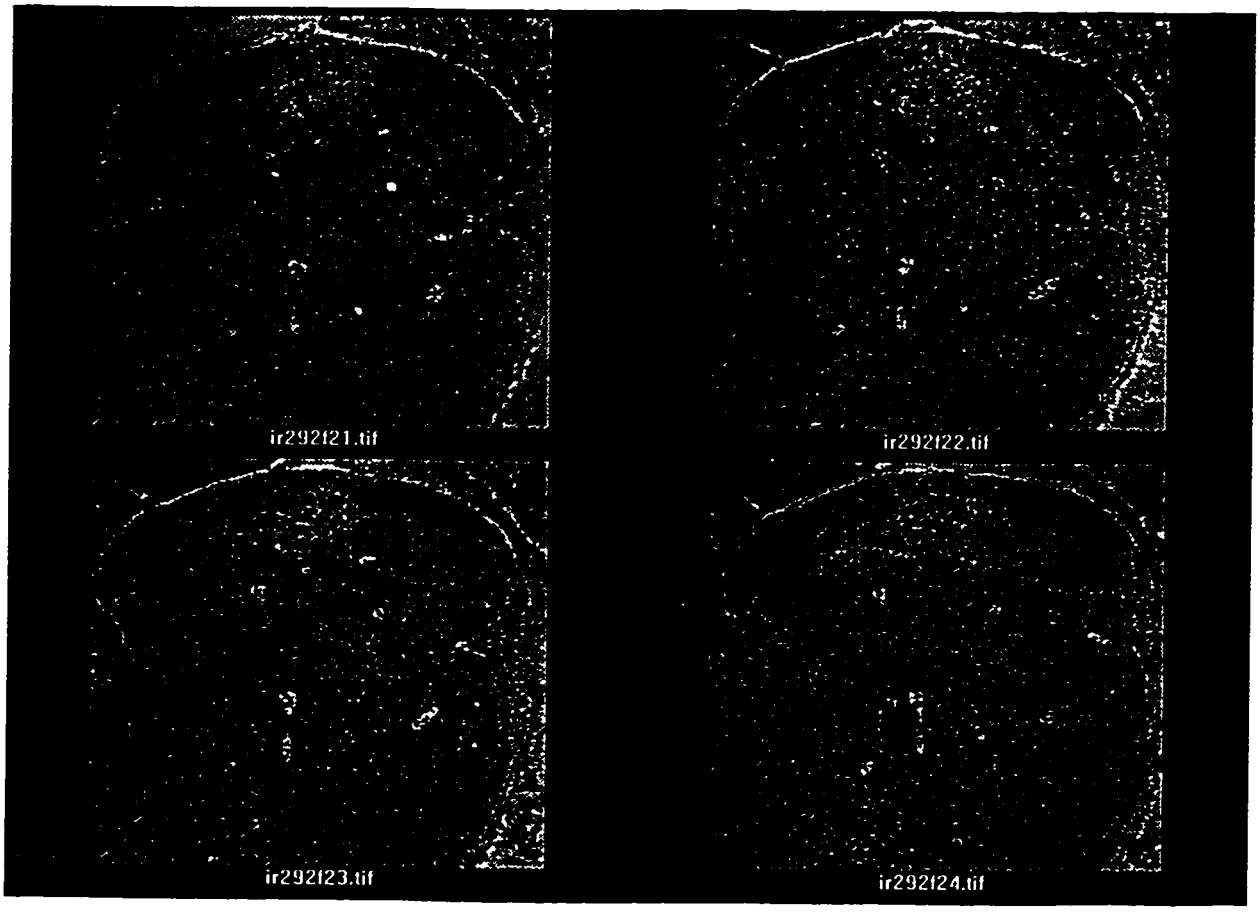
ir292f21.tif
ir292f22.tif
ir292f23.tif
ir292f24.tif

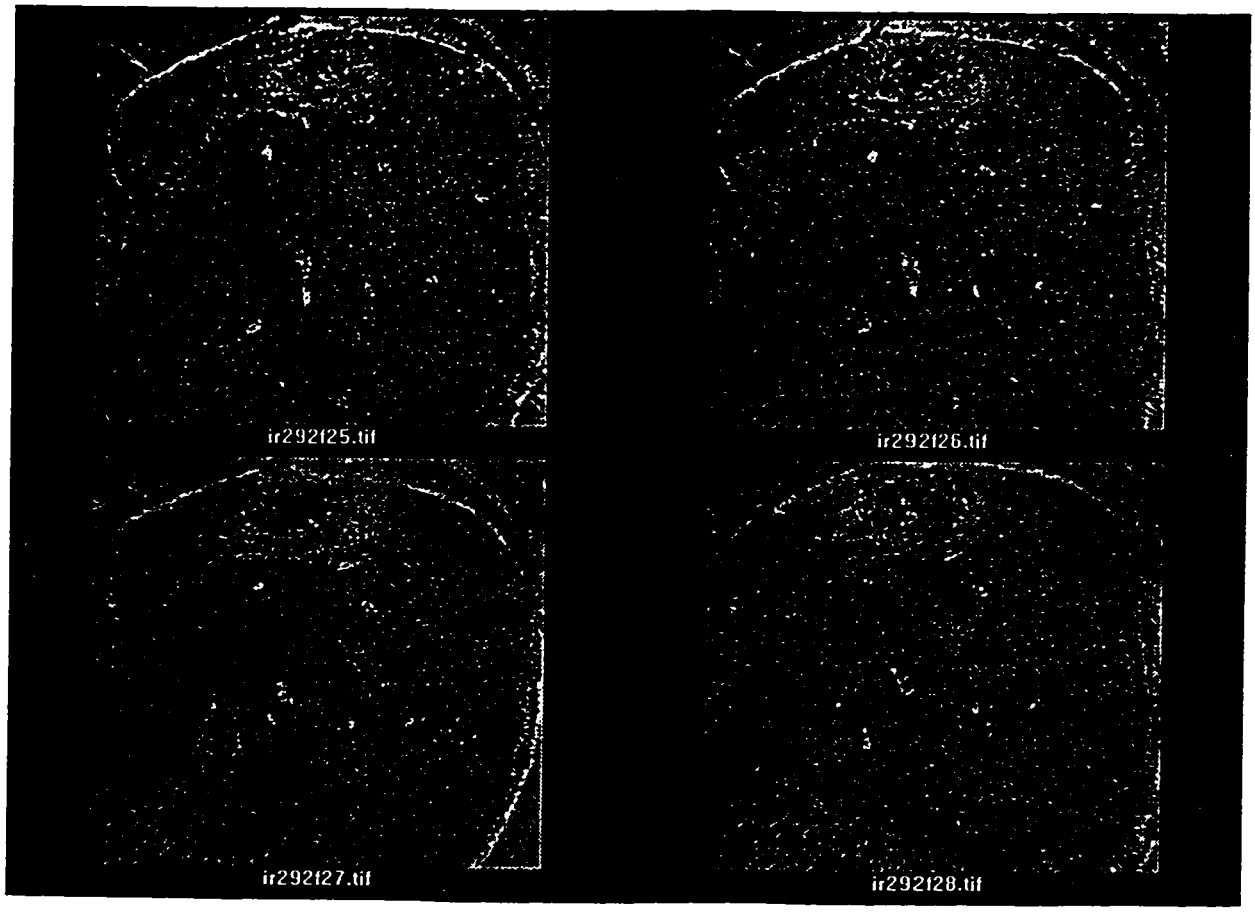
ir292f25.tif
ir292f26.tif
ir292f27.tif
ir292f28.tif

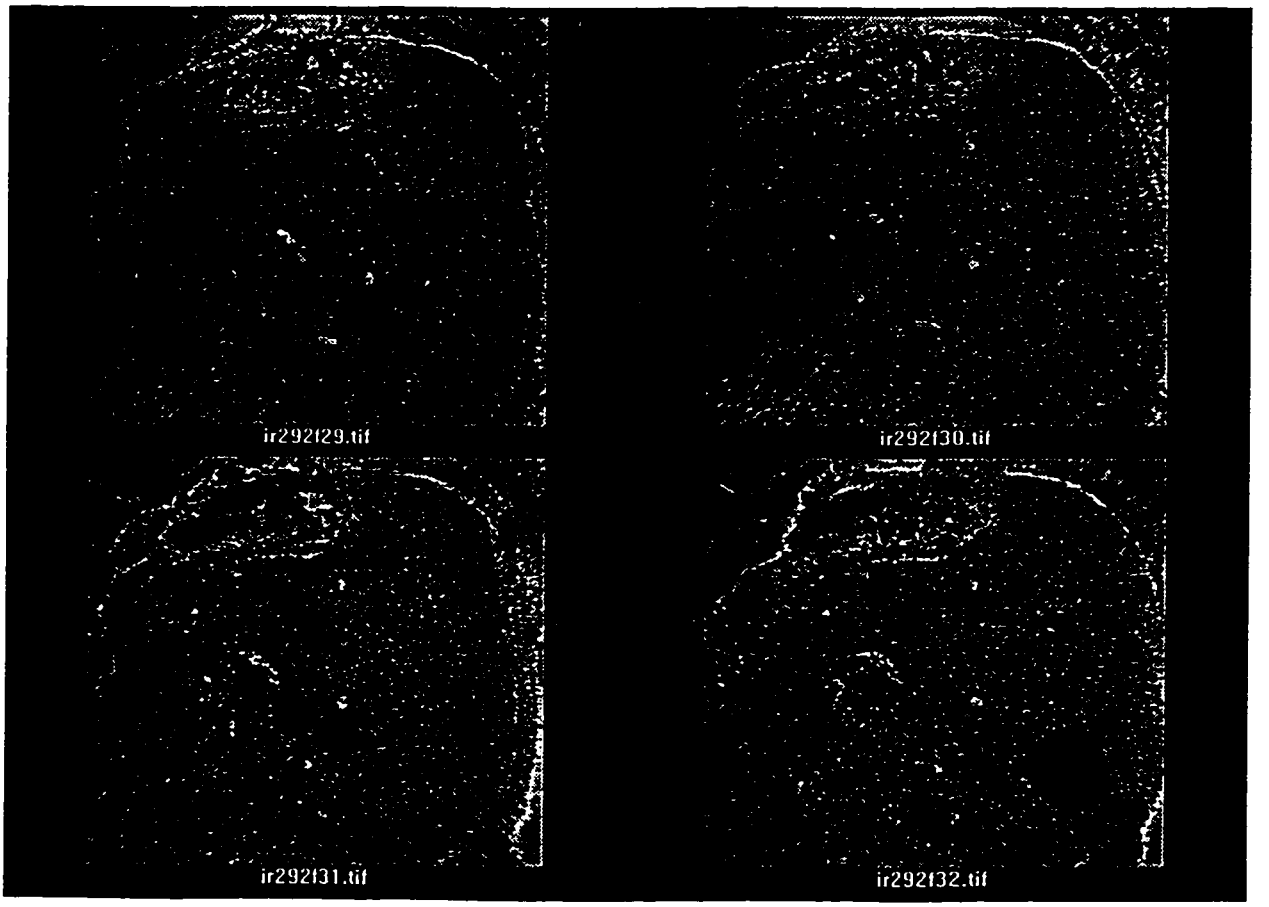
ir292f29.tif
ir292f30.tif
ir292f31.tif
ir292f32.tif

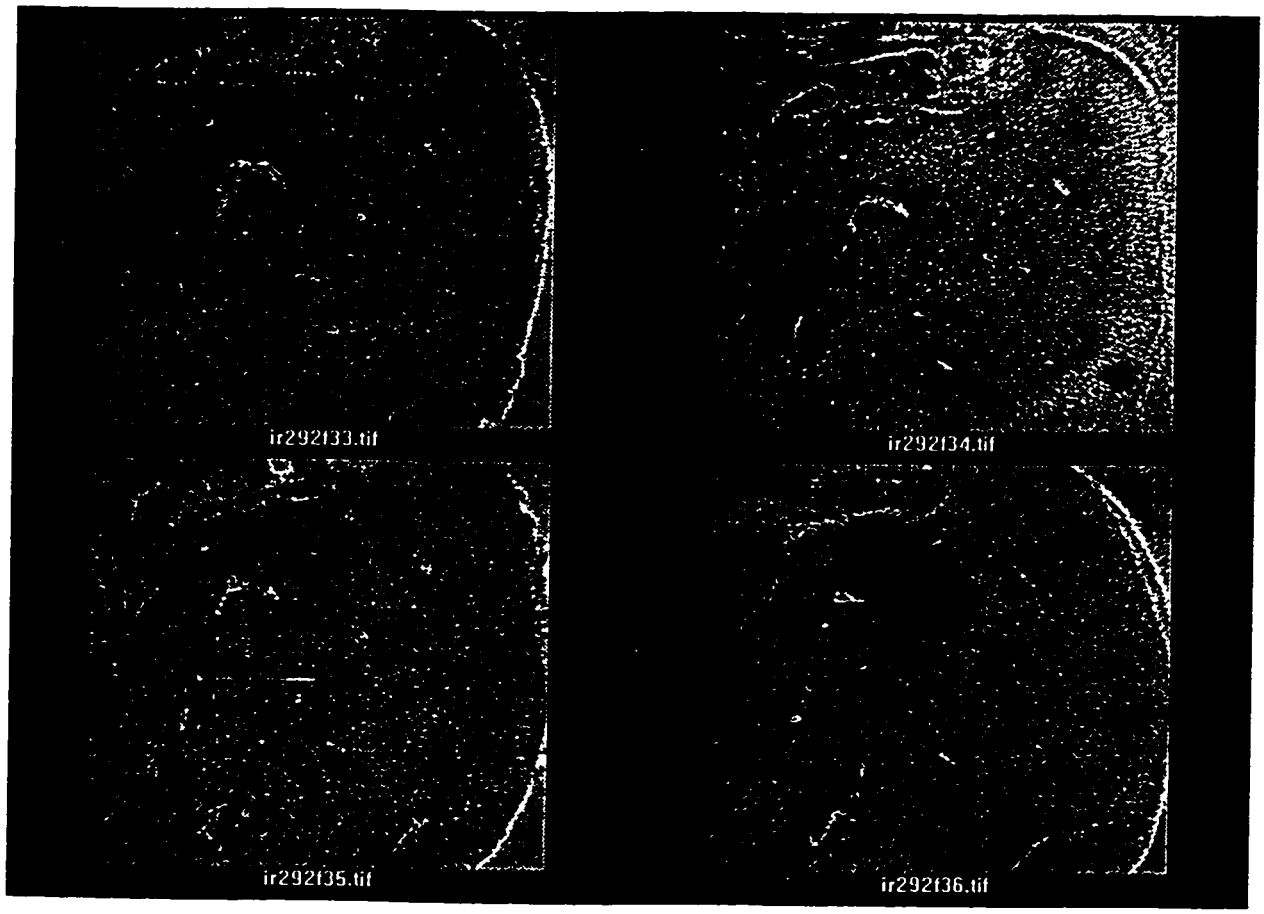
ir292f33.tif
ir292f34.tif
ir292f35.tif
ir292f36.tif

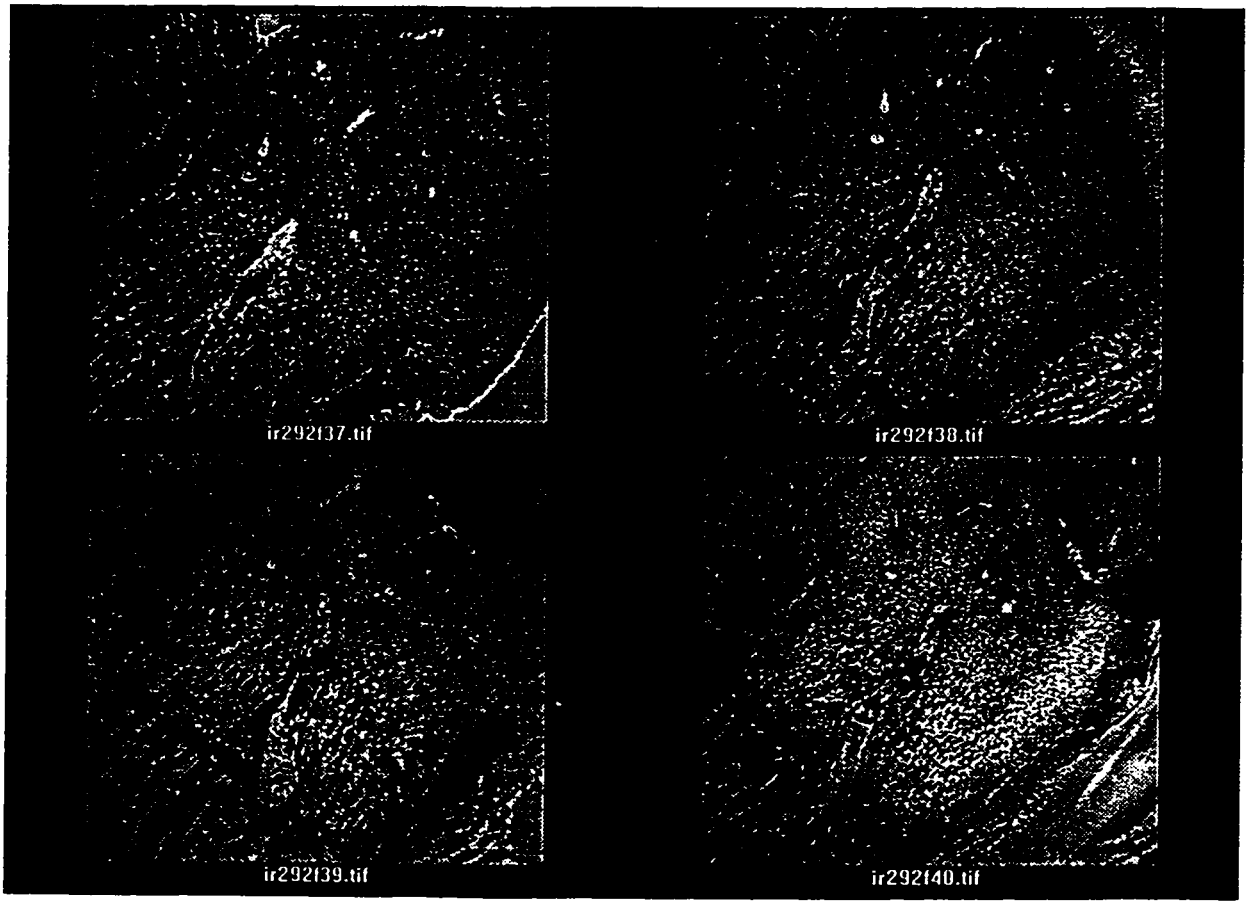
ir292f37.tif
ir292f38.tif
ir292f39.tif
ir292f40.tif

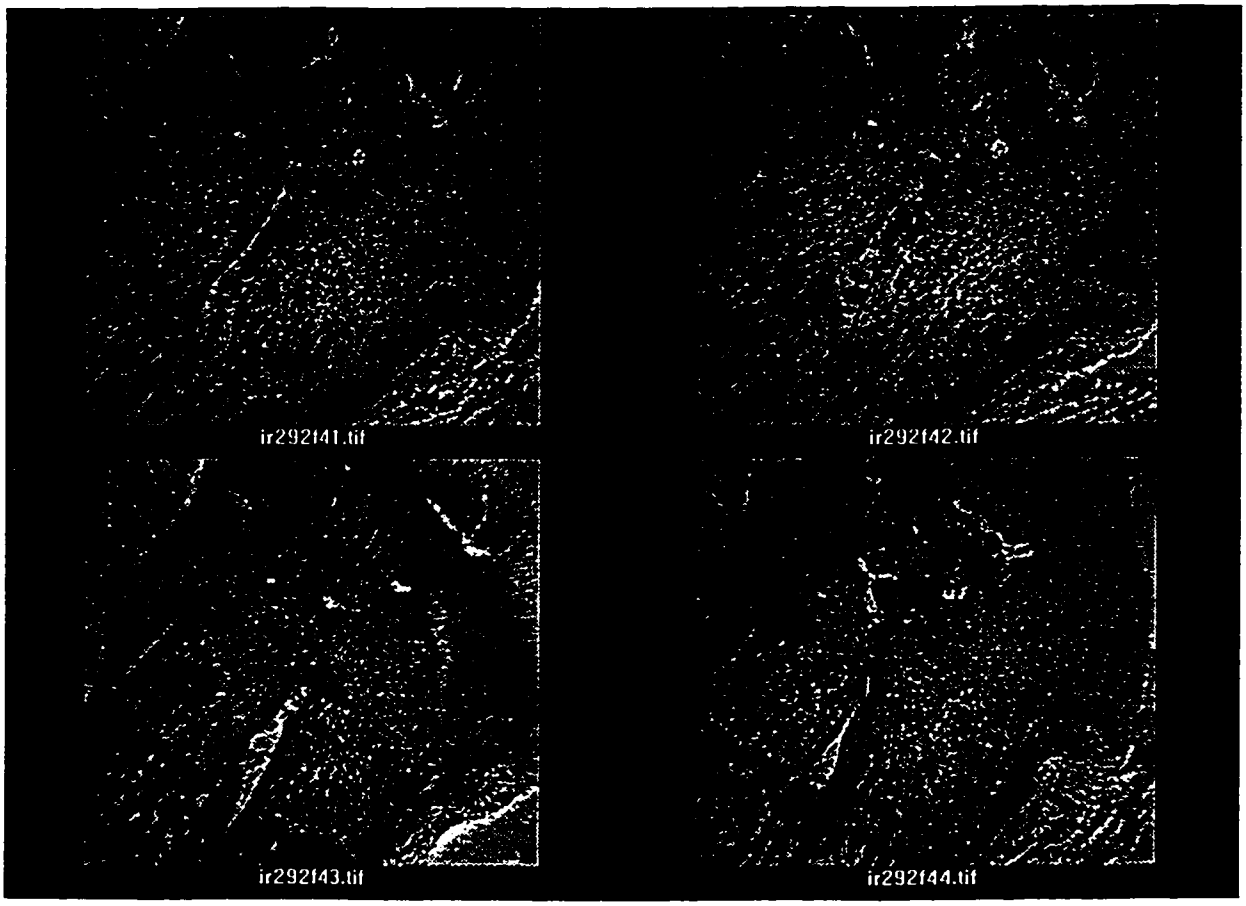
ir292f41.tif
ir292f42.tif
ir292f43.tif
ir292f44.tif

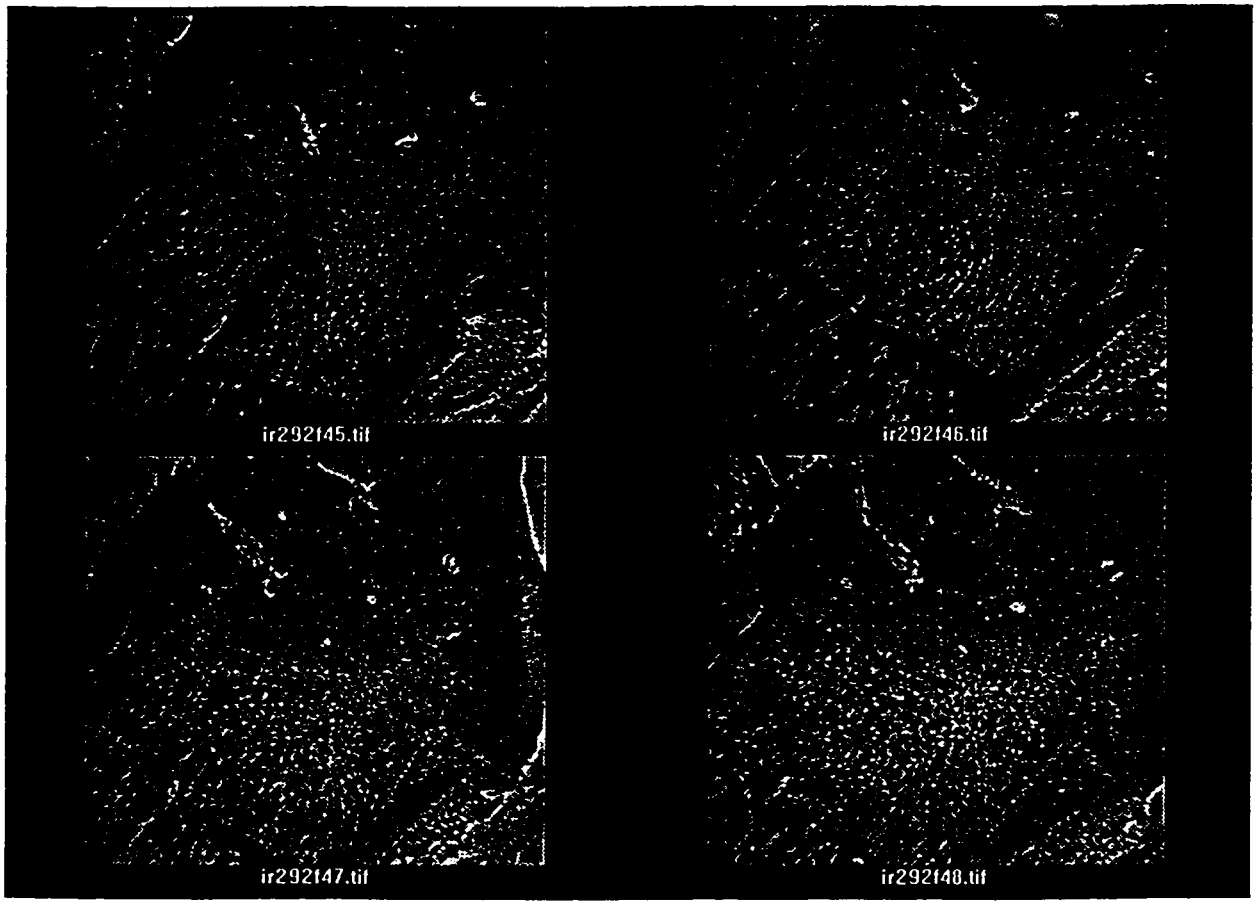
ir292f45.tif
ir292f46.tif
ir292f47.tif
ir292f48.tif

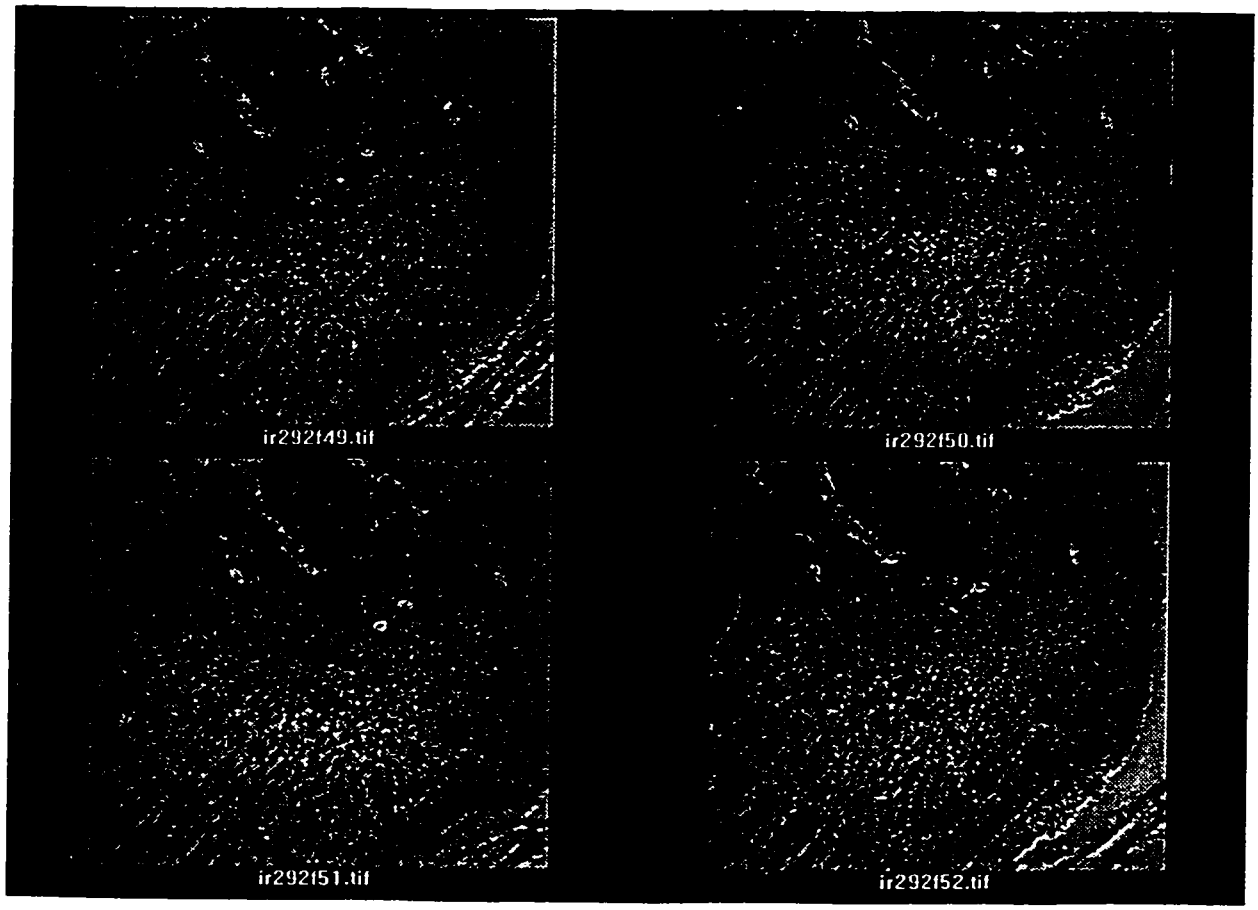
ir292f49.tif
ir292f50.tif
ir292f51.tif
ir292f52.tif

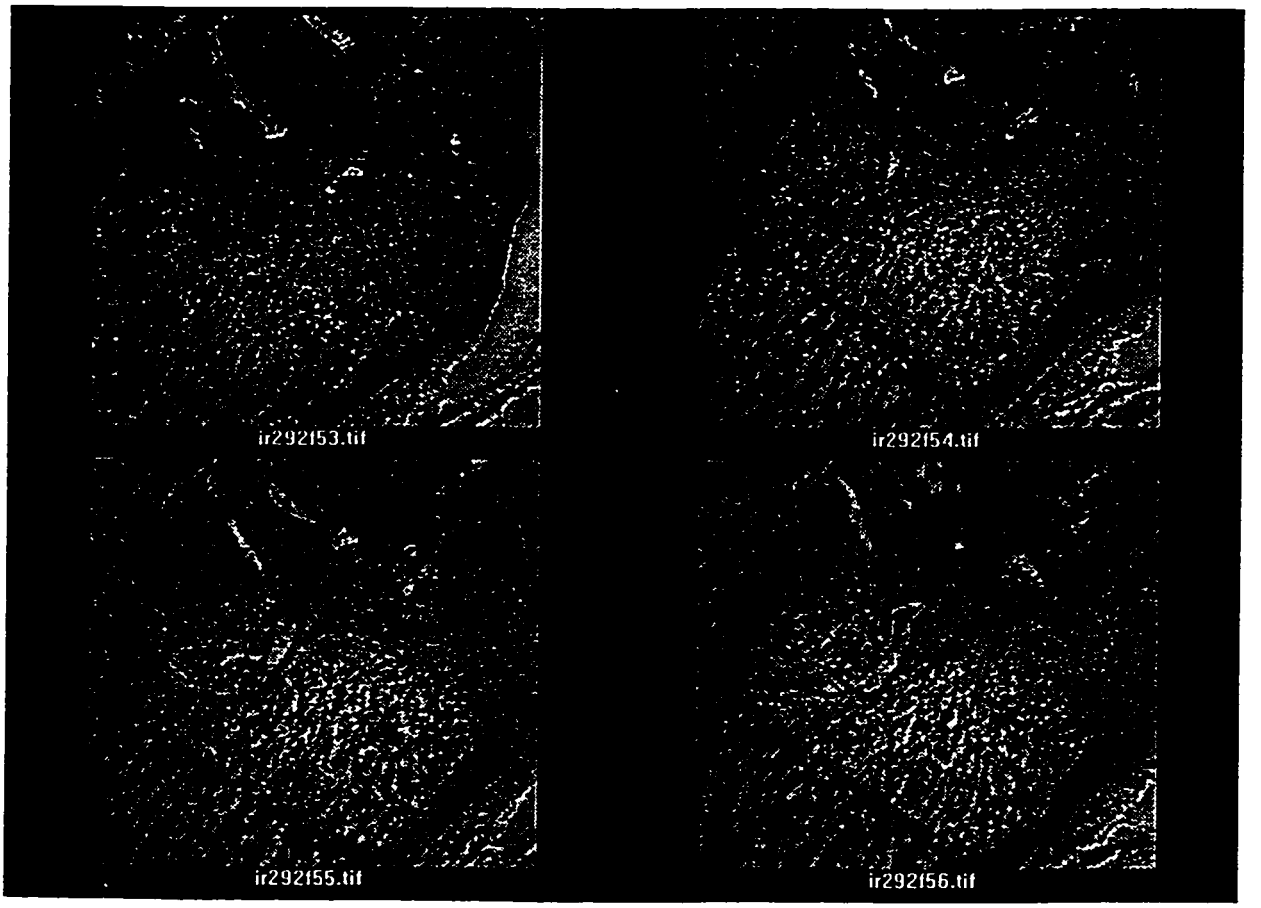
ir292f53.tif
ir292f54.tif
ir292f55.tif
ir292f56.tif

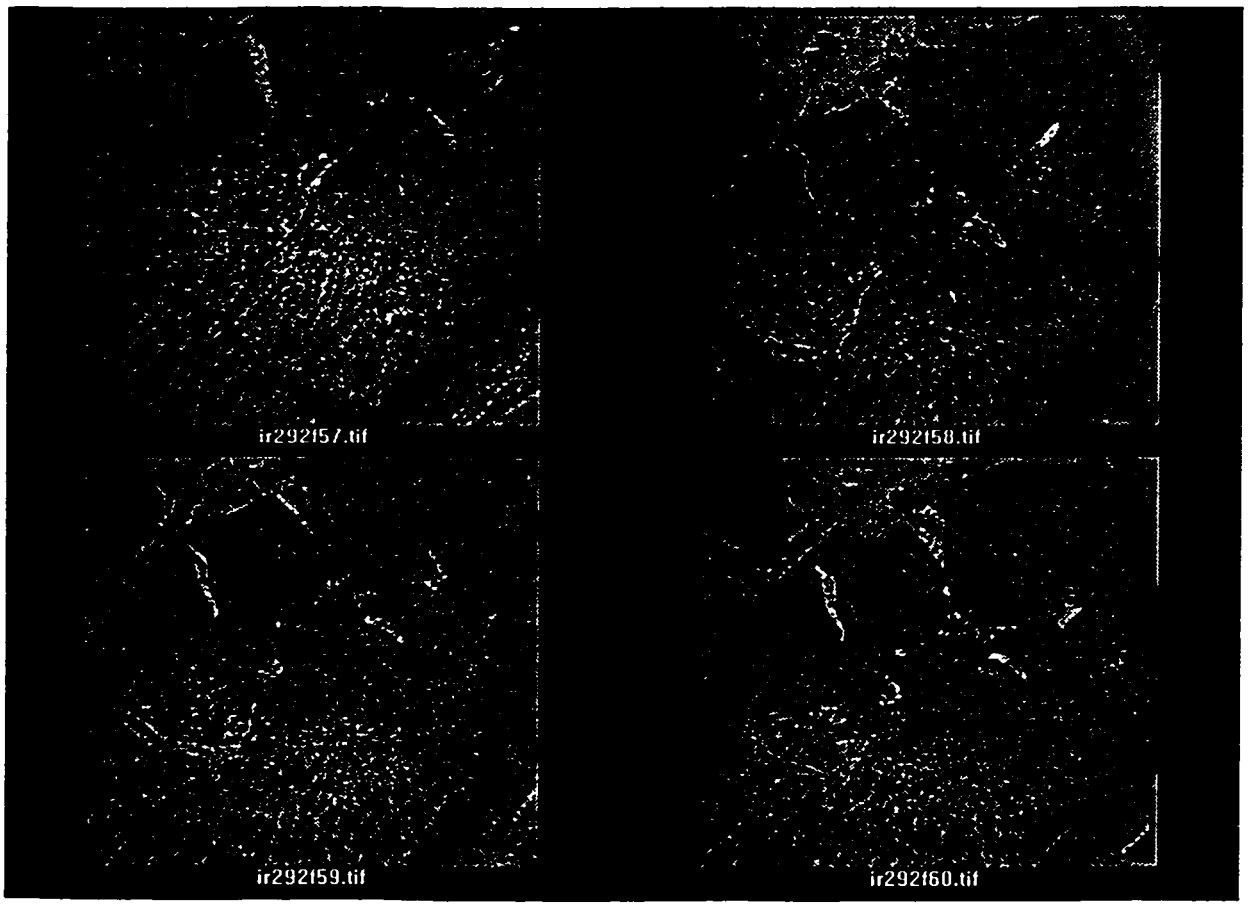
ir292157.tif
ir292158.tif
ir292159.tif
ir292160.tif

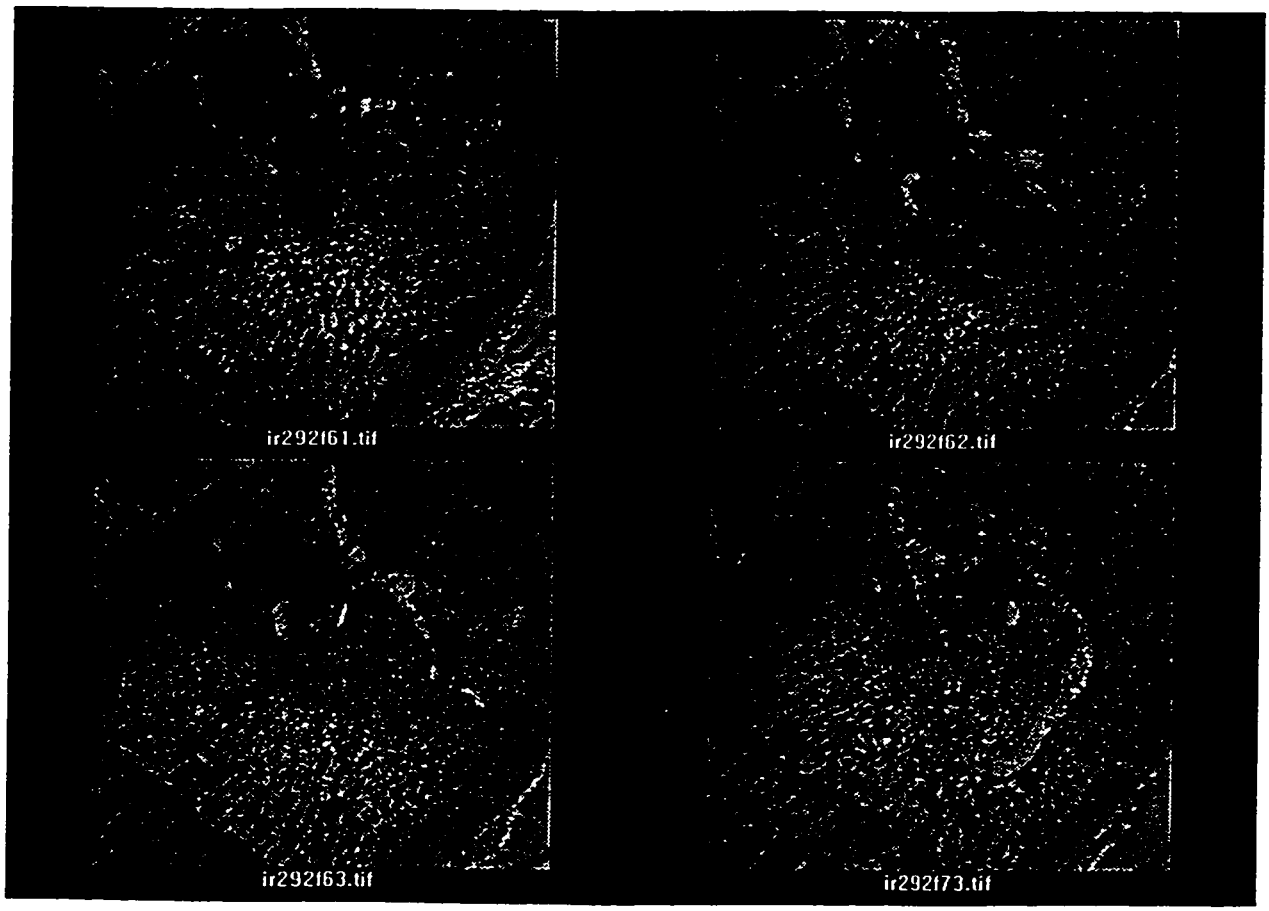
ir292f61.tif
ir292f62.tif
ir292f63.tif
ir292f73.tif

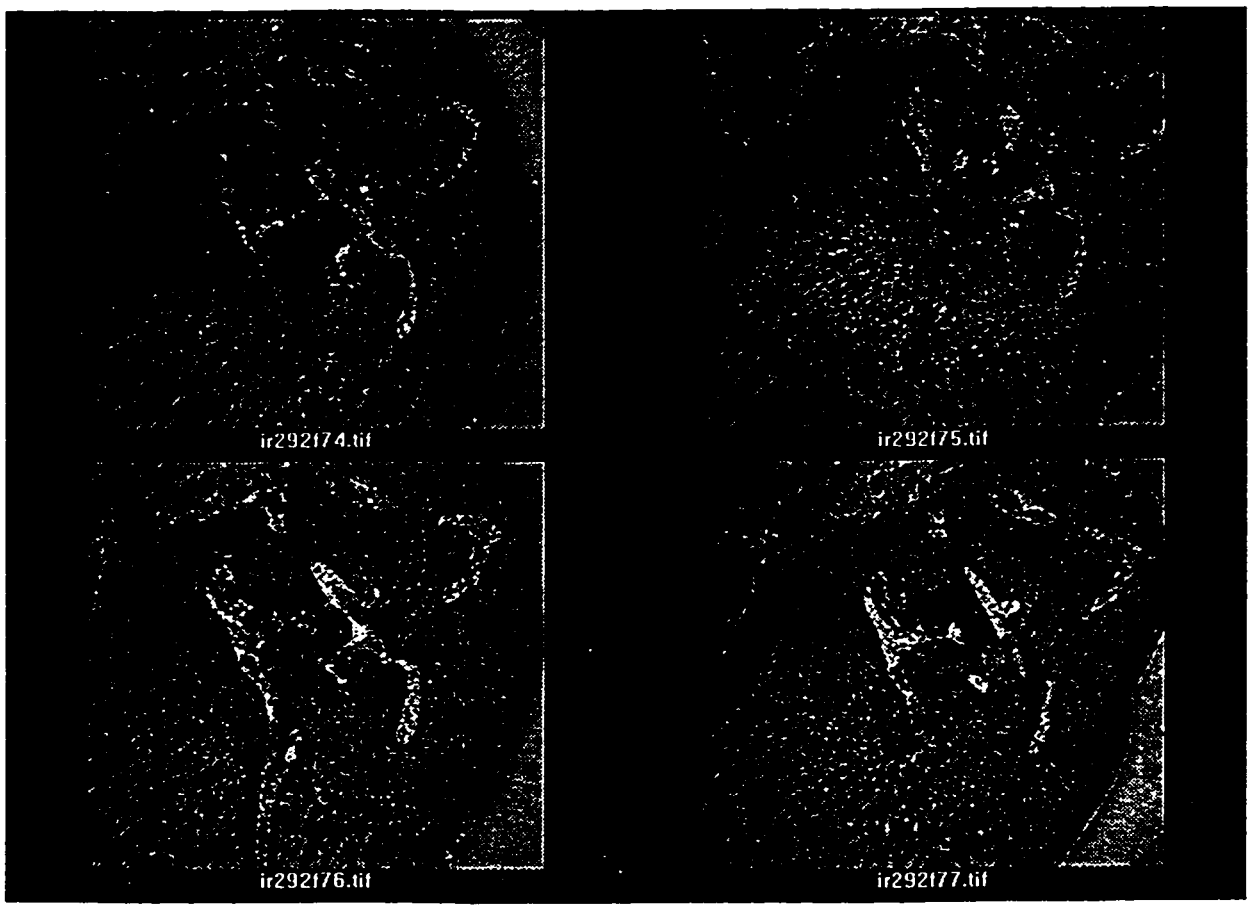
ir292f74.tif
ir292f75.tif
ir292f76.tif
ir292f77.tif

APPENDIX C.2

DIGITIZED SLIDES OF SERIALLY SECTIONED DISTAL FEMORAL EPIPHYSEAL TRANSPLANT IN THE CHICK CHORIO-ALLANTOIC MEMBRANE

This appendix illustrates the lack of cartilage canal development within the rabbit chondroepiphysis when placed on the chick chorio-allantoic membrane. The specimen corresponds to that seen in Figure B.5 on page 106. Although blood vessels surround the epiphysis in a loose connective tissue matrix (seen as the surrounding wispy-grey material), no classical canalicular erosions are evident. There is a faint suggestion of partial vascular erosion (seen clearly as a finger-like indentation in slide "etr11009.tif" on page 134, to the top-left of the chondroepiphysis). However this proved to be the only occaision in all three transplanted samples of rabbit chondroepiphyses.

All slides have been digitized at a magnification of x15.

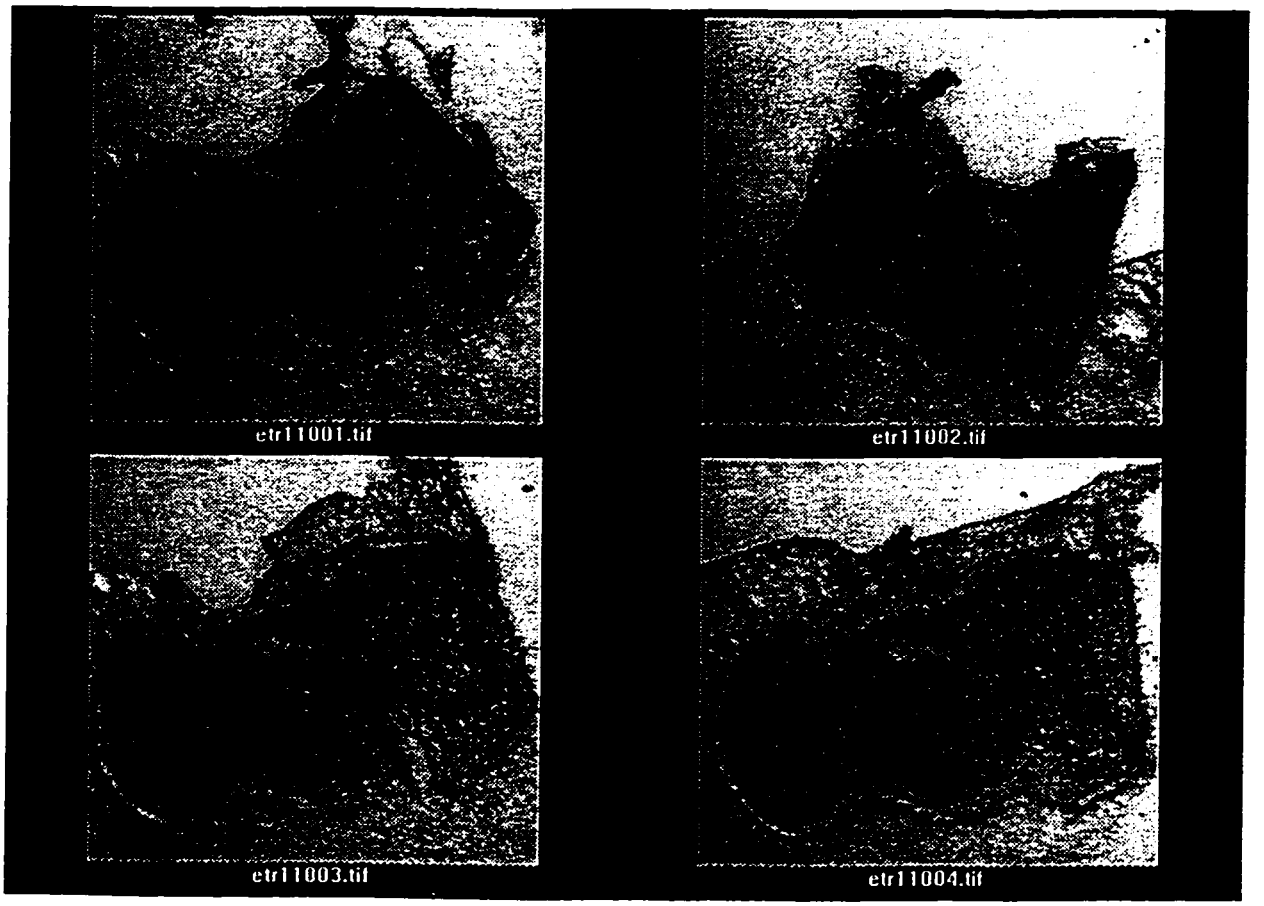
etr11001.tif
etr11002.tif
etr11003.tif
etr11004.tif

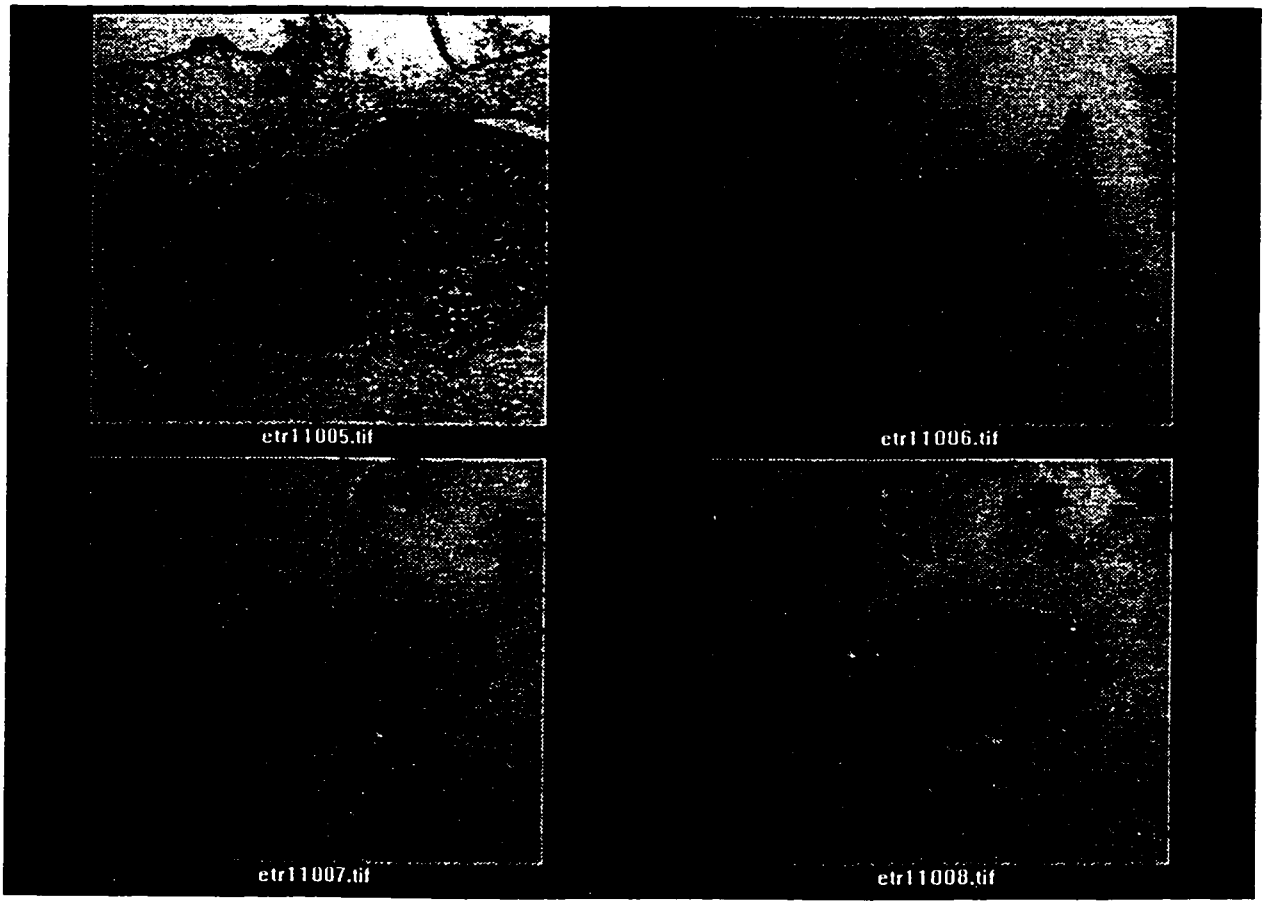
etr11005.tif
etr11006.tif
etr11007.tif
etr11008.tif

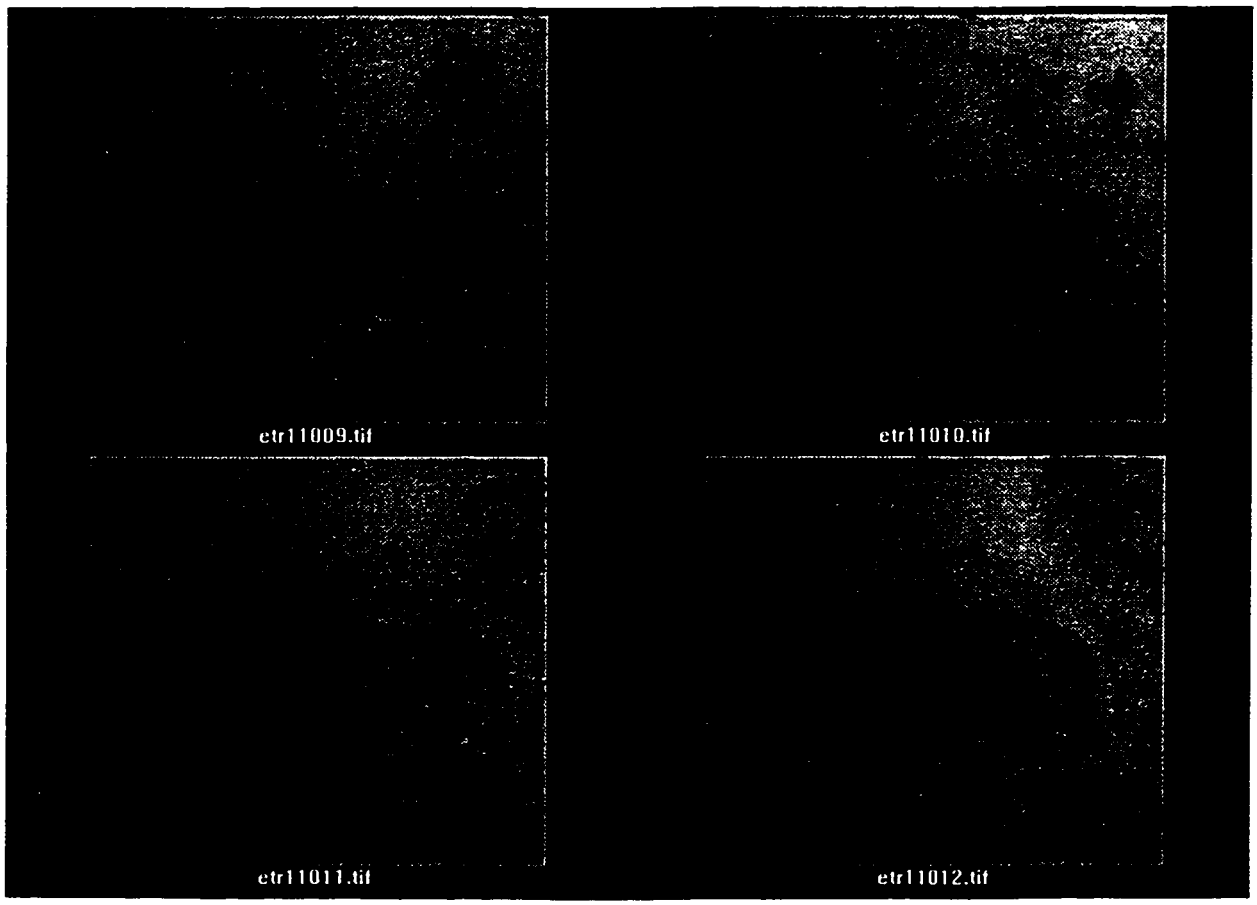
etr11009.tif
etr11010.tif
etr11011.tif
etr11012.tif

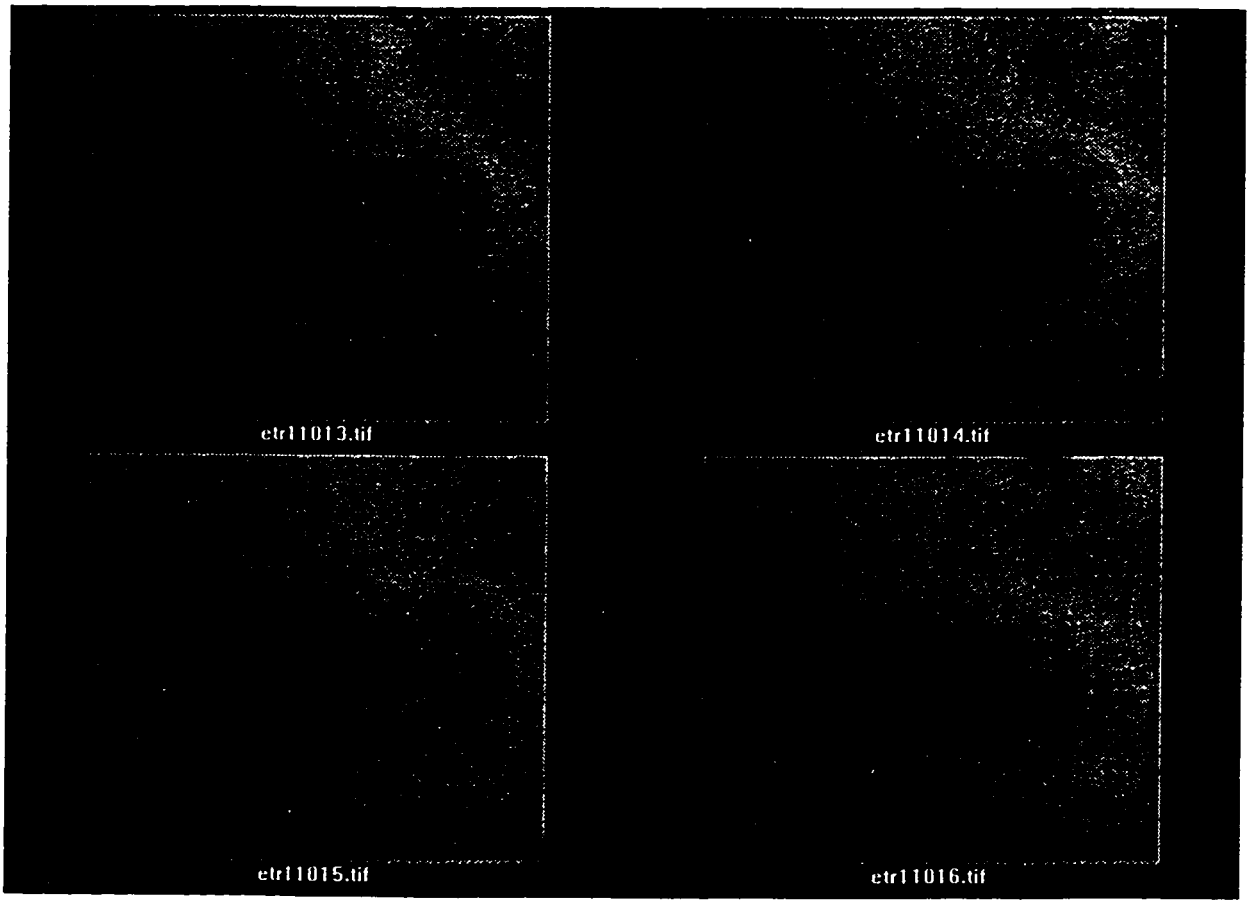
etr11013.tif
etr11014.tif
etr11015.tif
etr11016.tif

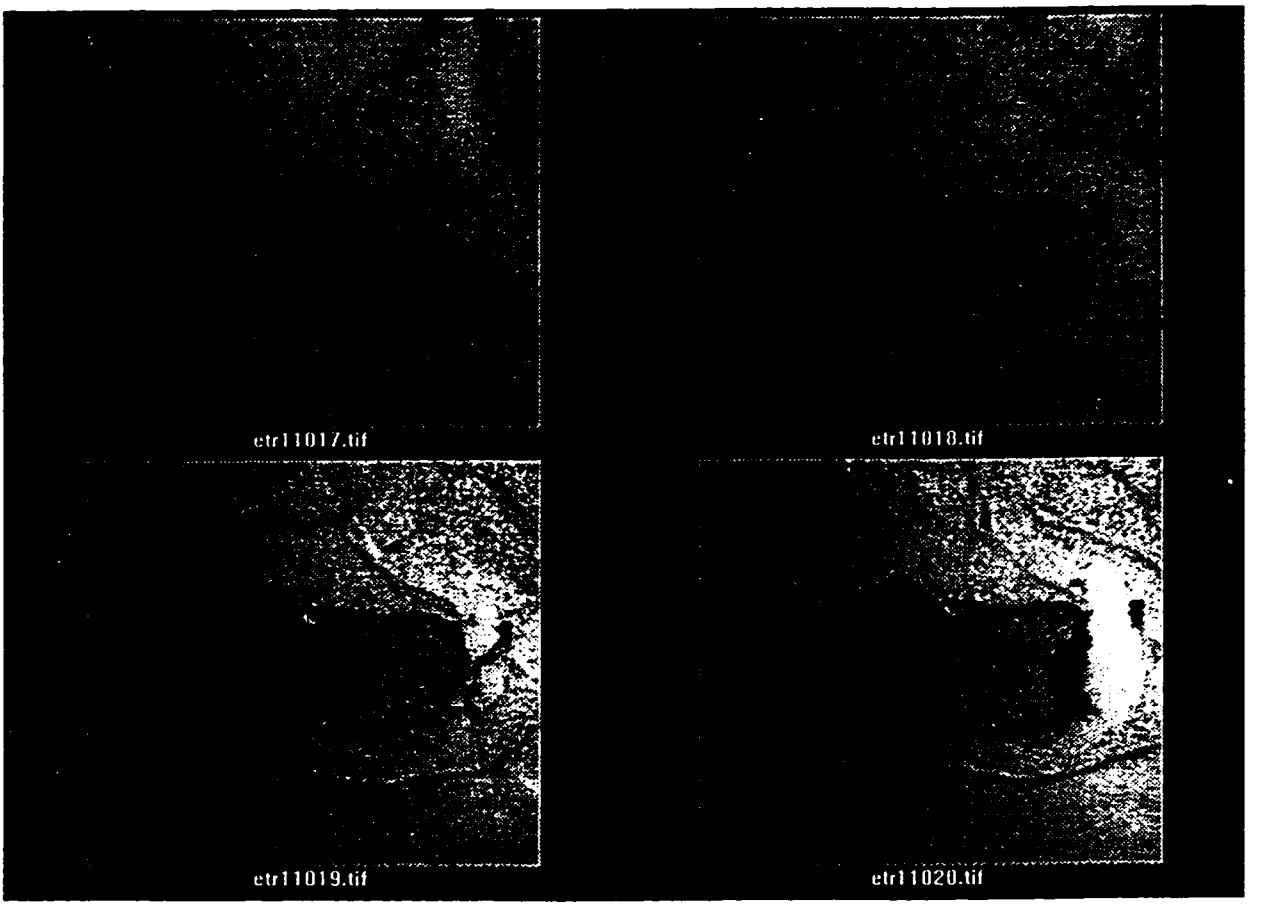
etr11017.tif
etr11018.tif
etr11019.tif
etr11020.tif

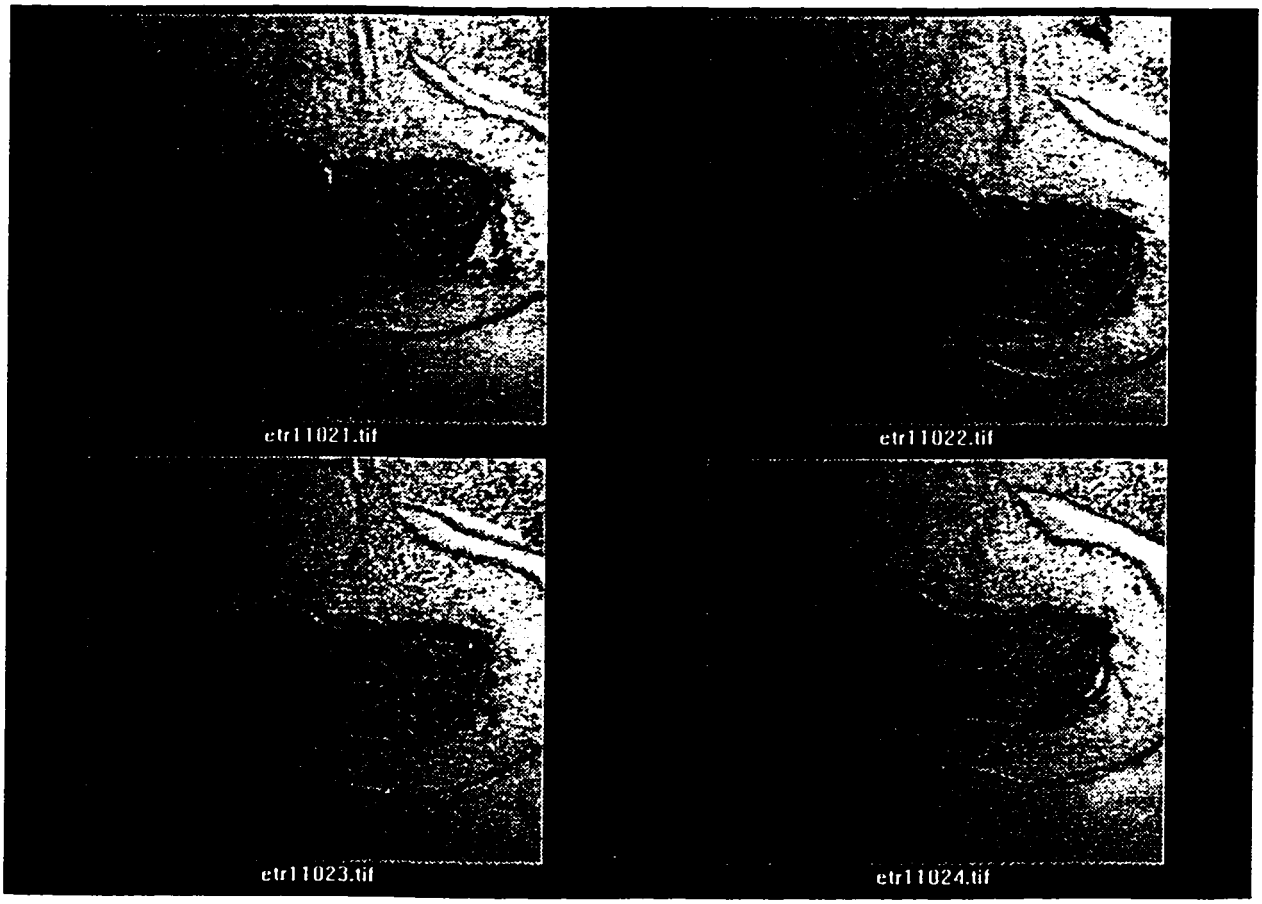
etr11021.tif
etr11022.tif
etr11023.tif
etr11024.tif

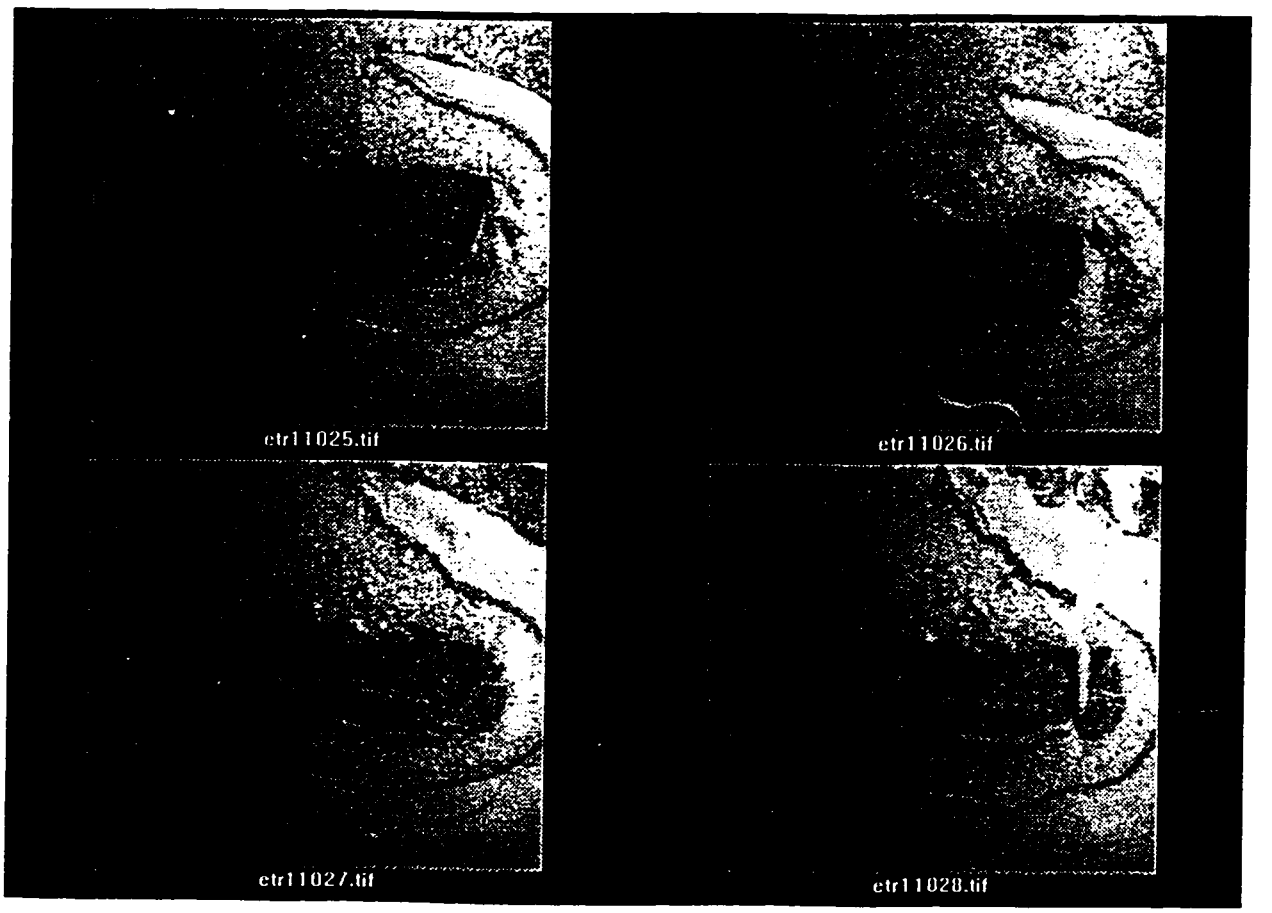
etr11025.tif
etr11026.tif
etr11027.tif
etr11028.tif

IMAGE EVALUATION TEST TARGET (QA-3)

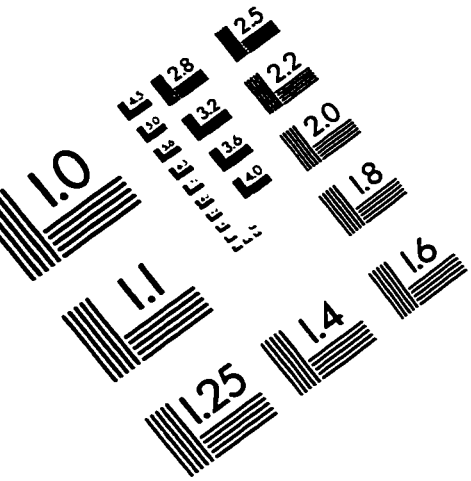

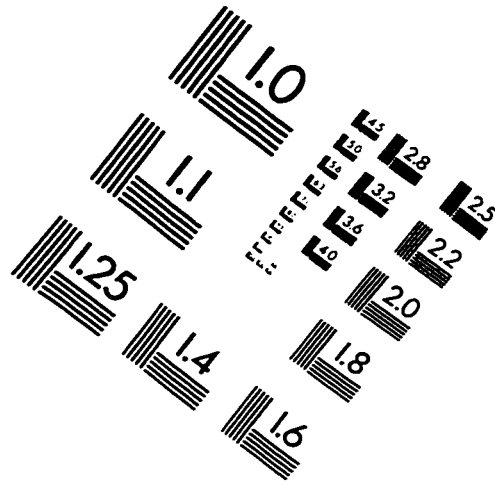

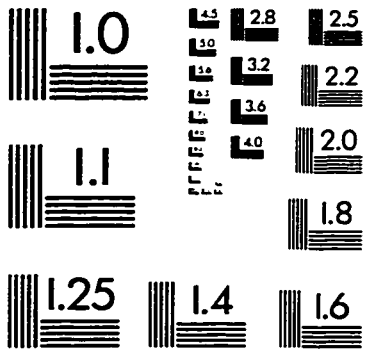

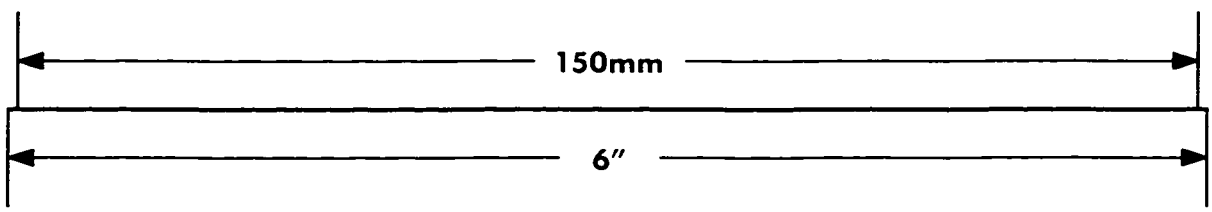

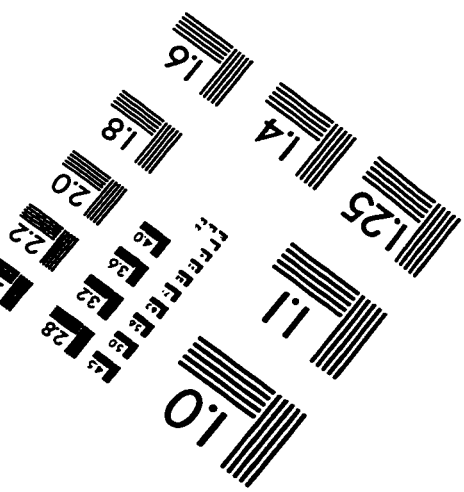

APPLIED IMAGE, Inc
1653 East Main Street
Rochester, NY 14609 USA
Phone: 716/482-0300
Fax: 716/288-5989
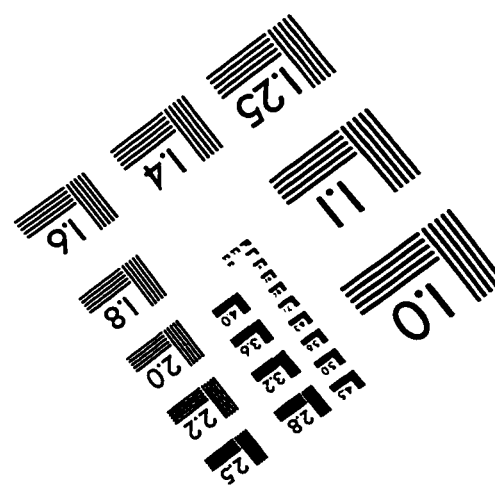
© 1993, Applied Image, Inc., All Rights Reserved